Atmospheric Correction of New Zealand Landsat Imagery

A thesis presented in partial fulfilment of the requirements for the degree of

Master of Philosophy
in
Earth Science

at Massey University, Palmerston North,
New Zealand

Sam Stafford Gillingham

2002

Abstract

In this study, MODIS data for New Zealand was downloaded and evaluated as input to the 6S atmospheric correction model. Data for one year were downloaded for aerosols, water vapour and ozone and trends of this data were studied. The sensitivity of retrieved reflectance of several targets to changes in the atmospheric components as seen in the MODIS data were also analysed. Several methods were developed for using this data for atmospheric correction and the output compared to a commercial atmospheric correction package (ATCOR 2).

In addition, ground measurements were used to confirm the accuracy of the MODIS data. This involved both data obtained from NIWA and readings taken with a hand held MICROTOPS instrument. These readings showed that the MODIS data has some inaccuracies. This can result in a significant error in the retrieved reflectance, especially for darker targets, such as forest. Therefore caution should be exercised when using aerosol values from MODIS in an atmospheric correction. However, the results for water vapour and ozone were reasonably close, giving confidence for using MODIS ozone and water vapour in atmospheric correction.

Ground measurements were also taken of targets with a GER 2600 Spectroradiometer and these readings compared to the atmospheric corrections of the same targets. This confirmed the accuracy of the atmospheric correction methods.

Acknowledgements

I would firstly like to thank my supervisors James Shepherd and Mike Tuohy for their time and thoughtful advice throughout the preparation of this thesis.

Financial assistance was gratefully received from the Massey Masterate Scholarship and from my parents, who in addition provided much support and advice.

Thanks must also go to Landcare Research for providing facilities and equipment, and to all the people there who assisted me directly, and indirectly.

To NIWA, Lauder who provided me with the ozone data very promptly and willingly.

Lastly, I thank John Dymond and Olivia Hamid for their invaluable assistance with preparing the final drafts of this thesis.

Contents

List of Figures

Chapter 1

Introduction

1.1 Aim

This project was undertaken in response to a question posed by Dr James Shepherd at Landcare Research, Palmerston North. He had a simple approach to correcting Landsat scenes for atmospheric effects. This approach was reliant on average monthly atmospheric data collected at Lauder, Central Otago. The atmospheric correction was performed in addition to a number of processes that Landcare had developed for removing the effect of sun angle and topography in satellite images. Dr Shepherd wanted to know whether his approach to atmospheric correction could be improved by using daily atmospheric data acquired by the Terra satellite.

The aim of the project thus became: to determine the best approach for atmospheric correction given the limitations of data availability and available computing power. NASA had made data from the MODIS (Moderate resolution imaging Spectroradiometer) sensor publicly available. This project will use MODIS data to determine how the important contributors to scattering and absorption in the atmosphere vary over the course of a year. These results will be used to assess the sensitivity of various targets to the changes in concentrations seen in the atmosphere over New Zealand. In addition, some techniques for performing atmospheric correction will be developed.

The 6S model attempts to retrieve pixel reflectance by taking into account gaseous absorption, scattering by molecules and aerosols, and variations of surface reflectance [45, 46]. Absorption is estimated for each spectral band of the satellite along the direct paths between the sun, target and sensor. Estimating scattering is complicated by the effect of photons being scattered toward the sensor that have not been reflected from the surface. In addition, some photons will be scattered toward the sensor that have

reflected off a nearby target. Lastly, there is the effect of trapped photons interacting with the atmosphere and surface repeatedly. The effect of adjacent targets is calculated using a weighting function that is primarily dependent on aerosol concentration.

Previously when using the 6S model to perform atmospheric correction, a suitable atmospheric model had to be used, such as the US Standard Atmosphere 1962. With the characterisation of the New Zealand atmosphere obtained, it should be possible to input into 6S average values for the time of the year, or ideally, the conditions for the Landsat scene if available. Lastly, some measurements on the ground will be taken to confirm the accuracy of the MODIS data and of the atmospheric corrections.

No work has been done on atmospheric correction of Landsat scenes of New Zealand (apart from the work of Dr James Shepherd at Landcare Research). Attempts to characterise the concentrations of New Zealand atmospheric constituents that contribute to scattering and absorption has been restricted to ground measurements in Lauder, Central Otago [21] and Christchurch [16].

As for the atmospheric correction of Landsat scenes, there has been some work on removing the effects of localised pollution by Liang *et al.* [28] who review some of the more commonly used techniques for atmospheric correction. A new method is proposed to overcome the limitations in these existing methods. This method first requires the creation of lookup tables of different atmospheric quantities and their radiative transfer code solutions. This is done for increased processing speed. Next the aerosol optical depth must be estimated. This is done by histogram matching between areas affected by haze and those that are not. The scene is classified by land cover type by using bands 4, 5 and 7 which are less affected by aerosols. Reflectance matching is then performed over the scene to estimate the aerosol optical depth. The result is then corrected for surface adjacency effects. This is done by considering the effect of neighbouring lighter of darker pixels. The created lookup tables are then used for calculating the surface reflectance.

Hu *et al.* have looked into using SeaWiFs (Sea-viewing Wide Field-of-view Sensor) data to atmospherically correct Landsat imagery over aquatic environments [24]. SeaWiFs has bands similar to MODIS and is able to measure aerosol optical depth over aquatic environments. There is a time lag of 1-2 hours between passes of Landsat and SeaWiFs, the effect of which is assumed to be negligible. Further, there are differences in viewing geometry and bandwidth, which are compensated for. One of their conclusions is that ignoring polarisation in the atmospheric model, or choosing an incorrect aerosol type, can lead to large errors in the correction. This is because the signal from

the sea is so small compared with the errors that can be introduced by the atmosphere.

Zhao *et al.* have used the 6S model to atmospherically correct an area of wetland in Japan [48]. The purpose is to develop a technique for measuring surface albedo for climate models. They compared the results of the atmospherically corrected Landsat 5 data with ground albedo measurements. The average error was 6%. To improve accuracy, more information on the spectral reflectance was recorded with a Spectroradiometer. A method was developed to correct the albedo calculations using these data. They also found that it is reasonable to compare atmospherically corrected pixel values with point albedo measurements on the ground.

A good summary of atmospheric correction techniques is presented by Lu *et al.* [29]. In addition they discuss the problems they encountered trying to build an historical sequence of atmospherically corrected images of the Amazon basin for the purposes of change detection. Generally, the actual composition of the atmosphere at the time of image acquisition was not available. The different techniques developed so far were evaluated, and it was decided to go with a variant of the dark object subtraction technique. This technique involves identifying a dark area in the image. This area may be a lake or dense vegetation. The amount of aerosol in the atmosphere is then estimated by studying the strengths of the different bands over this dark target. Due to the historical nature of the images used and the lack of calibration data for them, a number of techniques for estimating calibration data were also evaluated.

Song *et al.* analyse eight different atmospheric correction techniques and their effect on classification accuracy for Landsat TM data [44]. They conclude that atmospheric correction is not necessary when classifying a single scene if the training data are in the same image. This is because the atmospheric correction does not add any new information. They also conclude that the correction is unnecessary for change detection if training sites are identified on each image in the sequence. However, if the training sites are not on the image being classified, then atmospheric correction is required. They also conclude that the most accurate correction they evaluated was a modified dark object subtraction that took into account the effects of Rayleigh scattering. Chavez [19] gives a more detailed description of the modified dark object subtraction method.

For finding the albedo of the bottom of the ocean and its vegetation cover, Zhang *et al.* used Landsat TM data [47]. Their first task was to remove the effects of noise and striping in the imagery. This step is important because of the high noise over dark targets that the TM sensor exhibits. A number of different techniques were developed to

remove this noise. The approach favoured used Fourier analysis and numerical filters and is claimed to reduce noise by up to 25%. As for the atmospheric correction, the Rayleigh and aerosol scattering contributions were removed by assuming the properties of the atmosphere. Problems were encountered caused by the low dynamic range of the TM sensor, but the results for the albedo were consistent with measured values.

Another study using 6S for atmospheric correction was carried out by Ouaidrari and Vermote [38]. They were looking at atmospherically correcting Landsat TM data. The water vapour and ozone data to be input to the model was extracted from climatology data. Aerosol Optical Depth was estimated using the dark target approach. Clouds were detected and removed using a ratio between red and near infrared bands. Performance of the atmospheric correction was improved by interpolating the correction based on runs from 16 cells over the scene. Ground measurements were performed on prairie grass and compared to corrected Landsat TM scene. The results indicate a very close match in the visible channels. The adjacency effect correction developed help to improve the contrast of the scene.

1.2 The Terra Satellite

The Terra Satellite was launched from Vandenberg Air Force Base, California on 18 December 1999. Its purpose is to monitor global climate change. For this it is equipped with a variety of sensors for monitoring the earth and the atmosphere. It is 3.5m in diameter, 6.8m long and has a mass of 5190kg, and was carried in to space by by an Atlas-IIAS expendable launch vehicle. The orbit taken by the satellite is a near circular sun-synchronous orbit with an inclination of 98.2 degrees, an altitude of 705km, and an orbital period of 98.88 minutes. The orbits of the satellite can be predicted using [3]. The orbit is designed so the satellite crosses the equator at 10:30am local time when the sun angle is reasonably high and the cloud cover over the land is minimal. The sensors on board Terra record a wide range of electromagnetic frequencies and through some complex processing provides a wide range of information on the atmosphere. The lifetime of the satellite is expected to be six years.

In total all the instruments on the satellite transmit to the recording stations 194 gigabytes per day. The NASA ground network receives these data through the TDRSS (Tracking and Data Relay Satellite System) network in two 12 minute bursts each orbit. The ground station is at White Sands, New Mexico, and three satellites in geosynchronous orbit relay the data from Terra. During normal operation, commands are

sent to the satellite using S-Band. The actual data that have been recorded is transmitted from the satellite using the Ku-Band Single Access (KSA) at 150 megabytes per second. Terra can also transmit data over the X-Band for transmitting real time and recorded data directly to users at other ground stations. The data collected are sent to the Earth Observatory System Data and Information System (EOSDIS) for processing. This is the central processing centre for both Terra and Landsat in addition to other related satellites. Should the TDRSS system be unavailable, then there is a series of backup ground stations that provide a back up link using the S-Band. These stations are located at Poker Flats, Alaska; Svalbard, Norway; and Wallops Island Station, Virginia [2].

1.3 MODIS

The MODIS (Moderate Resolution Imaging Spectroradiometer) is a sensor aboard NASA's Terra satellite. One of the aims of this sensor is to detect and model climate change by collecting data on the composition of the atmosphere [1]. These datasets are made available free of charge and can be downloaded over the Internet from the MODIS atmosphere data products page [6]. The data are divided into three levels: level one is the raw unprocessed data; level two has had further processing performed on it; level three has had an additional level of processing and covers the whole world. In this study, the level two data are of most interest as it has information about atmospheric components at a good spatial resolution. Each file in this level corresponds to a measurement taken on a satellite pass. The Internet access allows the user to search by location and request the data returned by a search. The level two data are subdivided into the following products:

- Aerosol Product.
- Water Vapour Product.
- Cloud Product.
- Atmosphere Profile product.
- Cloud Mask Product.

In this study the aerosol, water vapour, and atmosphere profile (for ozone) products are used. These are described in more detail in the following in Sections 1.4, 1.5 and 1.6.

As mentioned above, level three products are also available. These have had another level of processing applied to them and cover the whole world. Because of this their spatial and temporal resolution has been decreased. They are divided into the following products:

- Daily Global Product.
- Eight-Day Global Product.
- Monthly Global Product.

It was intended to download the Monthly Global Product as part of this study to confirm that the summaries prepared using the level two data were correct. However the amount of data that had to be downloaded was very large (over 400MB a month) and became so time consuming the effort was abandoned.

The expression given for the error on the aerosol product over land is $\pm 0.05 \pm (0.20 * \tau)$ where τ is the aerosol optical depth. This expression indicates that as the aerosol optical depth increases, so does the error. For the water vapour product, the typical error over land is 10%. The ozone measurement is considered to be very accurate compared with other sensors so no error estimate is given [1].

1.4 Aerosols

Aerosols are microscopic particles suspended in the air. They can occur naturally as well as from human activities. Table 1.1 and 1.2 give a break down of the natural and anthropogenic sources of aerosols. The extreme variation in these figures means that comparisons are not very meaningful (the anthropogenic contribution is between 7 and 43% of the total). More recent analysis with the MODIS sensor indicates that 10% is a more accurate estimate for the anthropogenic contribution [5].

Allen *et al.* [15] have a more recent set of figures taken at Baring Head near Wellington, New Zealand. They took samples when the wind was blowing from the south to find the actual composition of aerosols over the ocean. These figures are presented in Table 1.3. They figures are probably closer to what would be seen for New Zealand. New Zealand is a small country in the middle of the ocean and heavily affected by oceanic air.

Lee *et al.* [27] comment on the sources of some of these aerosols. They mention that ammonia comes mainly from agriculture and the breakdown of animal waste. It

Table 1.1: Estimates of Natural Particles smaller than 20μm emitted into or formed in the atmosphere [18].

Type	Estimated Particulates (10^9 kg/year)
Soil and rock debris	100-500
Forest fires	3-150
Sea salt	300
Volcanic debris	25-150
Sulfate from H_2S	130-200
Ammonium salts from NH_3	80-270
Nitrate from NO_x	60-430
Hydrocarbons from plants	75-200
Total	**773-2200**

Table 1.2: Estimates of Man Made Particles smaller than 20μm emitted into or formed in the atmosphere [18].

Type	Estimated Particulates (10^9 kg/year)
Particles (direct emissions)	10-90
Sulfate from SO_2	135-200
Nitrate from NO_x	30-35
Hydrocarbons	15-90
Total	**185-415**

Table 1.3: Aerosols recorded at Baring Head (ng m^{-3}) [15].

Aerosol type	Winter	Spring	Summer
Methane- sulphonate	1.5	23	48
Non-sea-salt sulfate	115	139	187
NO_3^-	293	70	84
NH_4^+	44	39	59
SO_2	39	39	30
HNO_3	18	30	27
NH_3	74	42	31

reacts with sulfate and nitrate aerosols, plus nitric acid to produce both ammonium sulfate and ammonium nitrate aerosols. However, it is removed from the atmosphere very effectively by rain, and also by reactions with H_2SO_4 and HNO_3. Ozone at low altitudes is mainly produced by vehicle and industrial emissions and is responsible for the oxidising of nitric oxide into nitrogen dioxide.

Aerosols are of interest to climate scientists because they reduce the amount of sunlight that passes through the atmosphere to the surface. Further, there is an indirect effect where aerosols change the properties of clouds by aiding the formation of cloud droplets. Normally most of the aerosols in the atmosphere are in the troposphere where they are generally washed out by rain within a week. However, big volcanic eruptions can put aerosols into the stratosphere where they are not washed out and stay for months, reducing temperatures over the globe and contributing to beautiful sunsets. As well as through precipitation, aerosols can also just fall to the ground if the particles are large enough, or they can attach to vegetation and buildings. The lack of information on how different quantities of aerosol affect cloud formation, rainfall and temperatures is cited as the main reason that this information is being collected by MODIS [5].

Aerosols are an important part of this study because they scatter visible light. The signal at the sensor consists of energy from the target that has not been scattered away from the sensor, energy from the sun that has been scattered by the aerosols into the sensor without hitting the ground, and energy scattered toward the sensor from neighbouring targets. The particles that have the most effect are those with a diameter similar to the wavelength of light [18]. When calculating the scattering effect, the shape of the particle is assumed to be a sphere, as it is impossible to determine the true shape. The size distribution of the particles is generally chosen from a number of different distribution definitions. The index of refraction is also needed, which is dependent on the amount of water that is attached to the particle. Physical models are used to estimate the effect of aerosols on the brightness recorded at the satellite.

1.5 Water Vapour

Water vapour is recorded by the MODIS sensor for use in, among other things, understanding the hydrological cycle, interactions between water vapour and aerosols, earth's energy balance and climate [9]. The effect of water vapour is interrelated with that of aerosols because as humidity increases, condensation of water onto aerosols

Figure 1.1: Spectral Transmittance of H_2O [46].

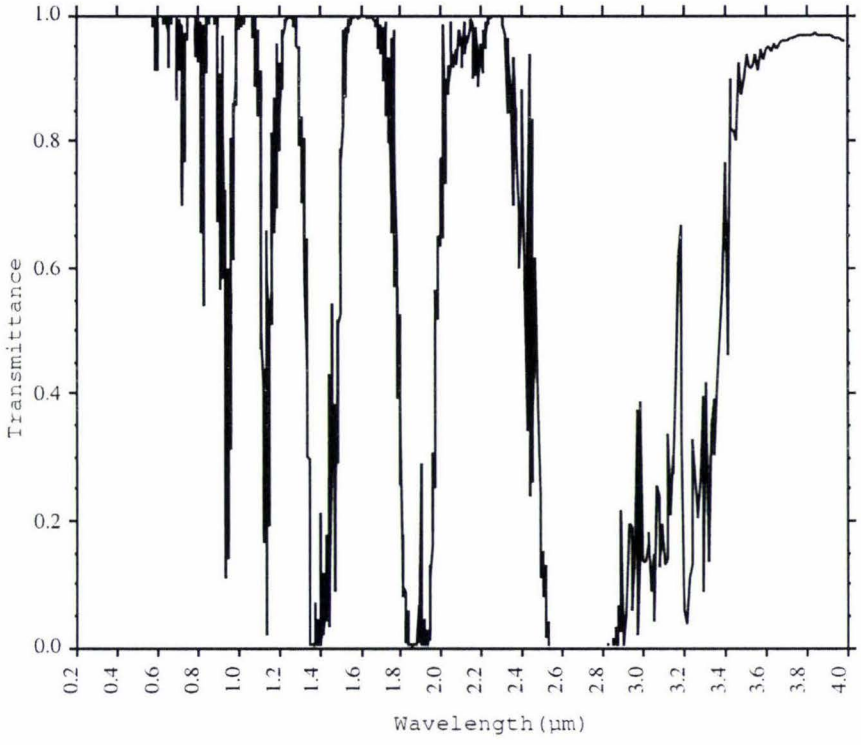

has an effect on the optics of the atmosphere when the relative humidity is above 30 to 40 percent, which is nearly always the case in New Zealand. The result of the condensation is that the particles increase in size causing the refraction indices to change and the extinction efficiency and amount of light scattered to increase [18].

Water is of interest in this study because it absorbs light at certain wavelengths and transmits at others (see Figure 1.1). Increasing amounts of water vapour in the atmosphere will result in greater absorption in the wavelengths that water vapour absorbs.

1.6 Ozone

Ozone is created as a result of high energy photons hitting oxygen molecules. The molecules break apart and then reform as ozone (O_3). This mainly happens in the stratosphere, resulting in an ozone layer 25-40km above the surface. Ozone is an effective absorber of ultra violet radiation, hence the concern over ozone depletion. However, ozone itself is not particularly stable and can be broken down by radiation and

chemical reactions. The chemical reaction of most concern derives from CFC's. Ultraviolet radiation splits chlorine atoms off CFC molecules. These chlorine molecules react with ozone, producing chlorine monoxide. This is unstable and when it reacts with a single oxygen atom, it produces an oxygen molecule and a spare chlorine atom that can destroy another ozone molecule. The reduction of atmospheric ozone in the last 50 years is not significant in the tropics, but is 4-5% in the mid latitudes per decade and 20 percent total in the arctic regions. In Antarctica the extreme cold makes the atmosphere more susceptible to ozone depletion and causes the "ozone hole".

Ozone is also present in the troposphere. It can be transported there by large weather systems from the stratosphere. In the troposphere, ozone can be created when ultra violet radiation reacts with pollution such as nitrogen oxide. Ozone is poisonous to plants, and also to people, in whom it can cause respiratory disease. Interestingly, it is increasing in concentration over many large cities even while the concentration is decreasing in the stratosphere because of this reaction with pollution [36].

In the stratosphere, ozone is useful for meteorology. It absorbs ultra violet radiation and the heat retained then determines the temperature profile and thus the circulation of the stratosphere. It also has been used as a tracer in determining circulation and transfer between the troposphere and stratosphere [35]. It is also possible to predict the location of jet streams by studying the gradient of ozone in the atmosphere [11].

It is from this background that interest has increased in monitoring the amount of ozone in the atmosphere. In the MODIS data, the product of interest is the "Atmosphere Profile Product". This contains the ozone readings and also has information on the stability of the atmosphere for the prediction of cloud formation and precipitation. The graph of transmittance through ozone is shown in Figure 1.2. Note how light is transmitted through most of the spectrum shown, but is absorbed strongly in the ultraviolet and weakly in the visibly wavelengths.

1.7 Other Atmospheric Constituents

The other main absorber is carbon dioxide, which along with water vapour is a main absorber at the near infrared wavelengths. However, its concentration tends to remain constant, so when modelling the atmosphere, a constant value can be input. The graph of carbon dioxide transmittance is shown in Figure 1.3. Nitrogen and Oxygen are the main atmospheric constituents, but they only have an effect in a small part of the spectrum. Once again the concentrations of these gases is known and constant [18].

Figure 1.2: Spectral Transmittance of Ozone [46].

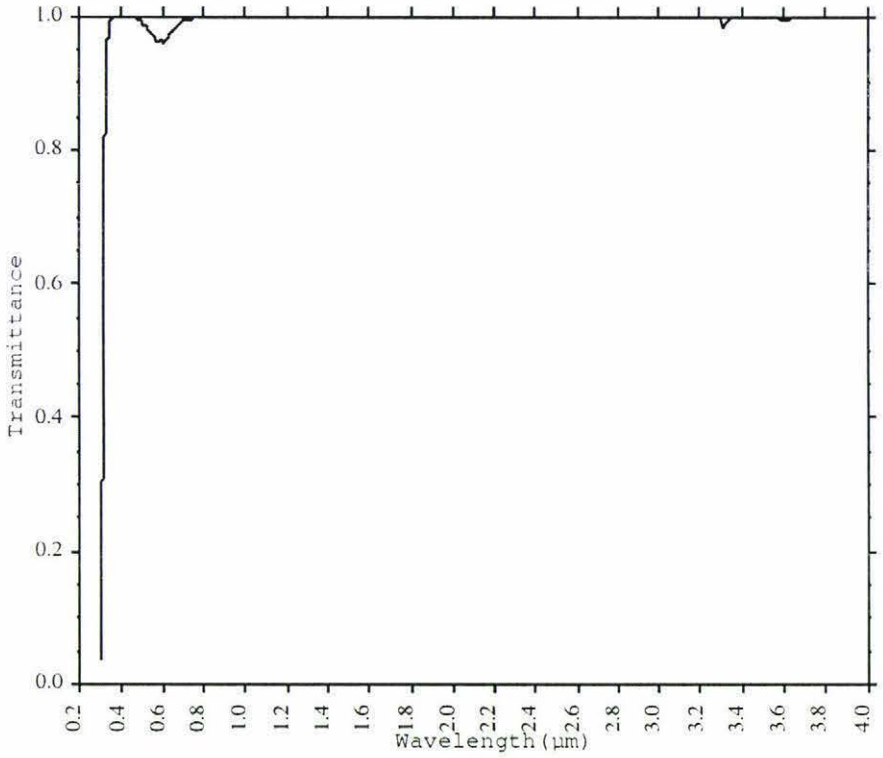

Figure 1.3: Spectral Transmittance of carbon dioxide [46].

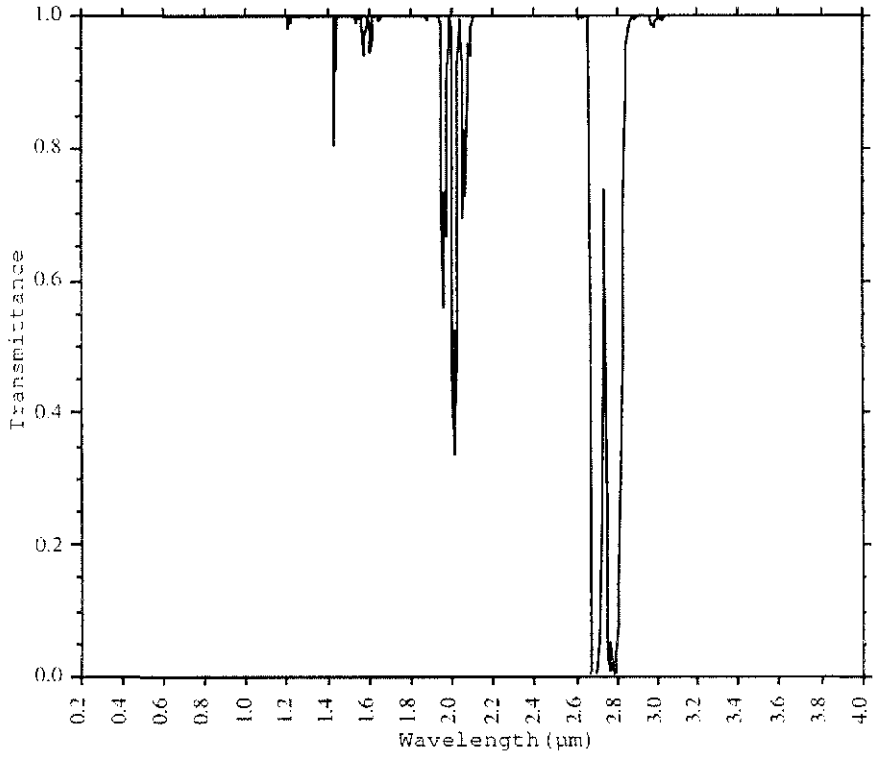

1.8 Landsat7

The Landsat7 satellite was launched by NASA from the Vandenberg Air Force Base on 15 April 1999 on a Delta II launch vehicle. Landsat satellites have been recording data of the earth since 1972 and Landsat7 is the most recent of the series. Landsat7 is in a similar orbit to the Terra satellite (see Section 1.2), but half an hour earlier. The orbit is designed so that each adjacent swath will be covered about 2 weeks apart in a westerly direction. At launch the satellite weighed around 4632 pounds. The main aim of the Landsat project is to provide remote sensing imagery of the earth for monitoring and managing the earth's resources. However, unlike MODIS data, Landsat7 data are not free, and has to be purchased from NASA.

Landsat7 uses the S-Band for receiving commands from ground stations, and the X-Band is used for downloading recorded data. Through this link it provides Earth Observatory System Data and Information System (EOSDIS) with 150 gigabytes of data per day. The actual orbital characteristics are continually monitored and the predicted flight path is computed up to 72 hours ahead. Decisions are continually made on how to manoeuvre the satellite so that it remains within the mission parameters.

Communication with ground sites is done when the satellite is in the line of sight from one of the ground recording stations that receive X-Band data. These are: Sioux Falls, South Dakota; Poker Flat, Alaska; Wallops, Virginia; and Svalbard, Norway. As well as these, Landsat makes use of the TDRSS (Tracking and Data Relay Satellite System) when it is not near a ground station. Landsat has some memory on board that it can use to record up to 42 minutes of data (100 images) when it is outside the range of a receiving station.

The sensor on board the Landsat7 satellite is called the Enhanced Thematic Mapper Plus (ETM+). A "scan mirror" sweeps across the track of the satellite. The energy is then focused on to a pair of mirrors that compensate for overlap and under-lap between sweeps caused by the movement of the satellite. The energy is then focused onto the primary focal plane which detects bands 1,2,3,4 and 8. Some of the energy is focused onto the "cold focal plane", which is cooled to 91 degrees Kelvin. This sensor detects bands 5, 6 and 7.

The spectral bandwidths of the Landsat7 sensor are given in Table 1.4. These bands (except Bands 6 and 8) are shown graphically in Figure 1.4.

The stated aim is to have $\pm 5\%$ radiance error on the calibration of the sensors for the life of the satellite [4].

Table 1.4: Bandwidths of the ETM+ sensor aboard Landsat7.

	Min (μm)	Max(μm)	Resolution(m)	Type
Band 1	0.45	0.52	30	Blue
Band 2	0.53	0.61	30	Green
Band 3	0.63	0.69	30	Red
Band 4	0.78	0.90	30	Near IR
Band 5	1.55	1.75	30	Mid IR
Band 6	10.4	12.5	60	Thermal IR
Band 7	2.09	12.5	60	Far IR
Band 8	0.52	0.90	15	Pan

Figure 1.4: The response of the ETM+ sensor aboard Landsat7 excluding Band 6 and 8.

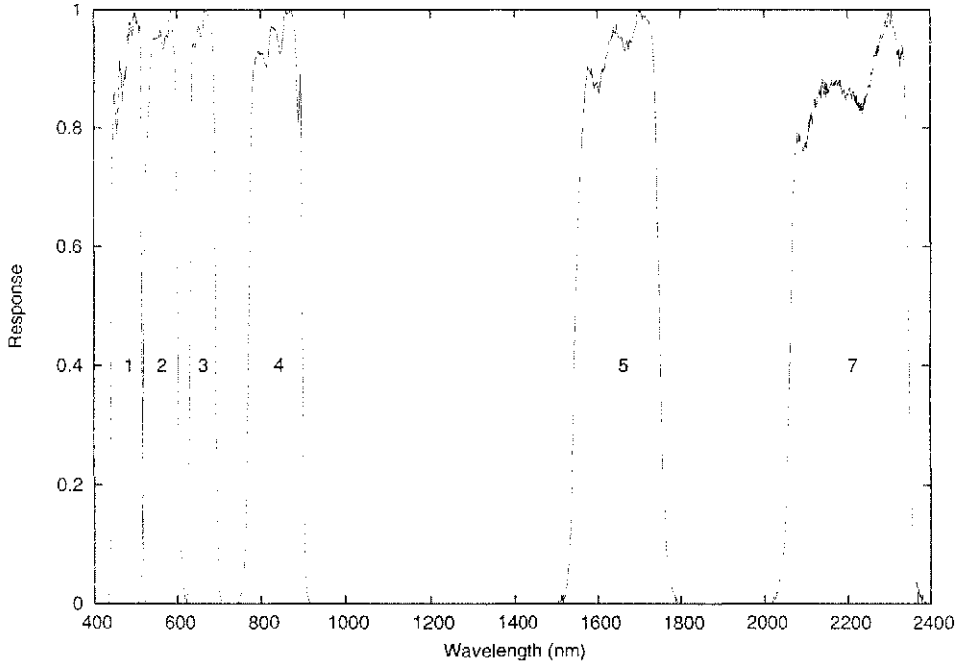

1.9 Landcare Research

Landcare Research is a Crown Research Institute that employs approximately 400 staff throughout New Zealand. One of the centres is based at Massey University, Palmerston North. This study was undertaken though both Massey and Landcare. Landcare conducts a research programme called "Fundamental environmental data, information and techniques Programme" which makes intensive use of satellite imagery. Through this programme many techniques have been pioneered for processing satellite imagery, in particular making Landsat imagery more useful for land-cover and habitat identification.

As part of this ongoing effort, methods are being developed to remove the effects of topography and sun angle from the imagery. These methods make the imagery more useful as they provide readings of the surface independent of sun, view angle and topography. Atmospheric correction is one area that requires further work to improve accuracy. Previously, the average monthly values at one site for aerosols, water vapour and ozone had been used. It was not known how much the actual values vary from place to place. This study will address this lack of knowledge and recommend to Landcare a method for performing atmospheric corrections. Combined with the other techniques that Landcare have developed, it should provide an accurate value for the actual ground reflectance with all other significant effects removed.

Chapter 2

Methods

2.1 Processing the MODIS data

The steps described in this section are summarised in figure 2.1.

2.1.1 Downloading the Data

The data were downloaded from the MODIS Atmospheric data products website [6]. Through this website, data can be downloaded a week at a time for a number of MODIS products. Notification of where and how to download the data are received via email.

It is likely for a given week that there may be twenty or so files. The file names are a sequence of 48 numbers and characters long, so setting up an FTP session manually can be difficult and error prone. This is a process which was automated using a program to read the email notification and download the requested data. One year's worth of data were downloaded for each product (Aerosol, Water Vapour and Ozone) and processed. In total, 70GB of data were obtained. If the data had been compressed, it would have only totalled around 17GB.

2.1.2 Extracting the Data

The files come from NASA in Hierarchical Data Format (HDF). Each HDF file contains a number of layers, each containing different information. The particular information contained in each layer is documented in the MODIS Atmosphere specifications [7, 8, 10].

The HDF User's guide [13] describes how to access the data in each layer using the HDF library, which is software that can be used to read the files. Using this library, the

raw data contained in these files can be extracted using a computer programme. Since the image processing for this project was to be done using ERDAS Imagine (the same software used by Landcare), it made sense for the layers of interest to be converted to Imagine format. ERDAS also supplies with Imagine a library for reading and writing Imagine files. Using both libraries it was possible to extract a given layer from the HDF file and save it in ERDAS Imagine format.

In addition, the gain and offset were applied to the data. The data are often packaged as integers to save space, so in order to obtain the original floating point data, these integers must be multiplied by the gain and added to the offset. However, MODIS data will have fill values for pixels where data were not obtained. Generally, this is specified as -9999. It is important to not apply the gain and offset to these values as it would hinder the detection of invalid data in future processing stages.

2.1.3 Rectifying the data

Once the files have been converted to ERDAS Imagine format, they then need to be rectified to the New Zealand Map Grid to be useful. Once this is done, all the data will be in the same projection, and will allow different files to be overlaid, or compared. Further, files from other sources can then be overlaid, such as maps of New Zealand. Rectification of the MODIS data can be done without selecting ground control points because there are layers in the HDF file that contain the latitude and longitude of each pixel in the image. Once these have been extracted, it is possible to rectify any other layer in the HDF file.

It it important to discard files that have few points inside the New Zealand Map Grid. A rectification done with few points will be of low precision, and also tends to indicate that very little, if any, of the data cover New Zealand. In addition, images where the only part that lies within the New Zealand Map Grid contains all fill values (-9999) get discarded as they serve no purpose in the analysis.

During processing, it was discovered that the geometric correction was generally a little inaccurate. The error was consistent and generally meant that there was a 3km offset to the west. Thus care needs to be taken when using these data that no dependence is placed on the absolute accuracy of the rectified data and this does have consequences for one approach to atmospheric correction, as will be shown later.

2.1.4 Calculating the cloud mask

Useful Landsat scenes are those that are taken when there is no significant cloud cover, as clouds prevent the sensor getting a good view of the surface. For the atmospheric data from MODIS to be useful for correcting Landsat scenes it also needs to be taken when there is no cloud cover. All the MODIS products of interest have a layer (called "Cloud_Mask") that contains, among other things, a flag specifying the amount of the pixel that is affected by cloud.

It is possible for MODIS to detect the fraction of each pixel affected by cloud because its sensors are of higher resolution than the data that are provided. Because a number of pixels from the sensors make up each pixel in the data used, the fraction can be calculated given the number of raw pixels affected by cloud. As only the pixels that have very little, or no clouds in them are of interest, a new mask is calculated for each file specifying which pixels have less than 30% cloud. This mask is then used in further processing to select pixels to analyse. For a full description of MODIS flags and how they are derived, refer to the MODIS Atmosphere QA Plan [20].

2.1.5 Managing the data

Once all the files have been processed as described above, some statistics need to be computed on the data on a monthly basis. This was done to reduce the data volume and to allow changes over time to be investigated. To this end, all the files for each month were analysed together and since they had been rectified were able to be treated as though they exactly overlaid each other. This enabled a comparison between each pixel in an image and a pixel at the same location in the others. Only pixels that contained little or no cloud cover were included as described in Section 2.1.4. Through this process, the following statistics for each of the co-located pixels were gathered for each month:

- Mean
- Standard Deviation
- Minimum
- Maximum
- Count

These values were used to calculate the statistics for each month as described in Section 2.1.6.

2.1.6 Obtaining statistics

For meaningful comparisons between the months, the data were summarised using the following measures:

- The mean of the layer that contains the mean of the pixels. This mean is weighted with the count of each pixel. This enables an understanding of how much aerosol is present for a given month and enables comparisons between the months. Refer to Figures 3.2, 3.6 and 3.9 for graphs of these values.

- The spatial variability of the values. This is an effort to find out how much the values differ over the whole image. This was calculated by finding the standard deviation of the mean of each pixel. This value was also weighted with the count of the values at each pixel. This value may be used to get an idea of the variation throughout the country. Since all the pixels are in different places, the standard deviation will give a measure of the spatial variability. For example, if a reading is taken for Otago, it will indicate how large the error may be if that value is used for Wellington.

- The temporal variability of the values. This value reflects the amount that the values vary over the month. This was calculated by finding the mean value for the standard deviation of each pixel. Since the standard deviation for each pixel is a measure of how much each pixel varies throughout the month, then the average standard deviation gives a measure of how much the picture varies temporarily over a month. This value gives an idea of how much the values vary throughout the month. For example if the monthly average value was applied to a day in that month, this value should give an idea of the error it will have. Refer to Figures 3.3, 3.7 and 3.10 for graphs of the variability of the data.

These values were only calculated using pixels over land, coastal areas and ocean that was less than 50km from land. This was done using a "Land Mask" file that contained non zero values for pixels to be included. The reasoning for this is similar to that for the cloud mask - Landsat scenes that are useful are over land or very close to it. Therefore for a representative statistic, only pixels specified by the land mask values

were included . Statistics were also calculated for the whole New Zealand Map Grid for comparison.

2.1.7 Processing data for each product

The following is a discussion of the specifics of product processing . One factor affecting all the product types is that for June 2001 there were only data for the first fifteen days of the month.

Processing Aerosol data

The data that were extracted from the aerosol product was the "Raw Optical Depth" for both Land and Ocean at 550nm. This was chosen because the coastal areas are of use as well as the land because of the influence the sea has on New Zealand. For a description of how this is derived see [26]. 550nm is also the wavelength that the 6S model [46] uses for its calculations. These data are available in 10km pixels and is re-sampled to 5km pixels during rectification. The files that contain this information are around 12MB each and there are generally over 200 per month.

Processing Water Vapour Data

Like the aerosol data, the water vapour data are available for every satellite pass over New Zealand. There are two data sets within these data that provide a measure of the amount of water in the column of atmosphere. One is at 1km pixels and is only available for satellite passes in daylight hours and uses Near Infrared to make the measurements. The other is available 24 hours and has 5km pixels. However the 5km data suffer from serious accuracy problems as described in [12]. Because of this it was decided to download only the larger files that contain the 1km data. For a discussion of how these data are derived, refer to [22].

Like the aerosol data, there are over 200 of these files a month, but due to the higher resolution of the files their size is 20MB per file.

Processing Ozone Data

Ozone data are available as part of the MODIS Atmospheric Profiles product [31]. The "total ozone" layer within this product contains 5km pixels. However there is more information within these files, such as atmospheric stability and temperature profiles. Because of this the requested files are larger than the other products (33MB). Due to

Figure 2.1: Data Processing steps for each Data Layer (Aerosols, Water Vapour and Ozone).

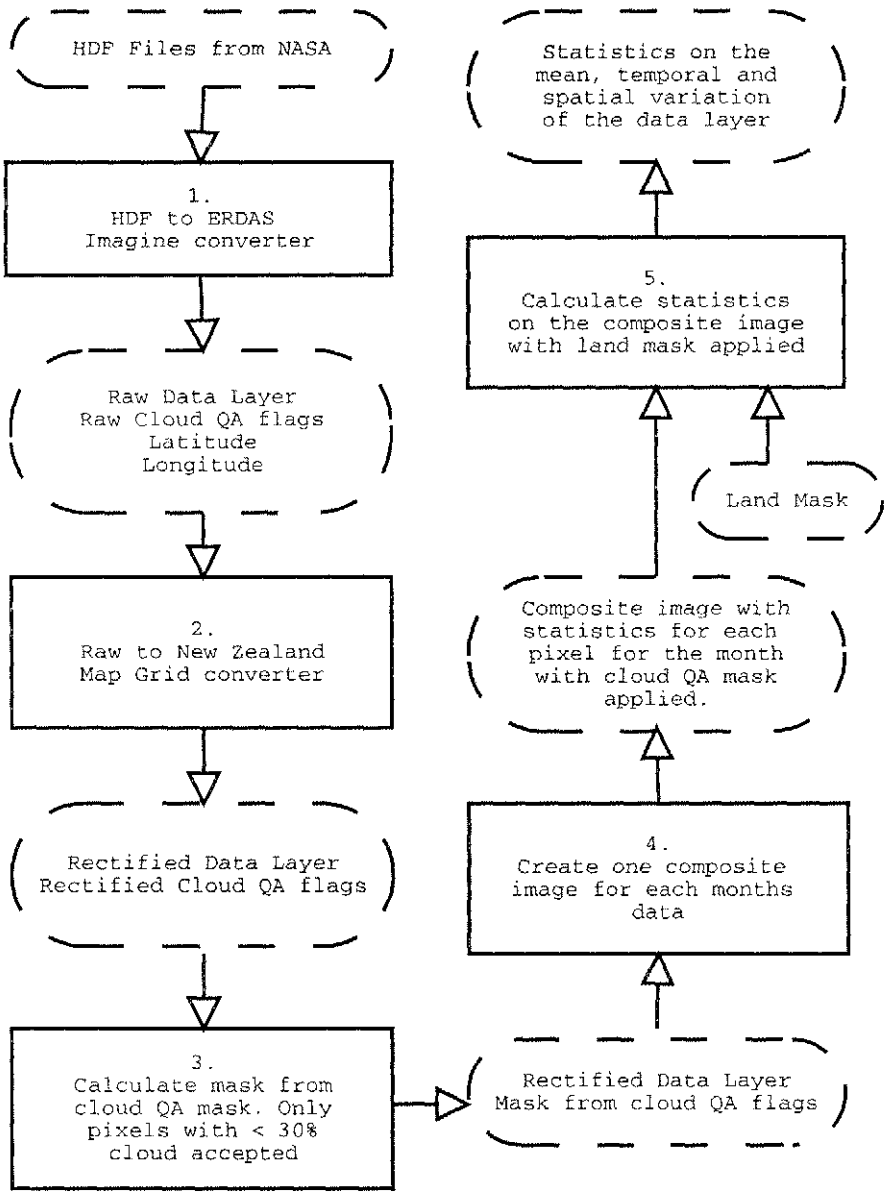

the sheer number of files that are available from NASA (around 55-60 files a week) and the time it would take to download them all, it was decided to download only a selection of the files. It was also decided to give a fair temporal distribution that every third file was to be downloaded, giving roughly the same amount of raw data as for the aerosol product. This means around 20 files a week.

2.2 Sensitivity Analysis with 6S

Once all the data is obtained for the behaviour of the New Zealand atmosphere using the steps outlined in Section 2.1, it needs to be fed into a model to predict how the observed variation affects satellite imagery. One of the models that has been written to do this is 6S [46]. This model as it stands contains information on various commonly used satellite bands and their widths. However it does not contain information on the Landsat7 bands. Modifications were made to 6S so that it knew about Landsat7 and was able to predict atmospherically corrected reflectance from surfaces for the Landsat7 wavelengths. Modifications were also made to the code so that the results were output at a higher number of decimal places to aid the precision of further processing.

The model returned values for a number of different parameters. The values recorded were:

1. Atmospherically corrected reflectance of the target. This is what the sensor would have seen had there been no atmosphere.

2. Direct Solar Irradiance. The amount of energy that hits the sensor which has come directly from the target (and from the sun before that).

3. Atmospherically Diffuse Irradiance. The energy that hit the sensor, but come from a nearby target, not the one being measured, due to scattering.

4. Environmental Irradiance. Energy that was received at the target from its surrounding area, and then reflected up to the sensor.

The inputs into the 6S model for each target studied were:

1. Radiance. This was obtained for a target by finding the value in the Landsat scene for a particular band and applying the gain and offset as specified in the Landsat header information for the layer.

2. Geometrical conditions. The solar zenith and azimuth angles were set to those specified in the Landsat header information. The satellite zenith and azimuth angles were both set to zero because Landsat7 takes its images looking directly down.

3. The total amounts of aerosol, water vapour and ozone. The profile of water vapour and ozone throughout the atmosphere is inferred using the US Standard 1962 model.

4. Date. The model was given the date when the earth is closest to the sun (21 December) which would give the brightest radiance from the surface. This was done because most satellite images are taken of New Zealand during the southern hemisphere summer so it is representative. This input parameter does not vary the final result very much.

5. Aerosol type. This was set as maritime because this accounts for most of the aerosols over a small island country like New Zealand.

6. Altitude. The altitude of the target is taken from a DEM. 6S is also told that the readings are taken from a satellite.

7. Ground reflectance. The reflectance of the target was given as zero and the reflectance of the surrounding environment was given as that of green vegetation. The size of the target was given as 20 metres. This information is used by the model to calculate the strength of the signal at the satellite given the input from the sun. However, of interest is the change in strength of the signal between the target and the satellite to calculate the atmospheric correction and the ground reflectance values are not used for this and are included for completeness.

Some representative targets were chosen (a forest, pasture and soil target) from a Landsat scene and determined the actual reflectance by inputing the MODIS values for aerosols, water vapour and ozone for the pixels over the targets. The model was run again, keeping the amount of water vapour and ozone the same but changing the amount of aerosols input over an arbitrarily large amount. This was to give an idea of how the output reflectance is affected by changes in aerosols. This experiment was repeated with water vapour, and then ozone to get an idea how changes in the amounts of these affect the retrieved reflectance.

With the values collected for the New Zealand atmosphere, the above experiments were repeated. The amounts of aerosols, water vapour and ozone were changed

through the amounts seen from the one year's worth of MODIS data. The was to give an understanding of how sensitive the retrieved reflectance is affected by the changes in the New Zealand atmosphere for the targets selected.

2.3 Ground Atmosphere Measurements

These measurements were used to check the accuracy of the MODIS data. A MICROTOPS II sensor (see Figure 2.2) was used for this purpose. The MICROTOPS II is made by the Solar Light Co. This device takes readings at a variety of wavelengths when pointing at the sun. The readings are then used to calculate the amount of ozone, aerosols and water vapour in the atmosphere. The wavelengths are as follows:

- 305.5nm
- 312.5nm
- 320nm
- 940nm
- 1020nm

The instrument works by comparing wavelengths where there is absorption with wavelengths where there is not. Thus for measuring ozone, the three UV wavelengths are used (305.5, 312.5 and 320nm). The amount of ozone can be calculated from a ratio of wavelengths 305.5nm and 312.5nm, or with a ratio between 320nm and 312.5nm. The MICROTOPS instrument provides these figures along with an experimental result from combining the two values. These wavelengths are used because they have different ozone absorption coefficients. Knowledge of these coefficients makes it possible to calculate the amount of ozone from the signal strength at these wavelengths.

For calculating water vapour, the calculation is simpler. At 940nm water vapour absorbs the most, and at 1020nm it absorbs the least. By using the relationship between the two measurements the amount of water vapour can be found.

These measurements require knowledge of the amount of atmosphere the light has passed through. To calculate this the instrument needs to know the time of day (provided by an internal clock) and the location in the world (provided by a connected GPS unit). From this the angle to the sun can be found and thus the distance of atmosphere that the light must pass through as it travels from the sun to the unit [34].

Figure 2.2: View of MICROTOPS instrument (top) and operation on the roof of Landcare building (bottom).

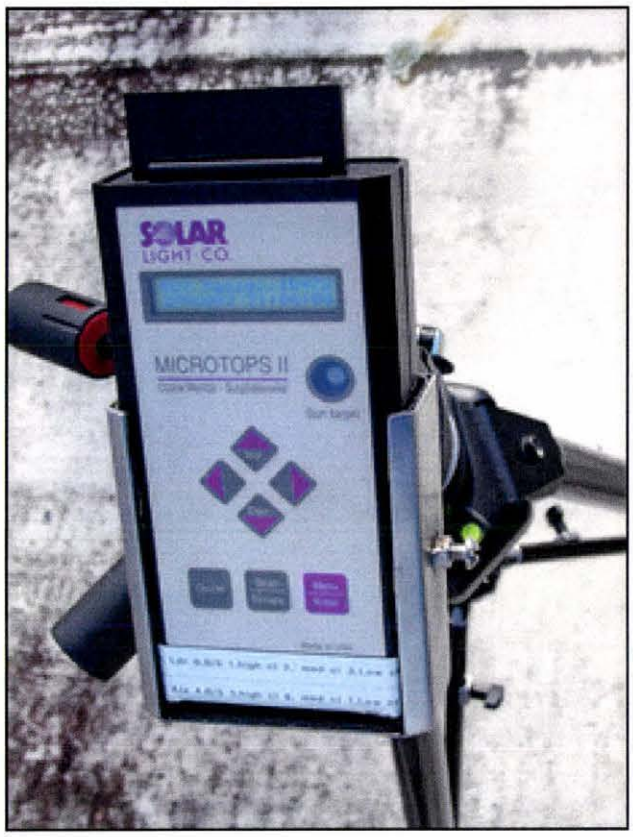

2.3.1 Measuring Aerosol Optical Depth

Aerosol optical depth (τ_{aer}) is unit-less and can be calculated by the following equation, above a height z [18]:

$$\tau_{aer}(\lambda, z) = \int_{z}^{\infty} \beta_{aer}(\lambda, d)\, dz \tag{2.1}$$

where β_{aer} is the extinction cross-section per unit volume for particulates. This is calculated using the following equation:

$$\beta_{aer}(\lambda) = \int_{0}^{\infty} \frac{dn}{dr}(r)\, \sigma(\lambda)\, dr \tag{2.2}$$

n is the number of particles, r is the mean size of the particles and σ is the extinction coefficient of one particle. This is computed from the Mie theory:

$$\sigma(\lambda, r) = \pi r^2\, Q_{ext}(\lambda, r) \tag{2.3}$$

where Q_{ext} is a non-dimensional efficiency factor.

The MICROTOPS instrument uses the 1020nm wavelength for calculating aerosol optical depth. However, this is not considered to be particularly accurate because it just uses the one reading. A more accurate approach is to construct a Langley plot which is a plot of the log of the raw voltage readings against the amount of airmass the energy has passed through. The readings are generally taken during a cloud free morning. At dawn, the light from the sun must pass through the most airmass, and this is reduced as the sun rises, reaching a minimum at midday (see Figure 2.3). The 1020nm wavelength was chosen for this because of low ozone and water vapour absorption of the signal and the low Rayleigh scattering. Readings were also made at 320nm, the other side of the 550nm used by MODIS for comparison and for consistency with Batchelor [16]. Measurements of aerosol optical depth at different wavelengths are not equivalent but can by related by the following equation[21]:

$$\tau_2 = \tau_1(\lambda_2/\lambda_1)^{-1.19} \tag{2.4}$$

The total optical depth of the atmosphere can be found by measuring the slope of the Langley plot. If it is assumed that the numbers that the instrument produces are related linearly to the solar irradiance, and that the earth is at its average position from the sun, the Beer-Lambert law can be written like this [16]:

Figure 2.3: Sun position for Langley readings.

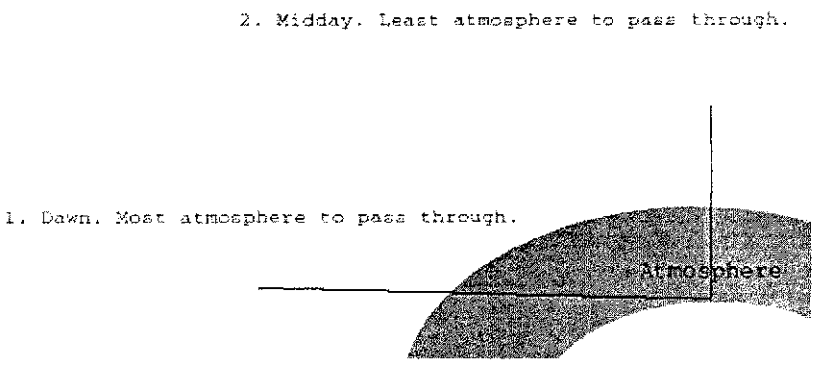

$$ln(V) = ln(V_0) - m_r \tau_{tot} \tag{2.5}$$

Where V is the output from the instrument and V_0 is the output of the instrument if it was at the top of the atmosphere, m_r being the ratio of the optical path along the angle to the sun to that at the zenith and τ_{tot} is the total optical depth. This equation is of the form $y = mx + c$ with the $-\tau_{tot}$ being the slope of the graph and $ln(V_0)$ being the y axis intercept.

To find the aerosol optical depth(τ_{aer}), the optical depth due to Rayleigh scattering(τ_{Ray}) and ozone(τ_{oz}) must be found as these are the three contributors to total optical depth in the UV spectrum [16]:

$$\tau_{aer} = \tau_{tot} - \tau_{Ray} - \tau_{oz} \tag{2.6}$$

The ozone optical depth was found using the ozone monitor that is part of the MICROTOPS II instrument. This is given in Dobson units. The amount of ozone in the atmosphere should remain constant through the course of the morning, so the readings were averaged. Because ozone optical depth results from absorption rather than scattering it occurs at certain wavelengths. The optical depth is expressed as:

$$\tau_{oz} = absolute\_cross\_section \times ozone \tag{2.7}$$

The absolute cross section is the amount of absorption presented by the ozone molecules. Tabulated cross sections for certain wavelengths and temperature profiles

are available [33]. The best temperature for stratospheric ozone is considered to be 226K [16]. This method requires that the ozone be expressed in molecules rather than Dobson units. 1 Dobson Unit= 2.69×10^{16} molecules cm^{-2} [14].

Rayleigh scattering is caused by the scattering of light by molecules in the atmosphere. This is distinct from scattering from aerosols in the atmosphere, which is known as Mie scattering. To calculate the Rayleigh scattering for a given atmosphere, pressure and temperature, both equations and tables can be consulted [39]. However, due to the discrepancy between the figures arrived at using calculations by Batchelor [16] and those in Penndorf's tables [39], it was decided to use the 6S model for calculating Rayleigh scattering, as it produces this as part of its output.

For this to work, 6S was given the characteristics of the filters used to collect the data. The shape of the filter curve was assumed to be Gaussian with the specifications given (2.4nm full-width at half-maximum, with a peak at 320±0.3nm and 10nm full-width at half-maximum with a peak at 1020±1.5nm). The standard deviation for such a curve can be calculated using the following equation where γ is the full-width at half-maximum value:

$$\sigma = \frac{1}{2}\sqrt{\frac{-(\frac{1}{2}\gamma)^2}{ln(\frac{1}{2})}} \tag{2.8}$$

6S was run using similar values to that given in Section 2.2, but was told that instead of the filter being that of the Landsat7 bands, it was the filter function of the MICROTOPS II 320nm and 1020nm filters given in 2.5nm intervals. From this, the optical depth due to Rayleigh scattering was obtained from the output.

2.3.2 Setting up the Langley Plot

Readings were to be taken over the course of a fine morning, when the effect of cloud is negligible. A site was chosen where the view of the sun was not obscured.

It was noted by inspecting the tables of Kasten and Young [25] that at low sun elevations, the rate of change of the amount of atmosphere the light passes through was much higher than at higher sun elevations (i.e. closer to midday). Thus to create a Langley Plot with an even distribution of readings, more readings must be taken in the early morning than closer to midday. With this in mind, a plot was created of the sun elevation for a particular day using the methods given in Meeus [30] and Michalsky [32]. An example of this can be seen in Figure 2.4.

Using this graph and the tables given by Kasten and Young [25], it is possible to

Figure 2.4: Sun Elevation for Massey University for the morning of 30 April 2002.

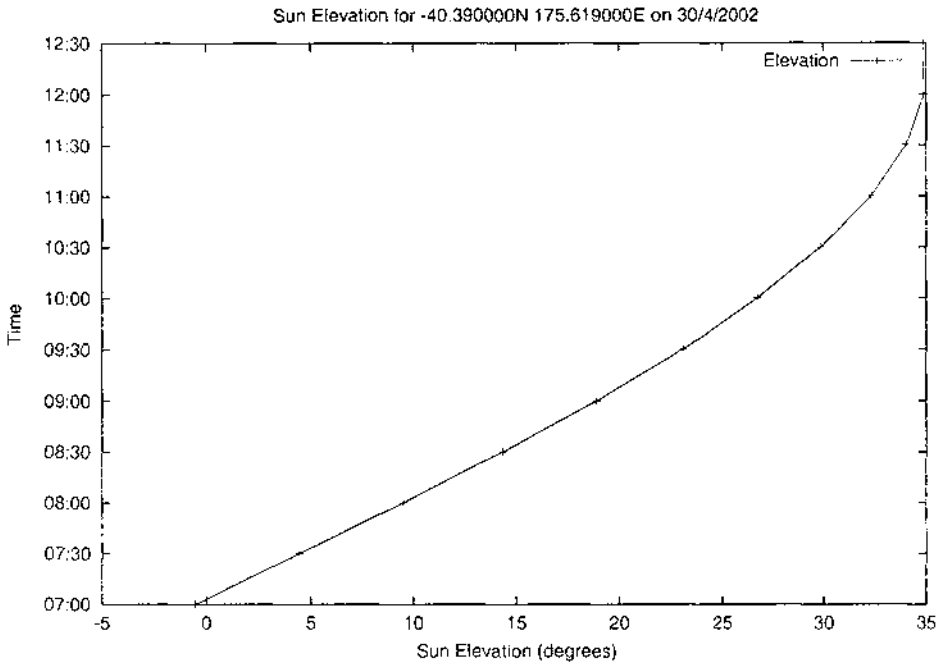

derive a set of times to take readings where the resulting plots on the graph will be at regular intervals of atmosphere. This is done for 30 April 2002 for one atmosphere spacing using Figure 2.4 as described below:

1. The amount of atmosphere for noon is looked up. Looking at the graph, 12:00pm corresponds to 35 degrees elevation. Looking up in the tables, this is 1.74 atmospheres.

2. To get an even plot, the next value is found by finding the time for around 2.7 atmospheres. Looking up in the tables, 2.75 atmospheres corresponds to 21.2 degrees. Looking at the graph, this is about 9:10am.

3. This is continued until 5 degrees is obtained which is the lowest sun elevation used. Any lower than this there is too much obstruction by trees and buildings and the readings are not likely to be very accurate due to the amount of atmosphere the light must pass through. The other times thus obtained are: 8:40am, 8:15am, 8:00am then five readings to about 7:35am.

4. The last five readings are a little difficult to read off the graph, so for the first 30 minutes, readings were taken every 5 minutes to be certain of getting good

readings while the amount of atmosphere was changing so fast.

Three or more readings were taken at each interval. Measurements were discarded that were deemed to be errors. The way this was done was to look at the signal values at 1020nm which should change in a linear fashion through the course of the readings. Readings unusually high or low against the trend were discarded. For the remaining readings, the signal values at 320 and 1020nm were obtained and plotted as a Langley plot and the slope of the graph was then measured. This was calculated by performing a linear regression on the data and the absolute value of the slope is τ_{tot}. The error in this measurement is given as one standard deviation. The variance of the slope can be calculated using the following equation [17]:

$$Var = \frac{\Sigma(Y - \overline{Y})^2}{N \times \Sigma(X - \overline{X})^2} \tag{2.9}$$

The ozone values recorded by the unit were averaged and converted to ozone optical depth (see Equation 2.7). The error given was of the range of values thus obtained.

2.3.3 Problems with the 320nm data

It was discovered early during the taking of the readings that the results based on the 320nm were of dubious value. Often the total optical depth as calculated using the Langley Plot would be around 1.1. Once the optical depth due to Raleigh scattering (0.91) and the Ozone Optical depth (~0.2) were subtracted, a very small residual resulted. It was decided that Rayleigh scattering and ozone could not be measured accurately enough for a reliable measurement of aerosol optical depth at 320nm. On the other hand, the 1020nm aerosol optical depth is more accurate due to a much smaller value for Raleigh scattering (0.008) and no Ozone Optical Depth at this wavelength.

2.3.4 Comparison with MODIS

To compare the MICROTOPS aerosol readings directly with MODIS, data need to be downloaded for the days that readings were taken in 2002. MODIS had data for each of the mornings that MICROTOPS readings were taken. These data were downloaded and processed to the same standard as the other MODIS data. This meant it was rectified and all cloud affected pixels removed. The remaining valid pixels that corresponded to the location of Palmerston North were found and the values then compared with those of the MICROTOPS.

2.3.5 MICROTOPS Ozone and Water Vapour data

As mentioned in Section 2.3, the unit records values for ozone and water vapour in addition to the raw values at the different wavelengths. These values are calculated each time a reading is taken.

There are three ozone readings made by the MICROTOPS. Two are based on ratios between different frequencies (305nm/312nm and 312nm/320nm) and the third is an experimental combination between the two that is supposed to compensate for the amount of air mass the reading was taken through (up to an air mass of 3.8 [34]). However, it was found that all three readings were affected to some extent as the amount of air mass changed. The compensation algorithm was not particularly accurate as not only did the values vary considerably, some of the values were much higher than those seen in the uncorrected ratio readings. This led to the conclusion that the ozone measurements were affected by the amount of air mass and that using the reading with the lowest air mass (midday) would be best. As mention in Section 2.3.2, three readings were taken at that time, so readings could easily discarded that were obviously different from the other two. The result used for ozone was the mid point value for both the uncorrected ratios from the last reading. The error between this and the actual values was around the stated error of 2.5% for the instrument [34].

There is only one value made available for the water vapour at each reading, and it seems reasonably stable. The average of these readings for the morning was taken. As described in the results, (Section 3.3) the water vapour readings seemed very low, and as such did not match the MODIS data. As an alternative, some water vapour data was obtained from NIWA as outlined in Section 2.3.6.

2.3.6 NIWA Ozone and Water Vapour

Due to the limited amount of readings from the MICROTOPS, one year's worth of daily readings of ozone taken at Lauder by NIWA (National Institute of Water and Atmospheric Research) was used. The data were recorded using a Dobson spectrophotometer and contains the total column ozone in Dobson Units for the entire year of the study. This is the same as the MODIS instrument measures so a direct comparison is possible between the two. The value for the MODIS data were taken from the pixel that contains the Lauder recording site (2248100E, 5567680N) from the monthly composites. As mentioned in Section 2.1, the geometric correction of the MODIS data can be up to 3km out. It was decided to ignore this error on the assumption there would be

little regional variation.

For the water vapour, it was possible to obtain daily readings from NIWA to address the limited amount of MICROTOPS readings. NIWA's climate database contains all of their readings for weather stations all around the country. A subset of these stations have balloon flights a midnight and midday every day. The data returned by these balloons was of use because it contains readings of dew point temperature and pressure as the balloon ascends through the atmosphere. The height for which dew point temperatures are available is generally up to 7000m. It is assumed there is very little water above this altitude. To obtain the precipitable water in the air that the balloon ascended through, the specific humidity must first be calculated. First the saturated vapour pressure e_s must be found at each reading using the equation given by Richards [40] as,

$$e_s = 1013.25 \exp(13.3185t_r - 1.9760t_r^2 - 0.6445t_r^3 - 0.1299t_r^4) \tag{2.10}$$

where $t_r = 1 - 373.15/T$ and T is the dew point temperature in Kelvin. From this the mass mixing ratio can be found, which is defined as the mass of water per unit mass of dry air. To find the mass mixing ratio (m) in gm/kg, the following equation can be used [42]:

$$m = \frac{0.622e \times 10^3}{p - e} \tag{2.11}$$

where p is the atmospheric pressure and e is the vapour pressure.

Then the specific humidity is found. This is the mass of water vapour per unit mass of moist air. To find the specific humidity (q) in gm/kg, use the following equation [42]:

$$q = \frac{m}{1 + m/10^3} \tag{2.12}$$

Once the specific humidity at each pressure level that the dew point temperature is given has been found, integration can be performed to find the precipitable water in cm using the following relationship [42]:

$$PW = \frac{10}{\rho g} \int_{p_s}^{0} q dp \tag{2.13}$$

Where p is the pressure in hPa, g is acceleration due to gravity and p_s is the pressure

at the surface. PW is in the same units that the MODIS data come in, so a direct comparison is possible.

Readings taken from Paraparaumu by released balloons were requested as this was the closest station with balloon readings to Palmerston North. These readings are taken twice a day, at midday and midnight. The data for the same timespan as the MODIS data were downloaded (1 November 2000 - 31 October 2001). The precipitable water for each reading was calculated. However, this will include days when is was raining. As mentioned in Section 2.1.4, pixels were removed from the MODIS data that had more than 30% cloud cover. Therefore the Paraparaumu data, on average would be much wetter than the MODIS. To address this, another table was downloaded from NIWA that held the amount of rainfall on an hourly basis. Readings for the balloon flights where there was any rainfall in the hour that the balloon was released were ignored. The monthly average water vapour amounts were then calculated from this and compared against data for the area of Paraparaumu taken from the MODIS composites.

2.4 Applying an Atmospheric Correction

In this section the various ways that an atmospheric correction can be applied to a Landsat scene will be discussed.

For all the corrections described in this section, a Landsat scene from the morning of the 5 December 2000 (NZ Time) was selected. This image had been sharpened using the higher resolution panchromatic band to 15m pixels. Further, the thermal infrared band had been excluded because of its lower resolution. This scene was subset into an area around Palmerston North approximately 48 by 42 kilometres. This area was chosen because it contained many interesting targets and would be much faster to process than the whole scene.

2.4.1 Spatial Atmospheric Correction

The idea of this system was to do the most accurate atmospheric correction possible within the limits of time and processing power. Data from the MODIS sensor taken 40 minutes later was retrieved and processed as summarised in Figure 2.6.

1km pixel size was chosen as the level to do the atmospheric correction because it was the best resolution offered by the MODIS data (water vapour). The other products were re-sampled to 1km as well. Values that were set as invalid by the MODIS processing were set to the average value of the rest of the data. The DEM of New Zealand

Figure 2.5: Comparison of different Atmospheric Correction Techniques.

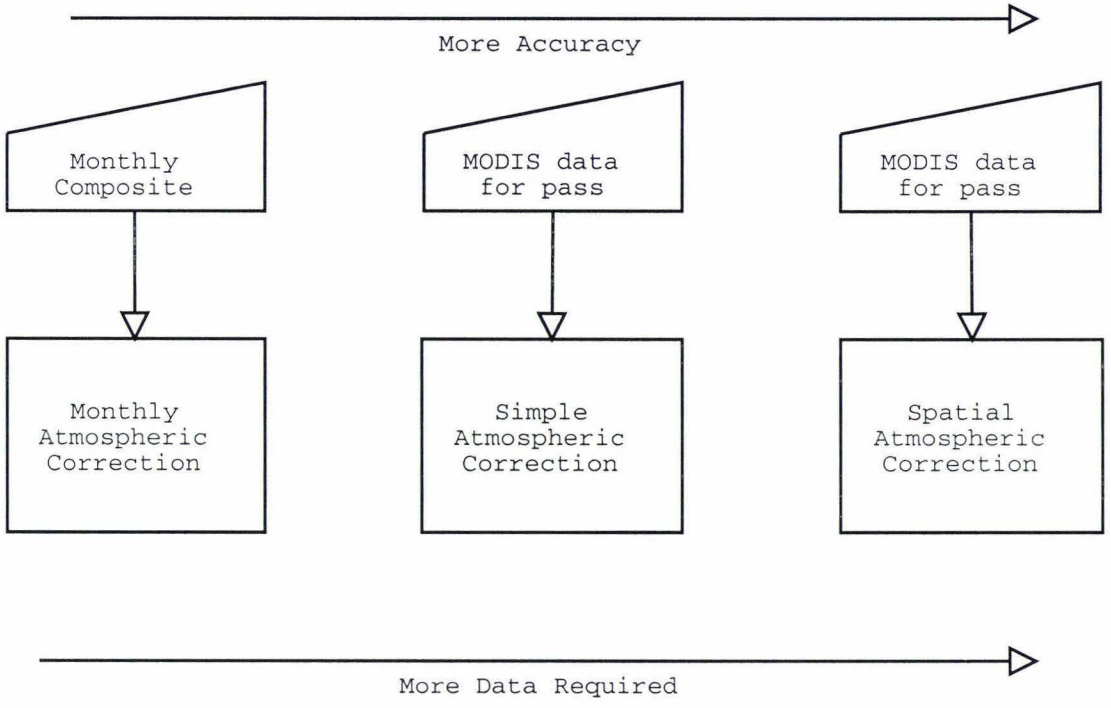

Figure 2.6: Spatial Atmospheric Correction Process.

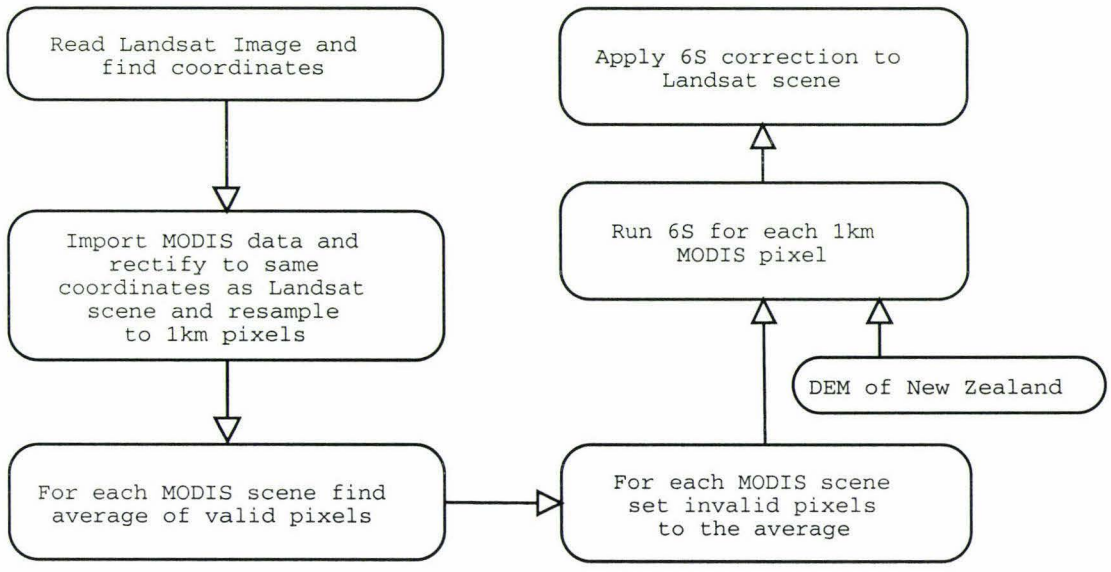

that was available was also 1km resolution making it easy for extracting the needed information for 6S.

6S produces three variables that can be used for converting measured radiance into atmospherically corrected reflectance. These are: xa, xb and xc. Each run of the 6S model gives a set of these. 6S was run for each 1km MODIS pixel. It was given the inputs of the aerosol, water vapour and ozone values from MODIS and the elevation from the DEM. Thus when this process is complete there are xa, xb and xc values for each 1km square over the image for each band.

When this correction is applied to the actual Landsat scene the actual measured radiance is found by applying the gain and offset for the scene to the pixel values. The atmospherically corrected reflectance is found using Equations 2.14, 2.15 (from [46]).

$$y = xa \times measured\_radiance - xb \tag{2.14}$$

$$corrected\_reflectance = \frac{y}{1 + xc \times y} \tag{2.15}$$

This is done for each Landsat pixel. Obviously, all the pixels in a 1km square will have the same values for xa, xb and xc, but different radiance values from the uncorrected Landsat scene. The resulting image then contains all the atmospherically corrected reflectance values for the Landsat scene.

2.4.2 Simple Atmospheric Correction

This correction is a simpler system that is not so intensive on computing power and time. The idea was to see if similar accuracy could be obtained with less processing. Only one set of atmospheric parameters was used as input. This was the average values for aerosol, water vapour and ozone for the MODIS data taken 40 minutes after the Landsat scene was recorded. Pixels that were invalid because they were set to -9999 by the MODIS processing were excluded.

To ensure that the experiment was similar to the spatial correction, it was decided to include the altitude in the calculations. A set of parameters (xa, xb and xc) was calculated by 6S for every 100m between sea level and the highest point in the scene. The intermediate heights between these values were interpolated. When applying the correction using Equations 2.14 and 2.15, the height of the pixel was found from a 15m DEM of the area and the appropriate set of parameters used. Therefore although the atmospheric data input into this method is a coarse average, the resolution of the

altitudes used to apply the correction is much higher than that in the Spatial Correction. This is something that could be improved in the Spatial Correction, but then 6S would have to be run for every 15m rather that every 1km - a large increase in processing time.

2.4.3 Atmospheric Correction using Monthly Composites

This process was intended as an approach that could be taken if the data from the MODIS sensor that is coincident with the Landsat scene is not easily available. The idea is that the monthly composite for the month of the Landsat image would be used. This may be from a different year, as it has been assumed that the atmosphere will follow similar trends each year. This assumption is untested by this project as only one year's worth of data were downloaded.

The area that the Landsat scene covered was found and the average values of the corresponding areas in the composites found. Thus average value was found from the monthly composites for aerosol, water vapour and ozone over the area of the scene. This is a weighted average of the values as the composites contain a count of values, as described in Section 2.1.5. These values where processed by 6S for every 100m between sea level and the highest point in the scene as done for the Simple Correction. These values were then applied using the 15m DEM as described in Section 2.4.2. Thus the processing is very similar to the Simple Correction, but it makes use of the monthly composite data.

2.4.4 Lauder Data Based Atmospheric Correction

The original atmospheric correction method pioneered by Shepherd and Dymond [43] at Landcare Research used data collected at Lauder, Central Otago. Mean monthly atmospheric profiles were obtained that included pressure, temperature, water vapour and ozone. Lauder is at 370m above sea level so the atmospheric data were interpolated down to sea level. The average atmospheric profile for the month of the image to be corrected is input directly into 6S.

For aerosols, sun photometer data from Forgan and Liley [21] was used. The monthly values for aerosol optical depth at 550nm (required for 6S) were interpolated from the actual wavelengths of the sun photometer (368nm, 500nm, 675nm, 778nm, 862nm). The aerosol optical depth at 550nm was corrected to sea level assuming a scale height of particulates of 1.2km [18]. Due to the location of the Lauder station,

these aerosol optical depth values describe a clear, inland atmosphere and may not be accurate for coastal areas where sea salt aerosols will occur.

The correction coefficients were calculated at 200m altitude intervals and the interpolation to actual pixel altitude was performed in the same way as the Simple Atmospheric Correction (see Section 2.4.2).

2.5 Atmospheric Correction using ATCOR

MODTRAN is an alternative model for looking at the effect of the atmosphere on satellite imagery, similar to 6S which is discussed in Section 2.2. There is a package called ATCOR which can be used in conjunction with the ERDAS Imagine software to do atmospheric correction which uses the MODTRAN model. The technical details are described by Richter [41]. There are two parts to the ATCOR model; ATCOR2 which does atmospheric correction of flat terrain, and ATCOR3 which does topographic and atmospheric correction. For the purposes of comparison with the methods developed, the simpler ATCOR2 module has been used.

2.5.1 How it works

Instead of using the actual atmospheric conditions at the time, as the other methods have attempted to, ATCOR uses a database of atmospheric correction functions. The parameters to these functions are:

- The standard atmosphere to use. In addition to the standard atmospheres that 6S has (tropical, mid latitude summer, mid latitude winter, subarctic summer, subarctic winter and US standard 62), it also supports arid, humid and autumn atmospheres.

- The type of aerosol. Supported types are rural, urban, desert, maritime and oceanic.

- Aerosol optical depth as a visibility estimate.

- Average ground elevation.

- Solar Zenith angle.

Therefore, in short this system is easier to set up as the MODIS data are not required. The accuracy of the standard models in the database and of the visibility estimation is relied on. In fact, there is no way to input the actual values for aerosol, water vapour and ozone into ATCOR.

However, there are a number of things that ATCOR can do that the other systems developed in this project cannot. These include:

- Haze removal.
- Allowing the standard atmosphere to be calibrated by matching the spectra of known targets.
- The ability to deal with spatially varying conditions by identifying dark targets.
- Support of many types of sensors.
- Having a graphical front end.
- Atmospherically correct the thermal band.

2.5.2 An atmospheric correction

To compare the performance of ATCOR with the methods described in Section 2.4, the same test Landsat scene (5 December) was processed with it. There are a number of of steps required. Set out below is a list of the information required with the corresponding information for the other systems:

1. The input image. The ATCOR module requires the original image as imported into Imagine format from the raw data. Unfortunately this means that the input data are not pan sharpened, rectified or stripped of the thermal bands. Therefore the data processed are slightly different from the other methods.
2. The date of acquisition of the imagery. For calculating the distance to the sun. The same as the other methods.
3. Order of the bands - set to default as the data has been input as requested. The other methods do not have an option to do this and expect the order of the bands to be fixed.

4. Output scale factors. Required for the output image to contain 8 bit integers but hold the reflectance values which are floating point numbers. The other processing steps output 16 bit integers with the scale factor of 10000. This defaults to a scale factor of 4, and this is left unchanged, meaning that the values must be divided by 4 to get the reflectance.

5. The name of the sensor, in this case "Landsat-7 ETM+". The other methods only accept Landsat 7 imagery.

6. The gain of the data. This is in case any stretch has been applied. This has not been done, so is is left at 1.0.

7. The sensor calibration file. ATCOR has the ability to apply a calibration of the sensor (the gain and offset). The gain and offset for the image is supplied from the ancillary data in the format requested. These values are also input into the 6S based processing methods, but ATCOR uses different units internally ($mWcm^{-2}sr^{-1}\mu m^{-1}$ instead of Landsat which uses $Wm^{-2}sr^{-1}\mu m^{-1}$). Therefore to create a calibration file for ATCOR, it is necessary to divide the values given for Landsat by 10.

8. Solar Zenith Angle. The same value is used as calculated for the other methods (34.4 degrees).

9. Aerosol type. Maritime used for consistency with the 6S based methods.

10. Model for thermal region for correcting the thermal band. The "mid-latitude summer" option was selected. The other methods do not correct the thermal band, and this band is not used for further analysis.

11. Visibility in km. The visibility calculated from the aerosol optical depth using Equation 3.1 is input. The aerosol optical depth used for this was the median of the MODIS aerosol product taken 40 minutes after Landsat scene (0.0905312). This gave a visibility of 72.1km.

12. The average height of the scene. The other methods use a DEM to apply the right correction for the height to each pixel. In this case it is 123m.

These differences are summarised in Table 2.1.

The accuracy of these inputs was checked by using the supplied SPECTRA module to match different predefined spectra with what would be found for the atmospheric

Table 2.1: Data required in ATCOR 2 and 6S based methods.

Item	ATCOR 2	6S based methods
Input Data	Must be raw image	May be pan sharpened
Date of acquisition	Date of image	Date of image
Order of bands	May be changed	Must be in fixed order
Output scale factors	Can be changed to suit data	Fixed at 1000
Sensor	Supports a range of sensors	Must be Landsat 7
Gain	Can compensate for stretch	Fixed at 0
Calibration of sensor	Different Units to Landsat	Same units as Landsat
Solar Zenith	Set to that of imagery	Set to that of imagery
Aerosol Type	Can be set, Maritime used	Can be set, Maritime used
Model for Thermal Band	Can be set	Not supported
Aerosol Optical Depth	Visibility input	Aerosol Optical Depth input
Target Height	Set as scene average	Uses DEM

correction for small areas on the ground. ATCOR 2 has a number of spectra recorded for comparison with Landsat 7. The ones that were relevant were tested and found to match the spectra very closely, so no fine tuning of parameters was required. A screen shot of this process is shown in Figure 2.7.

The correction was performed using the "constant atmosphere" option. ATCOR 2 has the ability to compensate for different atmospheric conditions in different parts of the scene. It uses dark targets and attempts to calculate different optical depths for different parts of the image. There isn't much variation in optical depth over the Landsat scene, and for the sake of simplicity the option was ignored.

ATCOR 2 also has a haze detection and removal algorithm. This was not as useful because there are no discernible areas of haze in the scene used; and because using it is not consistent with the other methods which that do not attempt haze removal.

2.6 Ground Cover Measurements

This section describes the steps taken to simulate the readings that the Landsat instruments would obtain if it was down at ground level. This will help determine the accuracy of the atmospheric correction as the results returned should ideally be the same.

Figure 2.7: Screen shot of ATCOR 2 Spectra Module.

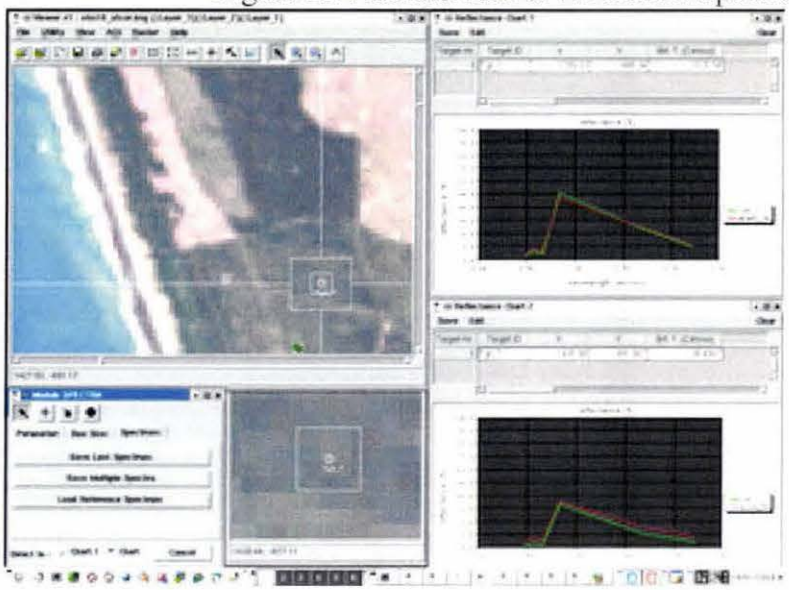

2.6.1 The Spectroradiometer Instrument

A GER 2600 Spectroradiometer supplied by Landcare Research Ltd. This is a portable instrument that records signal strengths from 312nm to 2557nm [23]. Before measuring targets, it is necessary to get a reference reading from a standard reflectance plate. The target is then measured and the ratio between the target and the reference is the reflectance. This instrument is mounted on a tripod and connected to a laptop with specialised software that communicates with the device and records all the readings taken. The instrument is supplied with calibration information for the sensor that must be loaded into the software before it is used.

The readings of the reflectance plate and the target are in radiances, and there will be a measurement of both at all the wavelengths (all 597 of them). Once the data have been downloaded off the laptop, the radiance of the target is divided by the radiance of the reflectance plate to obtain the reflectance for each wavelength. From these reflectance readings it is possible to apply the filter function of the Landsat sensor to simulate the readings that would be obtained by the Landsat sensor in each band had it been positioned at the bottom of the atmosphere. A picture of the GER 2600 instrument is shown in Figure 2.8.

Figure 2.8: The GER 2600 instrument mounted on its tripod.

2.6.2 Ground cover selection

Ideally, to check on the accuracy of the atmospheric correction, an area would be selected and measured at the same time as a Landsat pass. The corresponding scene would then be purchased and the corresponding pixel would be analysed. In practise this is not possible due to the expense of a Landsat scene ($1200) so there is a restriction of only using scenes taken in the past. This project was restricted to historical images that Landcare have in their archives.

To work around this problem it was decided to use invariant targets: those that do not change their spectral response over time. The resolution of the original Landsat data is 30m. To get enough pixels free from neighbouring target contamination a target that is at least 3x3 30m pixels is needed so the outside pixels can be discarded. This number would preferably be larger, so that the pixel values can be averaged. Surfaces which were considered included:

- Airport Runways
- Sand
- Car parks
- Rugby fields
- Artificial turf sports grounds

It was decided that most of these surfaces have variations in their reflectance over time. Airport runways can have many different shades of concrete along their length. Also gaining access to what is generally a secured area could be a problem. Sand changes its colour due to the amount of moisture it contains. Car parks can have different numbers of cars in them. The type and length of grass on a rugby field may have changed. The surface that was considered the best was the artificial turf. Luckily, not far away from Massey University there is an artificial hockey ground containing two hockey pitches. This ground is included in the subset of the Landsat scene corrected by the different methods as described in Sections 2.4 and 2.5.2. Since the image was taken, one of the pitches has been upgraded and its artificial turf replaced with a water based surface instead, probably altering its reflectance characteristics. However the other (more northern) pitch remains unchanged as a sand based surface. It was assumed that the reflectance of this surface will not have changed since the image was taken in December 2000. Spectra for the hockey pitch was recorded with the GER instrument

on a fine day when the sun angle was similar to what it was when the Landsat scene was taken and the results compared with the values in the corrected scenes for the area of the hockey pitch.

It was considered important to determine what was the behaviour of the correction over very dark areas such as lakes. Obviously, reflectance values for lakes should be very small, but not negative. Negative reflectance values are impossible and point to errors in the correction or the input atmospheric parameters. Lake Horowhenua was included in the Landsat scene subset and the results for the area of the lake for the corrected scenes analysed and compared to other reference spectra for lakes recorded by the GER instrument.

2.6.3 Applying the Landsat filter function

The GER 2600 instrument takes readings at 597 discrete wavelengths. This information is the spectral signature of the target. However, the Landsat sensor takes readings at a selection of these wavelengths and each band may include more than one of the GER 2600 wavelengths.

To simulate what the Landsat sensor would have obtained if it were put in the same position as the GER 2600, the Landsat filter function needed to be run over the data. This was done with a program already written by Dr James Shepherd at Landcare. This program suppresses the readings taken at frequencies outside that of the Landsat sensor and normalises the others under the graph of the Landsat sensor response. The result is the reflectance at each Landsat band. These values are used to compare the values obtained by the different atmospheric corrections with the values recorded by the GER instrument.

Chapter 3

Results

3.1 MODIS Results

This section presents the results of the analysis of the MODIS data as described in Section 2.1.

3.1.1 Aerosol Results

Composite Images

As an illustration of the data obtained, the pixel means for the composite images for the year of the study are reproduced in Figure 3.1.

The November image is distinctly brighter all over while the July image is mostly darker. This is consistent with the trend of the data recorded at Lauder [21]. The Southern Alps are not shown in either picture, due to cloud affected pixels being discarded. Another interesting phenomenon is the high values in coastal areas. In the November image there are very high values in Horowhenua, Manawatu and Wanganui. In December this area expands to include Banks Peninsula and Hawkes Bay.

Statistics

Figure 3.2 shows the mean levels of aerosol optical depth over the one year period of the study. Both the values for the entire area of the New Zealand Map Grid and figures for the New Zealand land area and coast are shown (refer to Section 2.1.6). It is noticeable that the land and coast averages are slightly higher. This is expected because there are more aerosols associated with dust and sea spray over the land and coast. It is noted that the highest values are in the summer and the lowest in the winter

Figure 3.1: Monthly Aerosol Composites

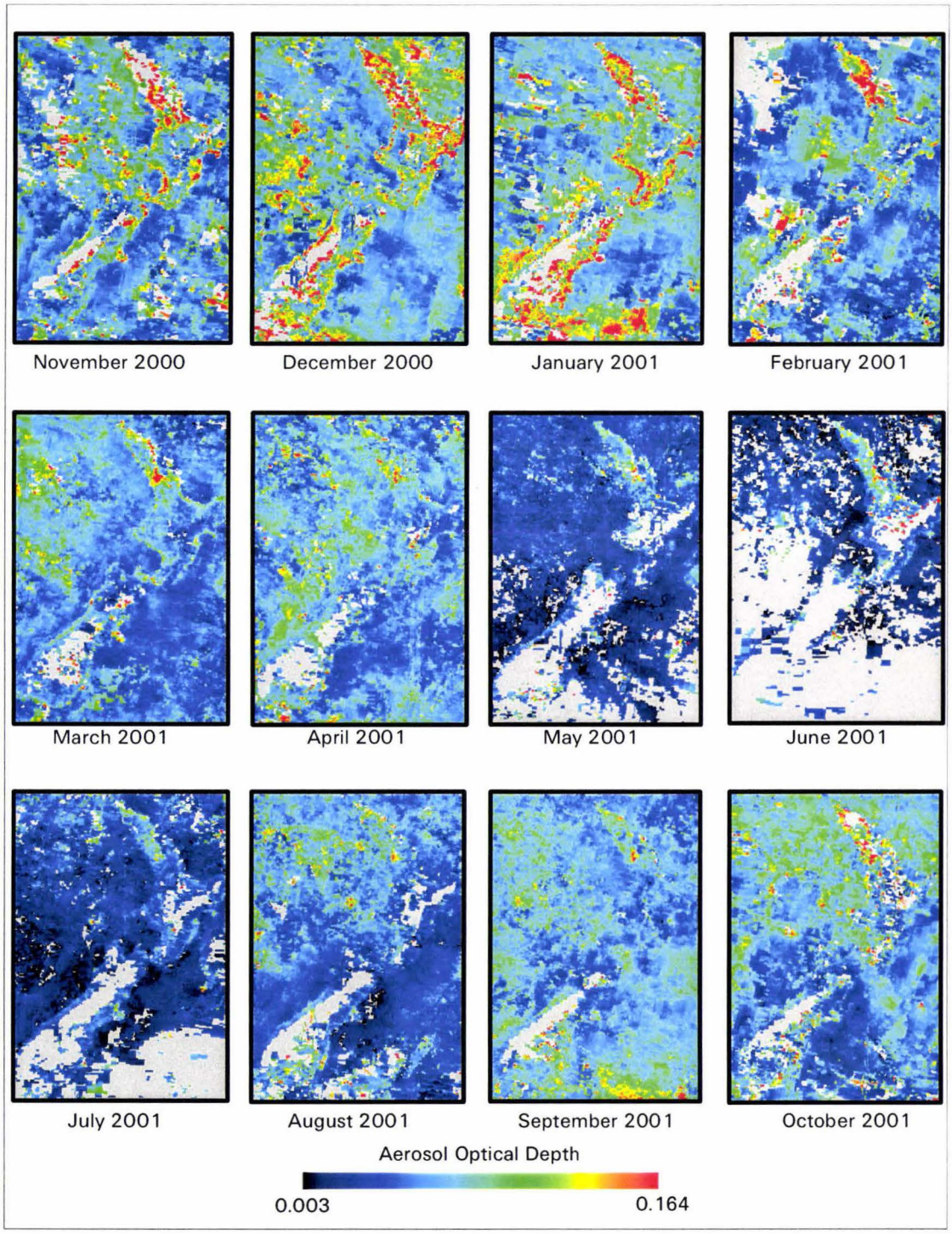

Figure 3.2: Aerosol Optical Depth for New Zealand over one year.

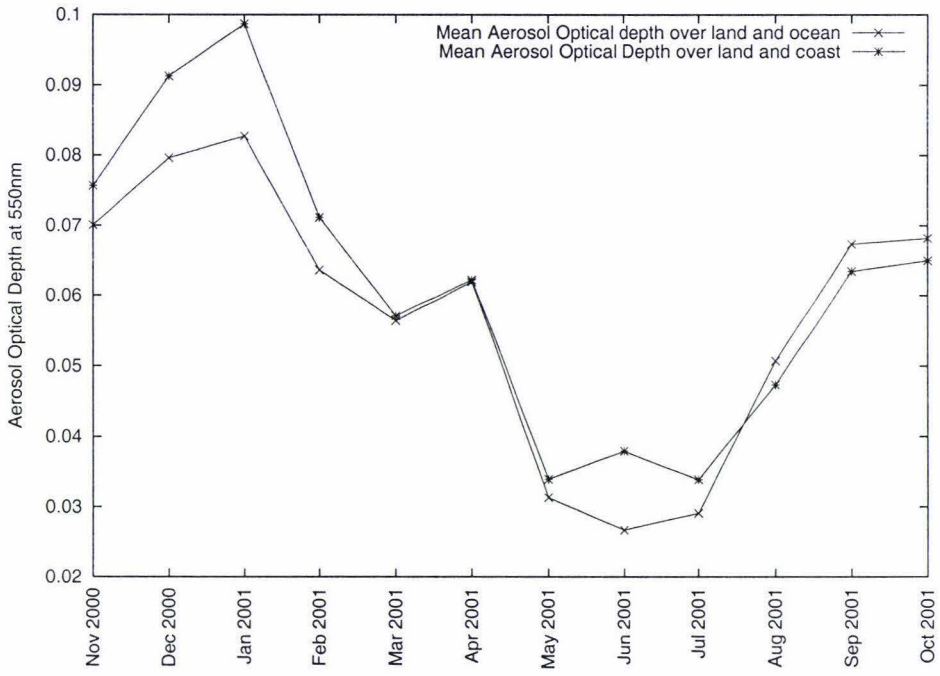

months. This makes sense because there tends to be more wind in summer and the increased water vapour in the air increases the optical depth.

Figure 3.3 shows the variation from the mean of aerosols over the year of the study. Both the spatial and temporal variability is shown. Overall the variability is less in winter than summer. The exception to this is the value for spatial variability for June 2000. This is much higher than the neighbouring months and is probably related to the fact that their was only 15 days worth of data available for that month.

Aerosol Optical depth can be converted to apparent visibility using equation 3.1 which is taken from [46].

$$v = exp(-ln(\tau/2.7628)/0.79902) \tag{3.1}$$

where ν is the apparent visibility in kilometres, and τ is the aerosol optical depth at 550nm.

Using this equation the apparent visibility can be plotted over the course of a year in figure 3.4.

Figure 3.3: Spatial and temporal variations in Aerosol Optical Depth over one year.

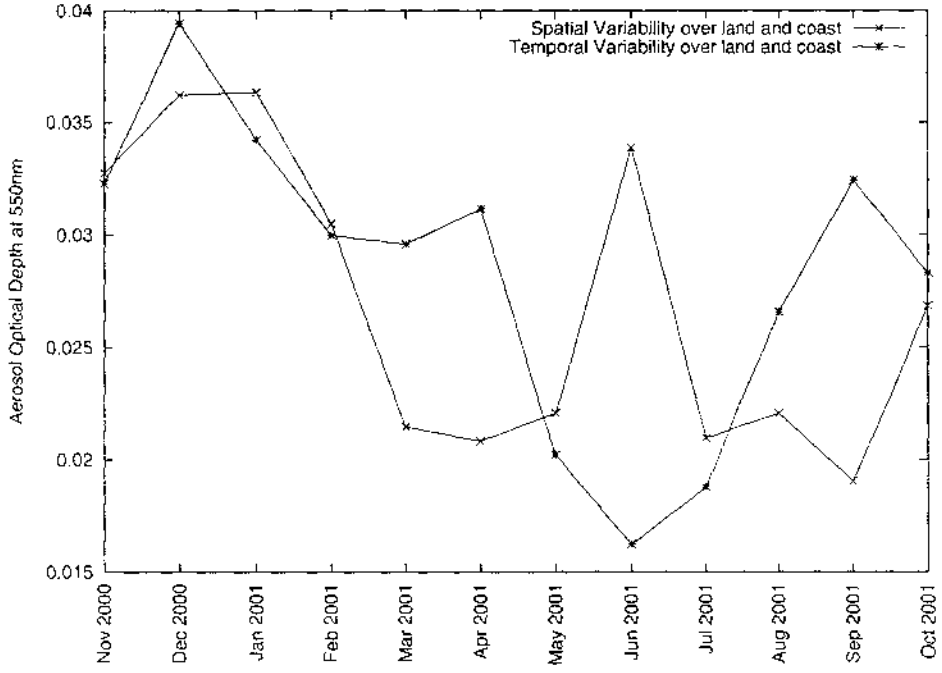

Figure 3.4: Apparent visibility over one year.

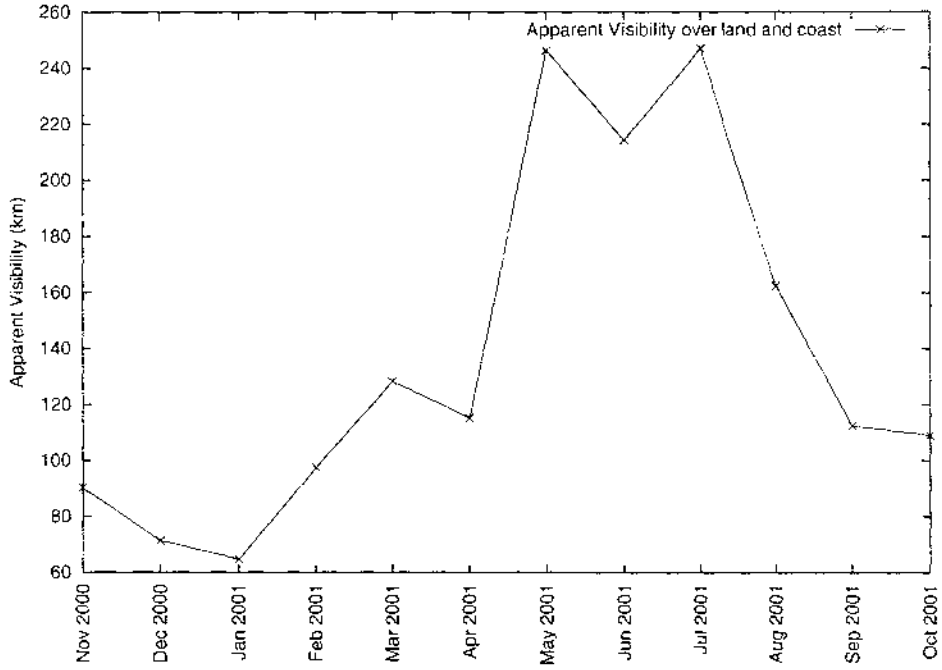

3.1.2 Water Vapour Results

Composite Images

Figure 3.5 shows the composites for water vapour. It is noted how the values of water vapour are high in summer, but drop down in winter. This is a similar trend to the aerosols.

Statistics

Figure 3.6 shows the average values of water vapour over the one year period of the study. The values peak in late summer and are lowest mid winter. This is due to the atmosphere being able to absorb more water when it is warmer. In winter the air is colder and thus cannot carry as much water vapour. The values over land and coast are slightly higher in summer than those over the whole map grid. In winter, however, the opposite is true. This could be because of the relative temperatures of water and land. In summer the land heats up more than the ocean, and in winter the sea is warmer than the land which loses heat easily.

In Figure 3.7, the spatial and temporal variations from the mean are shown. The variations in winter are less than those in summer, although this variation is more pronounced in the temporal variability.

3.1.3 Ozone Results

Composite Images

Figure 3.8 shows the ozone composites. Note how the range of values is much greater for ozone than for the other products. The trend over the year is roughly opposite to the aerosols and water vapour.

Statistics

Figure 3.9 shows the average ozone values over the year of the study. Values are lowest in late summer and peak in late winter. There is almost no variation between the values of ozone over the whole area of the New Zealand Map Grid and those taken over the land and coast. This is because ozone is not affected by land - it is present at very high altitudes (see Section 1.6) and has no interaction with the land surface, unlike aerosols and water vapour. Ozone moves over the globe on high altitude winds and in the southern hemisphere, the "ozone hole" has an effect. It is possible that the drop

Figure 3.5: Monthly Water Vapour Composites

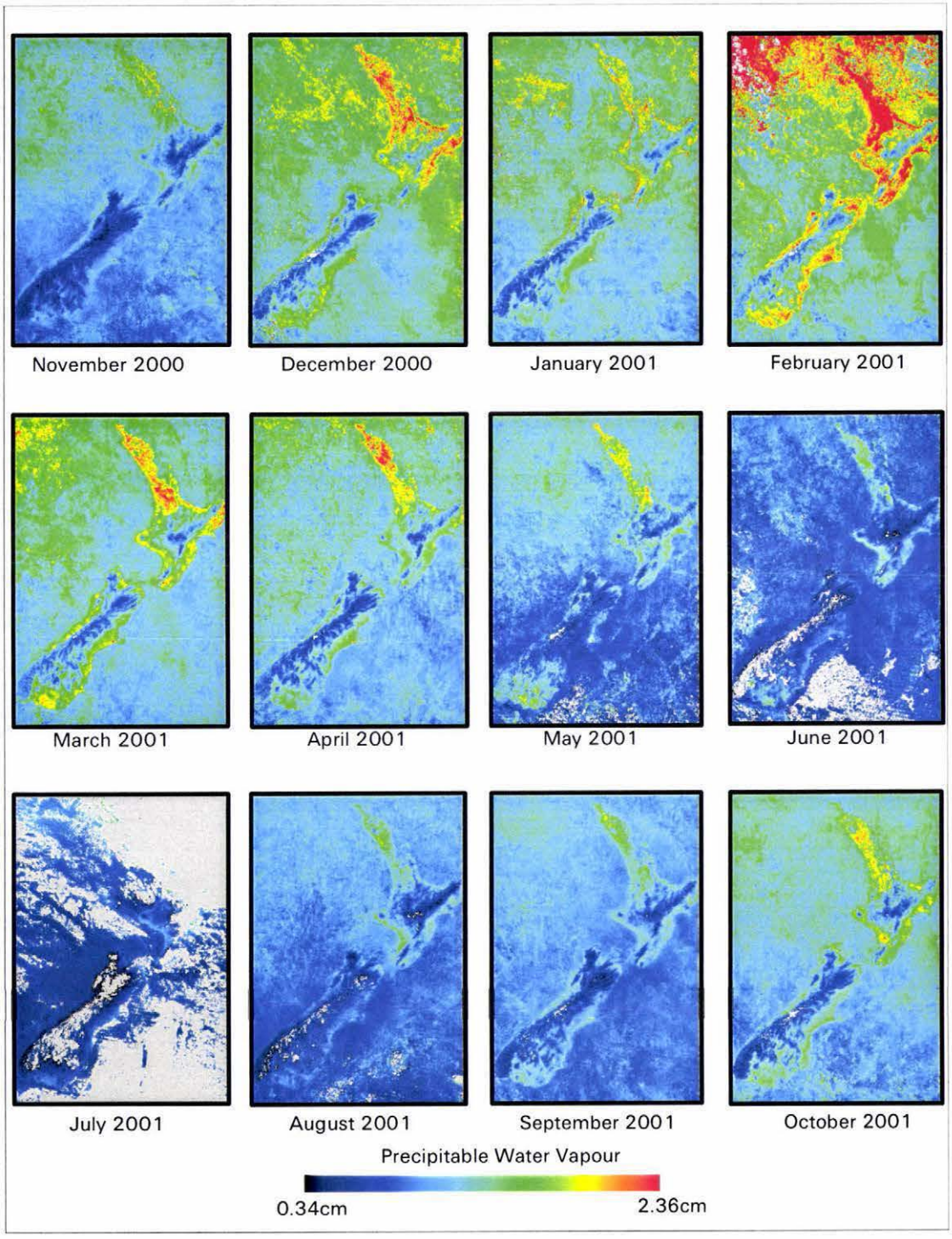

Figure 3.6: Precipitable Water Vapour for New Zealand over one year.

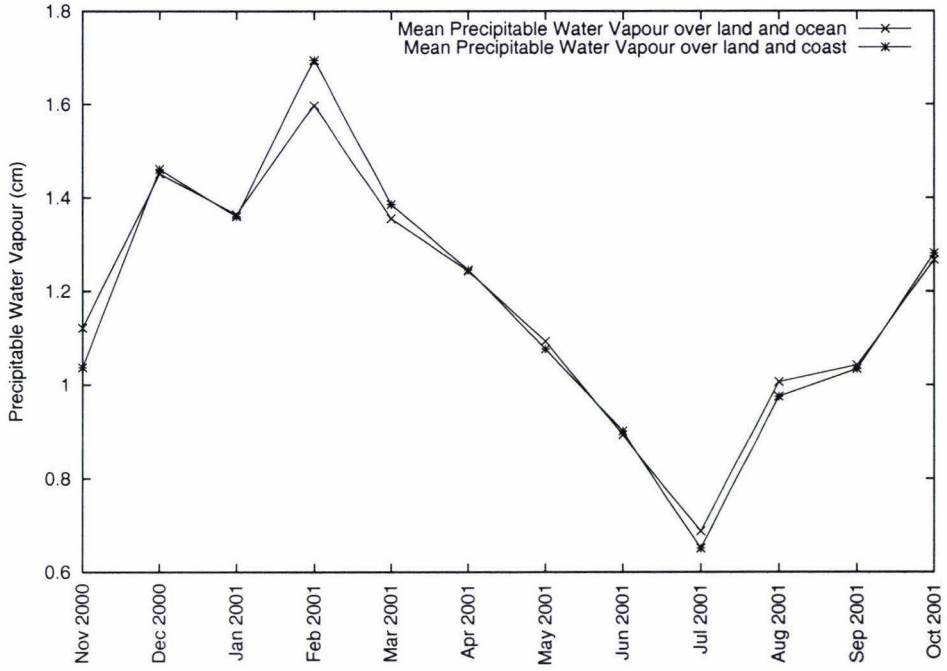

Figure 3.7: Spatial and Temporal variations of Water Vapour over one year.

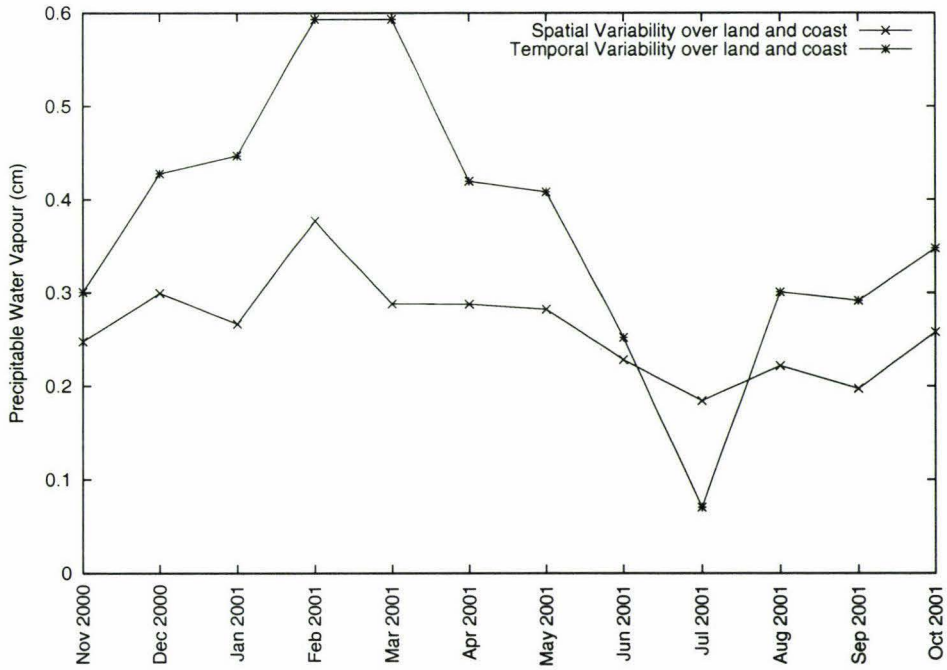

Figure 3.8: Monthly Ozone Composites

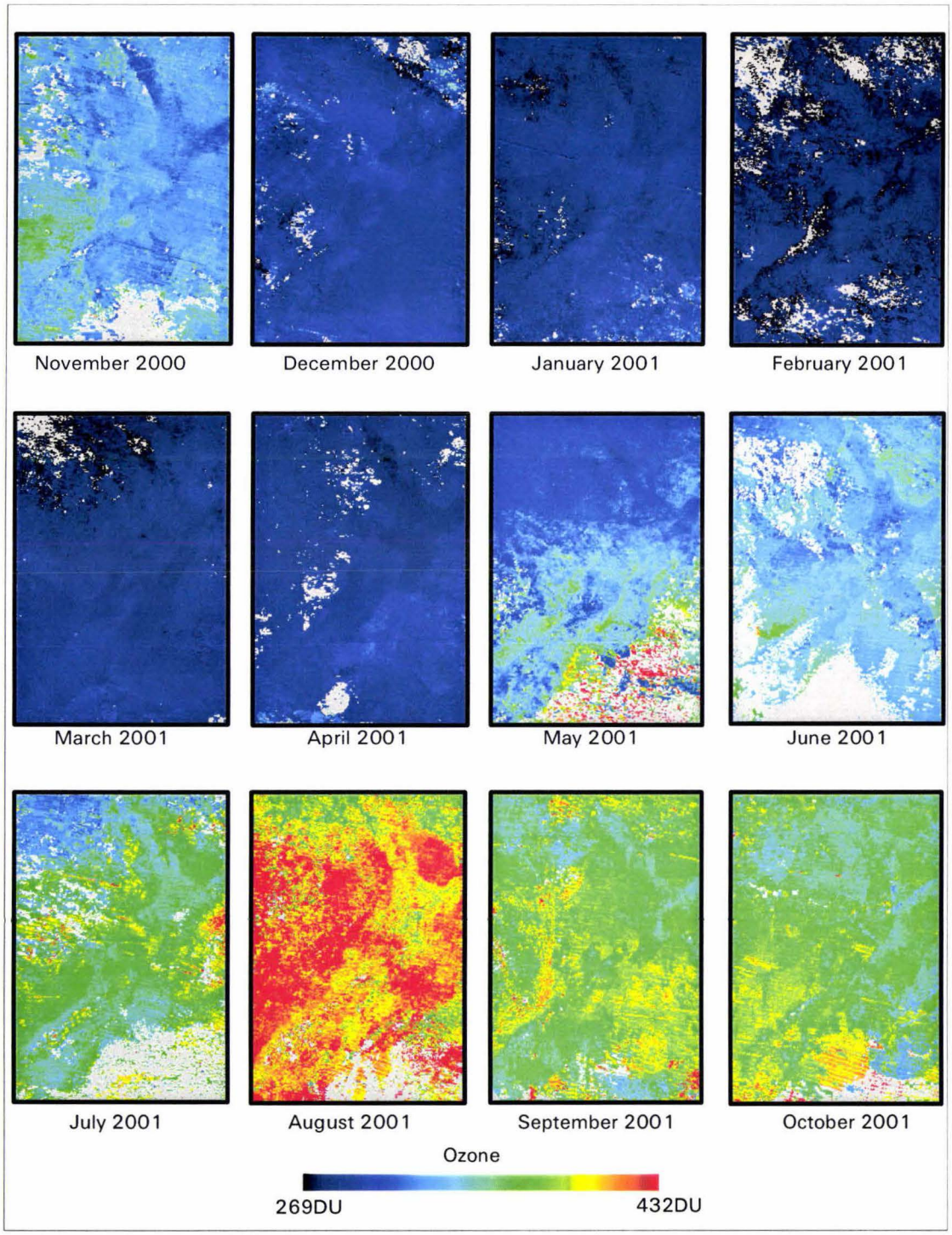

Figure 3.9: Ozone for New Zealand for one year.

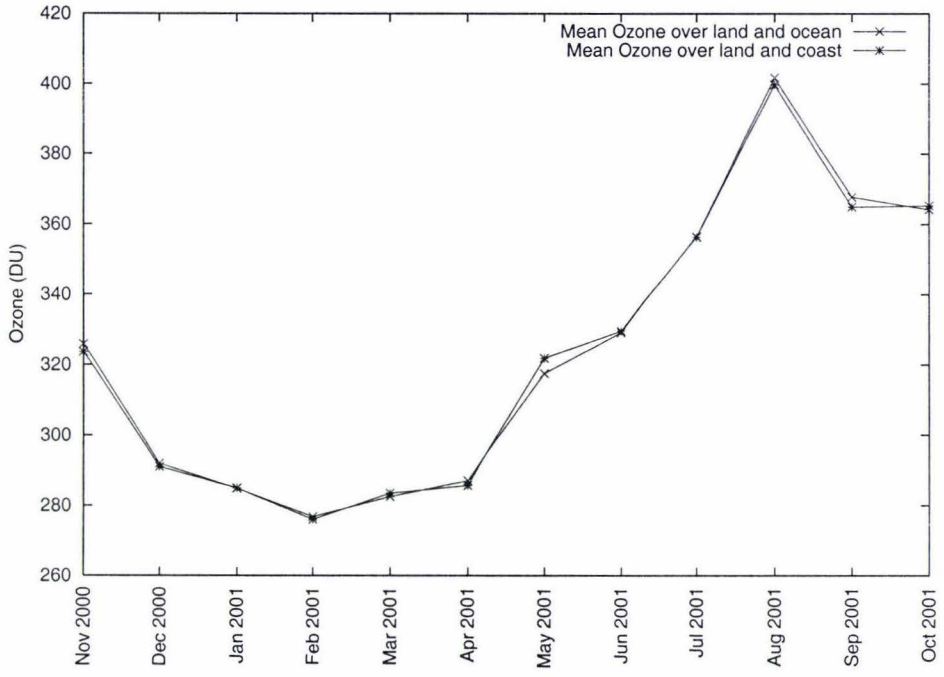

seen in late summer is related to the dissipation of the ozone hole over Antarctica at the same time, and the movement of this ozone depleted air over New Zealand.

For the spatial and temporal variations of ozone over the year, refer to Figure 3.10. Generally, the variability matches the trend of the average amount of ozone - lower late summer and higher in late winter.

3.2 Sensitivity Analysis Results

In this section the results of the 6S model with a variety of inputs are presented. The first set of inputs contained all the possible values that the three constituents could be. The second set contained the range of values seen in the New Zealand atmosphere.

The Landsat7 bands of interest are 1, 2, 3, 4, 5 and 7. This is because band 6 is thermal and hence targets are mainly emitting energy rather than reflecting at this wavelength, and therefore not of interest for this analysis. Band 8 is panchromatic, and because it is higher resolution it takes in a wide range of wavelengths to obtain the required energy, and therefore covered by the other bands. Section 1.8 has more detail on these bands. The inputs into 6S are described in more detail in Section 2.2.

Figure 3.10: Spatial and Temporal variations in Ozone over one year.

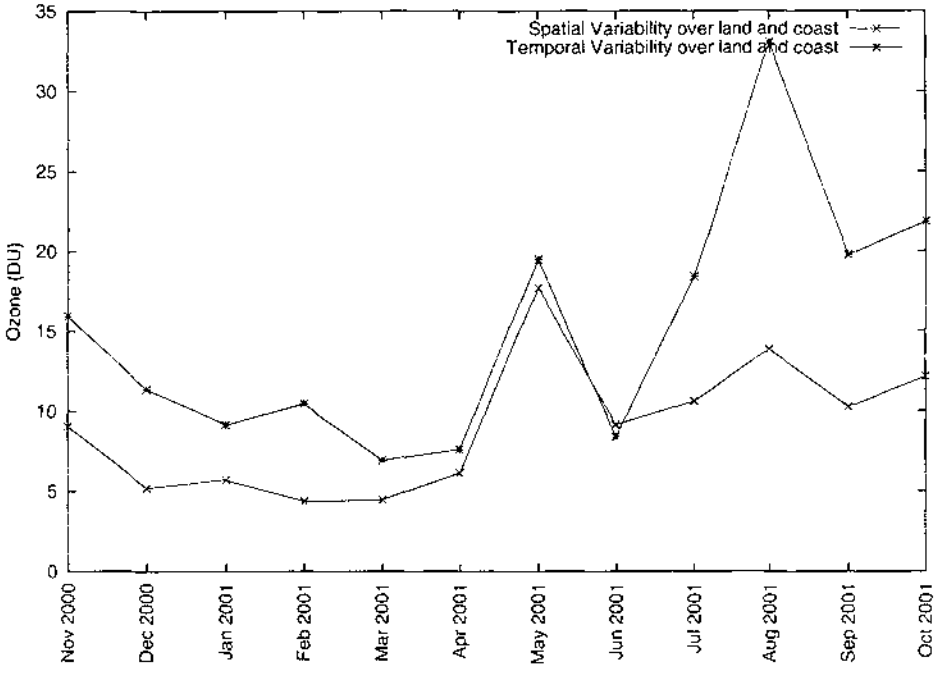

3.2.1 Result over all possible values

The object of this experiment was to examine how the different Landsat bands are affected by variations in the amount of aerosol, water vapour and ozone. To do this the input values were varied over a greater range than seen over New Zealand to make any trends in the results more pronounced.

Firstly three different targets were selected on a Landsat scene of the Wellington area for 4 December 2000. This was to study the behaviour of different cover types. These targets were:

1. A forest target. This was mature beech forest on the slopes of Mt Holdsworth in the Tararua Ranges (NZMG reference: 2714442E 6032912N).

2. A pasture target. This was a field in the Wairarapa that had a good cover of grass (NZMG reference: 2738232E 5977352N).

3. A soil target. This was another field in the Wairarapa, but was bare of vegetation (NZMG reference: 2730477E 6032717N).

Figures 3.11 and 3.12 show where these targets are on the December Landsat scene.

Figure 3.11: Selected Targets in December 2000 Landsat Scene (Red=Band 4, Green=Band 5, Blue=Band 3).

and what they look like when zoomed in. The image is 15m resolution. The actual radiances for these targets are summarised in Table 3.1.

Next the actual values from the corresponding MODIS data for aerosols, water vapour and ozone were obtained. The altitude of the sites was also obtained from a digital elevation model of New Zealand. These values are summarised in Table 3.2. It is noticeable how much drier the forest target atmosphere is. This is due to the altitude: most of the water vapour in the atmosphere would be below 1135m. Figure 3.13 shows this relationship with the NIWA Paraparaumu balloon reading which is closest in time to the Landsat scene (See Section 2.3.6). This shows that most of the water in the atmosphere is concentrated close to the ground. In fact, the NIWA data put the amount of precipitable water above 1135m at 0.269cm, which is close to the amount that MODIS gives; the discrepancy is small and is likely to be a result of errors and the fact that the readings are taken for different parts of the country.

6S was run with these values to obtain the value for atmospherically corrected reflectance for each target as described in Section 2.2. These numbers appear in Table

Figure 3.12: Close up of Selected Targets in December 2000 Landsat Scene.

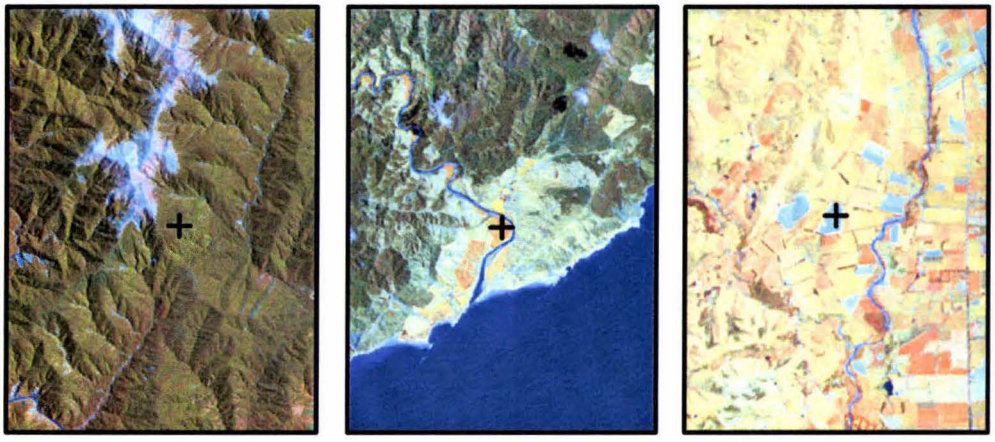

Table 3.1: Radiances for Targets in Wellington area. Atmospherically corrected Reflectance in brackets.

	Forest Target	Pasture Target	Soil Target
Band 1	38.79(0.006)	47.32(0.018)	73.70(0.092)
Band 2	27.82(0.021)	39.75(0.045)	75.56(0.14)
Band 3	15.43(0.018)	16.05(0.015)	73.64(0.18)
Band 4	76.00(0.26)	157.10(0.57)	76.97(0.27)
Band 5	6.16(0.10)	10.06(0.17)	19.11(0.31)
Band 7	0.74(0.036)	1.22(0.059)	5.07(0.24)

Note: Radiances expressed in units of $Wm^{-2}sr^{-1}\mu m^{-1}$.

Table 3.2: MODIS parameters for Targets in Wellington area.

	Forest Target	Pasture Target	Soil Target
Aerosol Optical Depth	0.065	0.113	0.082
Water Vapour	0.318	1.173	0.665
Ozone	277.8	291.6	304.6
Altitude	1135m	19m	157m

Figure 3.13: Specific Humidity vs Altitude for Paraparaumu.

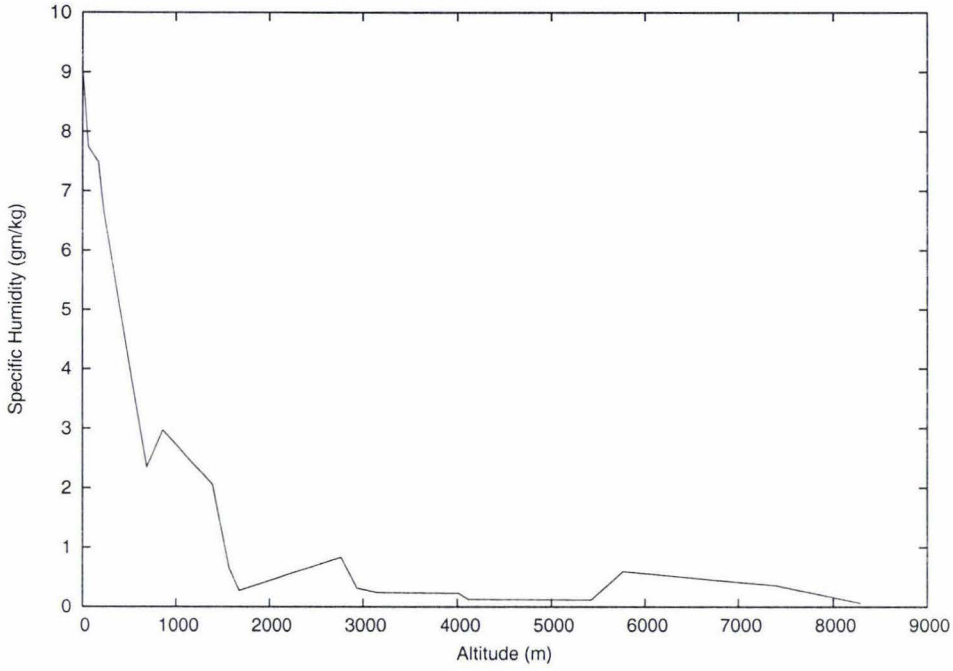

Table 3.3: Figures used for determining overall 6S model behaviour.

	Aerosol(Optical Depth)	Water Vapour(cm)	Ozone(Dobson Units)
Minimum	0	0	0
Maximum	1	4	500

3.1 in brackets. The model was then run for a range of values for aerosols, water vapour and ozone far greater than would would be seen in the New Zealand atmosphere. This was to estimate how the changes in the values affect the different bands. The altitude was kept constant. The values used are summarised in Table 3.3.

The results were then plotted as the percent variation from the actual values for reflectance shown in Table 3.1.

Aerosols

Bands 1, 2 and 3 (the visible) are affected the most by the changed amounts of aerosols over the targets (Figures 3.14, 3.15 and 3.16). Over all the targets, the visible bands show the most variation when the aerosols are increased in the atmosphere. However, the amount they vary from the actual values is different over the different targets. The forest target shows the most variation - up to 900% when the aerosol optical depth is set to 1. The pasture target has a smaller variation - about 550%, and the soil target

Figure 3.14: Variation in Forest Target due to Aerosol.

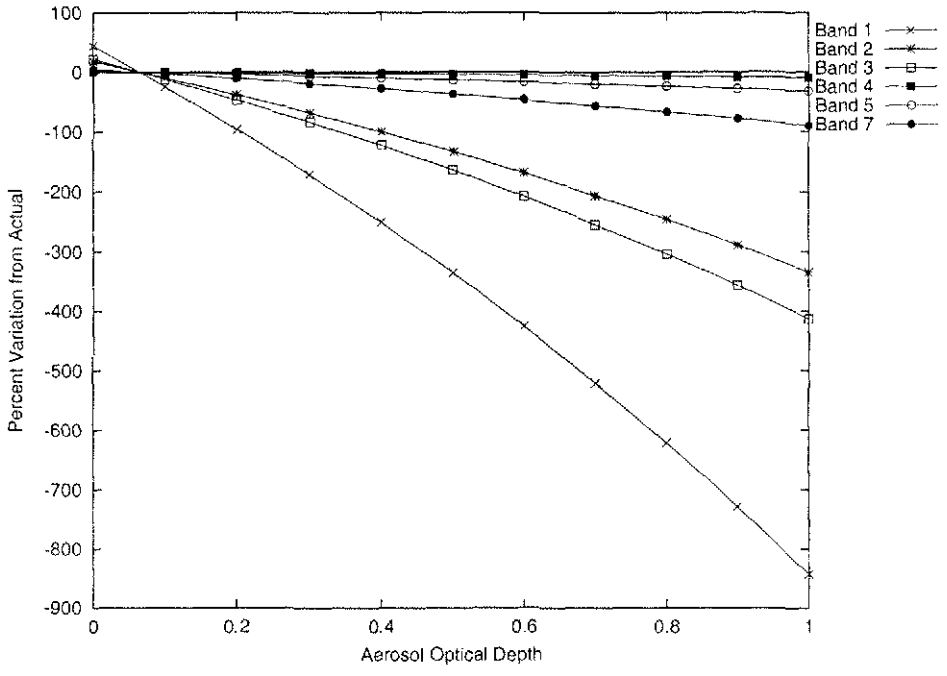

has the smallest variation - 100%. This is related to that fact that the forest target is the darkest, the soil the lightest target, and the pasture in between. Darker targets have a higher percentage variation because the atmospheric effects account for a larger proportion of the reflectance. It is interesting to note that the order in which the bands are affected in magnitude is not the same for all the targets. For the forest and pasture the targets, Band 1 (blue) is affected the most followed by Band 3 (red) and Band 2 (green). However, for the soil target Band 2 has more change than Band 3.

The reason that the graph slopes in the direction it does - the percentage reflectance decreases as the concentration of aerosols increases - is because of the scattering effect of aerosols. As the aerosols increase in the atmosphere, so does the amount of light hitting the sensor that has been scattered from all directions including energy that has come from the sun and been scattered back to the sensor without hitting the ground. The model counteracts this by reducing the apparent reflectance of the surface as the concentration of aerosols increases.

Band 7 (far infrared) is also affected by the changing aerosols for forest and pasture, but not as much as the first three bands. The other bands appear not to be affected much at all.

Figure 3.15: Variation in Pasture Target due to Aerosol.

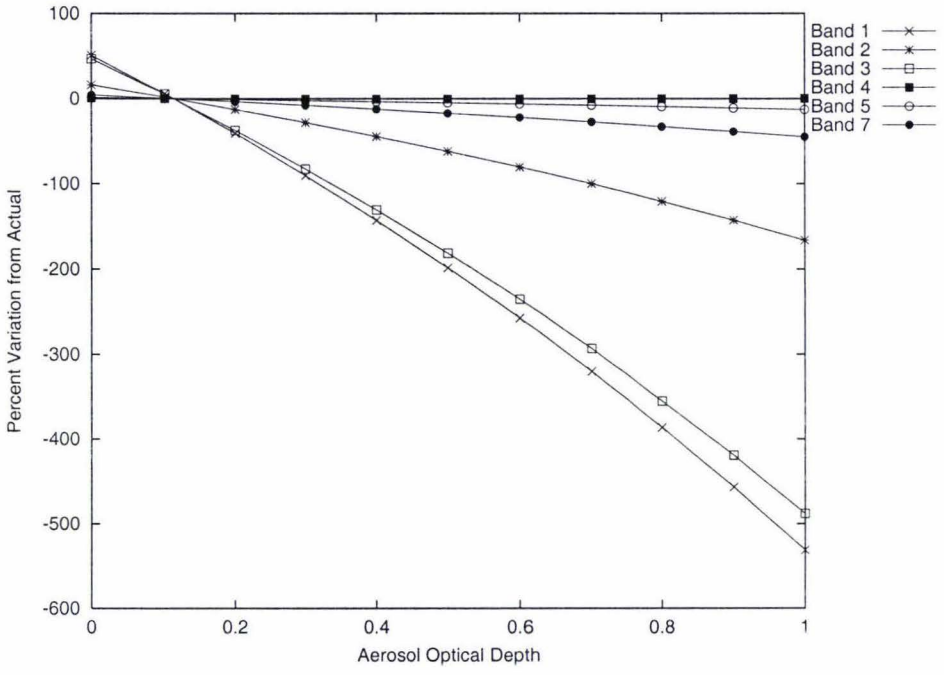

Figure 3.16: Variation in Soil Target due to Aerosol.

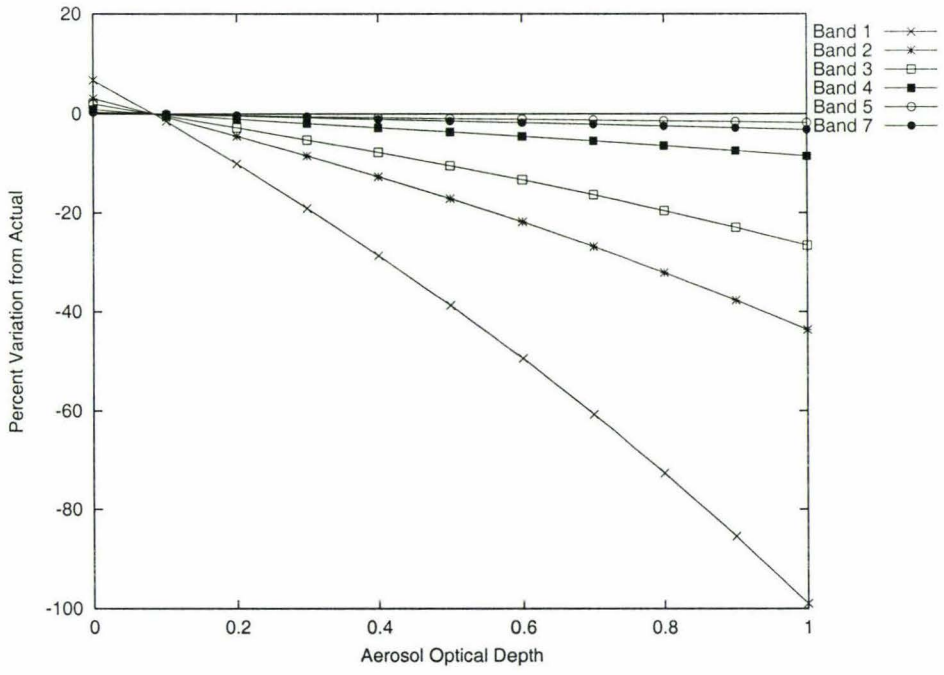

Water Vapour

When the amount of water vapour is increased from 0 to 4cm, the amount of variation this causes is not as great as with the aerosols (Figures 3.17, 3.18 and 3.19). All the targets are similar, with 6% being around the maximum amount that water vapour causes the reflectance to vary from actual for all the targets. However, the bands that are affected the most by water vapour are the infrared bands (4, 5 and 7). The order in which the bands are affected by the water vapour is the same for each target, unlike the the aerosols; Band 7 (far infrared) and Band 4 (near infrared) are affected the most; next then Band 5 (mid infrared), followed by bands 2 (green) and 3 (red), which are affected the same; lastly is Band 1 (blue), which appears not to be affected at all.

This behaviour is due to the way in which the bands are affected by the atmosphere. As can be seen in Figure 1.1, different parts of the spectrum are affected more by water vapour. These parts of the spectrum correspond to Bands 4, 5 and 7. The parts of the spectrum that are least affected by water vapour are the visible and thus the visible bands are not shifted as much by changes in the amount of water vapour.

Water Vapour displays the opposite behaviour to aerosols when it comes to the direction of variation from the actual. Where the amount of reflectance was reduced as the amount of aerosols was increased, it is increased for water vapour. This is because as the water vapour is increased in the atmosphere between the sensor and the surface more energy is absorbed by the atmosphere. This means that to compensate, the model must increase the amount of apparent reflectance at the surface to compensate for the increased absorption.

Ozone

Figures 3.20, 3.21 and 3.22 show the effect of ozone being varied between 0 and 500 Dobson Units. The forest target causes the most variation in the reflectance (15%), next the pasture (~11%), and lastly the soil (~6%). This is related to the brightness of the targets as described for the aerosols. Like the water vapour, the order of the bands affected remains the same. This is firstly Band 2 (green), then Band 3 (red) and then Band 1 (blue). The other bands appear to be almost unaffected by the variation in the amounts of ozone. To summarise, ozone, like aerosols, effects the visible spectrum and there is a difference in the magnitude of the effect between targets.

Ozone also exhibits similar behaviour to water vapour, in that, as the concentration increases, the amount of reflectance is also increased. This is because it absorbs energy in the same way that water vapour does.

Figure 3.17: Variation in Forest Target due to Water Vapour.

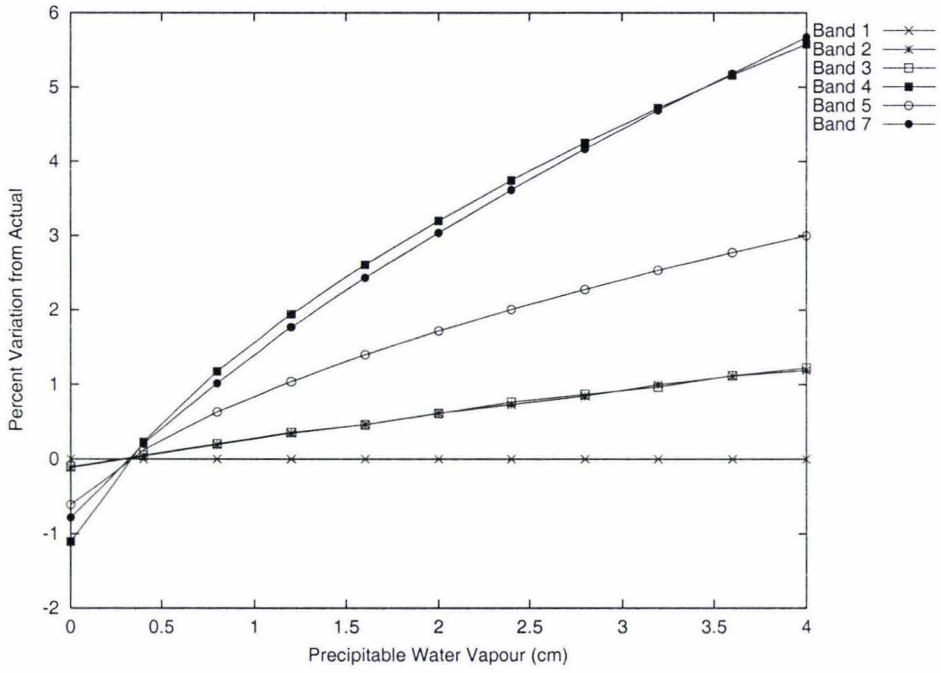

Figure 3.18: Variation in Pasture Target due to Water Vapour.

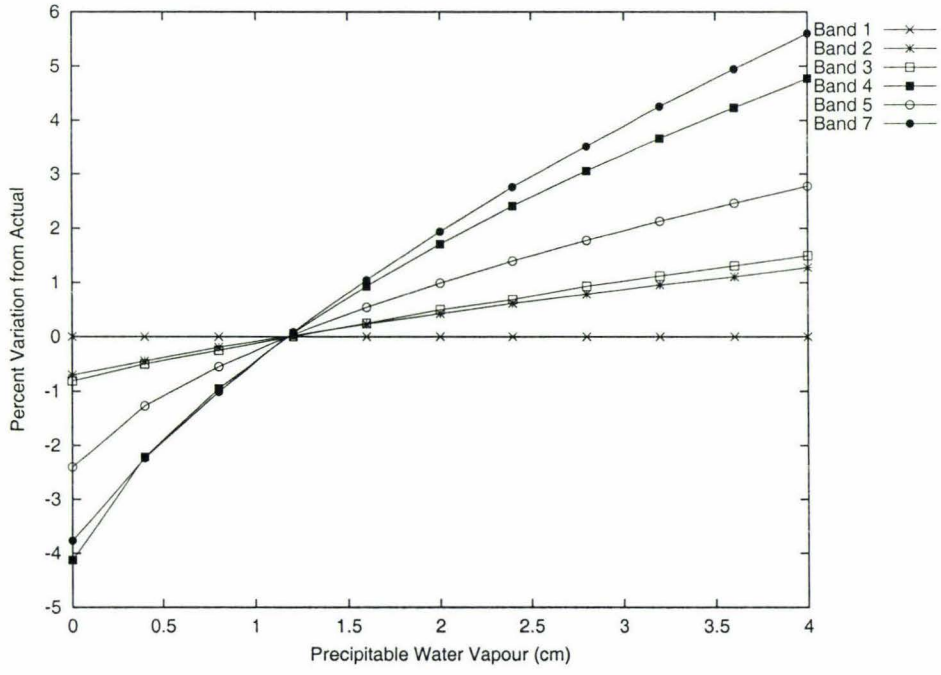

Figure 3.19: Variation in Soil Target due to Water Vapour.

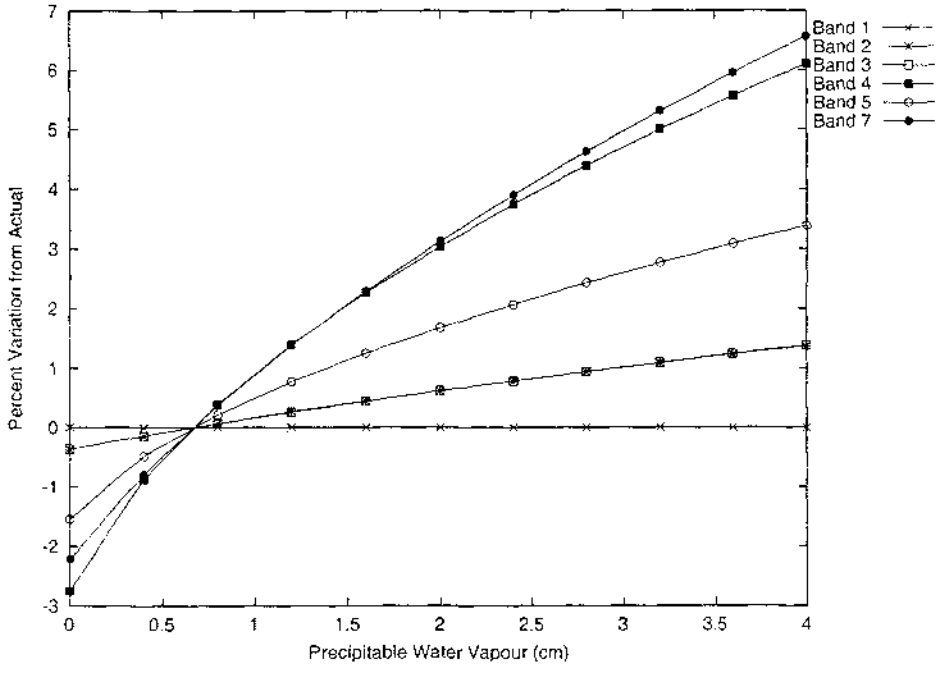

Figure 3.20: Variation in Forest Target due to Ozone.

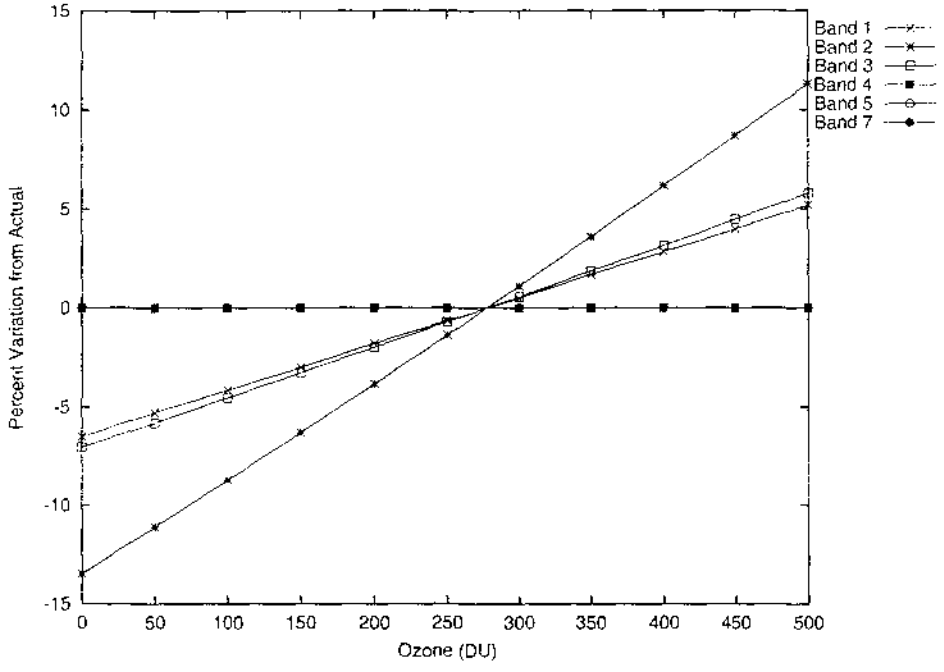

Figure 3.21: Variation in Pasture Target due to Ozone.

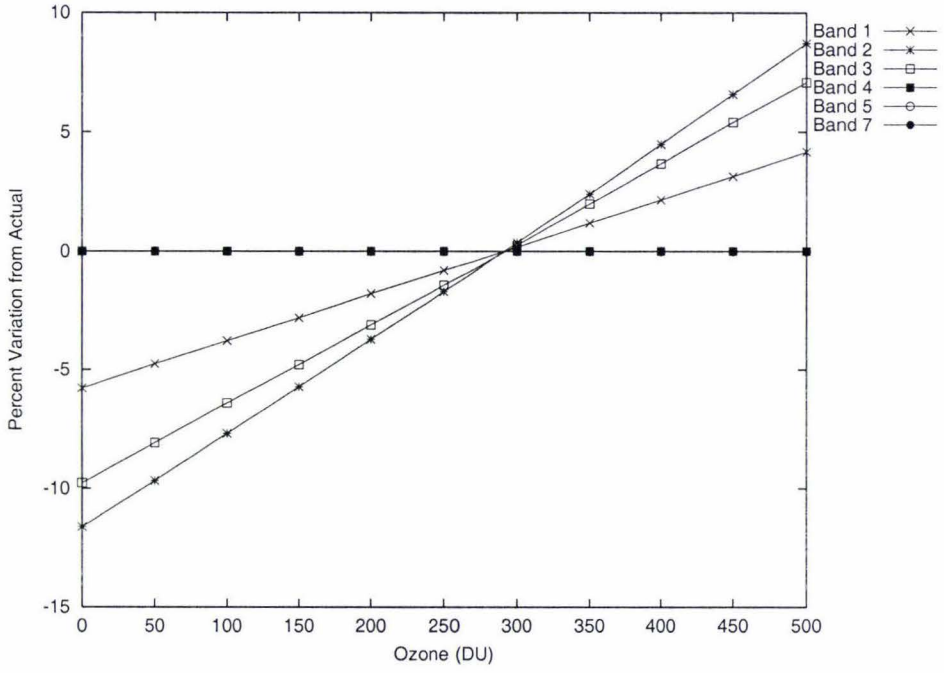

Figure 3.22: Variation in Soil Target due to Ozone.

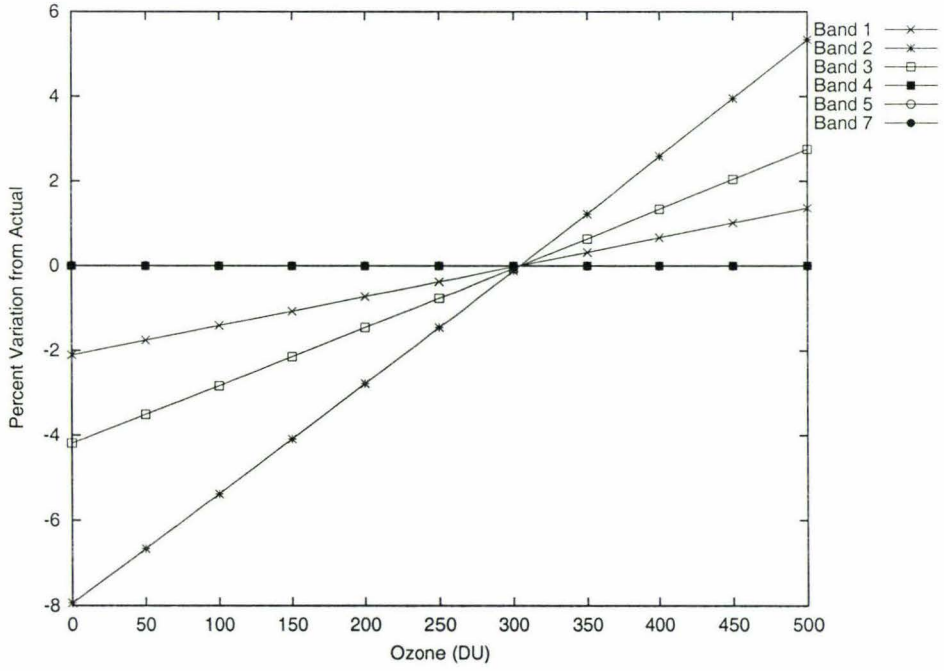

Table 3.4: 90 percent confidence values for the New Zealand atmosphere.

	Aerosol	Water Vapour	Ozone
Minimum	0.004	0.339	269
Maximum	0.164	2.359	423

3.2.2 Results for the New Zealand atmosphere

For a better idea of how much the Landsat scenes are affected by the variations in the New Zealand atmosphere, 6S was run with values that are typically seen over New Zealand. The same sites were selected as described in the Section 3.2.1.

Originally, it was intended to select the range of values for New Zealand by taking two standard deviations each side of the mean for each month and for each product. This would remove outlying values. However this assumes that the distribution of the pixel values is normal. This is true for the Water Vapour and Ozone data, but not for aerosols. The histogram for aerosols is skewed toward the lower values. This was pronounced enough that taking two standard deviations off the mean, as intended, resulted in a negative value for the lower bound.

Instead, it was decided to use an approach that would work for both normal and non-normal distributions. This involved creating a cumulative histogram for each monthly composite. The values at the 5% and 95% percentiles were chosen for aerosols, water vapour and ozone. These results are shown in Table 3.4.

The values in these ranges were graphed against the percentage variation from the actual figures for December 2000 (when the image was taken). Although these figures are just a "zoomed in" version of the figures for a wider range of values shown in Section 3.2.1, they show the variation in the New Zealand atmosphere and give the variation in retrieved reflectance to expect.

Aerosol

Figures 3.23, 3.24 and 3.25 show how the reflectance is affected by aerosols. They show that aerosols will affect forest targets by a maximum of 69%. For pasture targets this will be around 50%, and for soils, around 7%. The reflectance will be too great if the concentration of aerosols is underestimated, and too small if overestimated.

Figure 3.23: Variation in Forest Target due to Aerosol quantities in New Zealand.

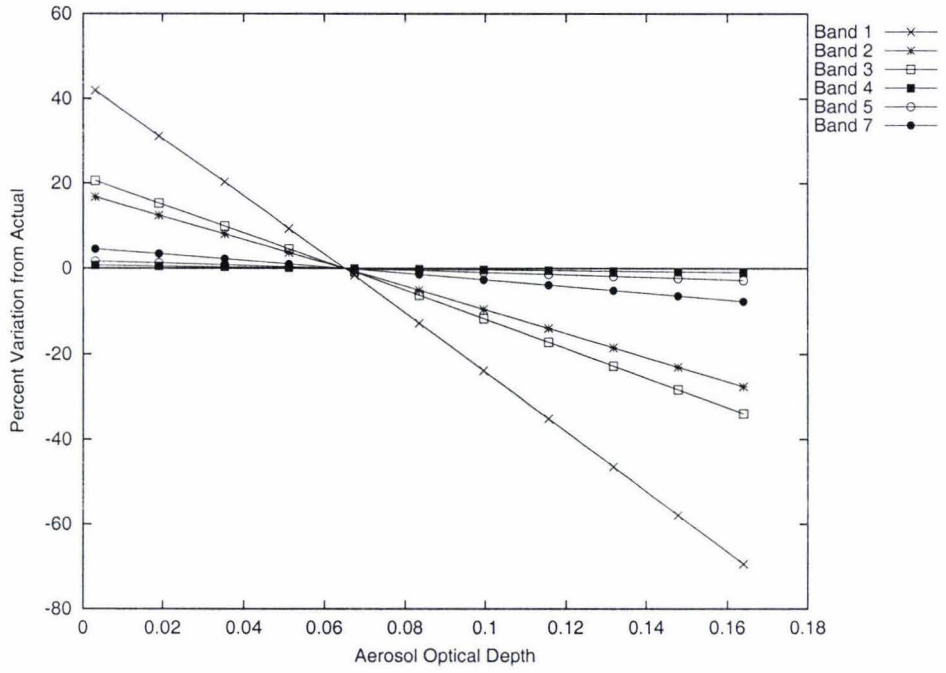

Figure 3.24: Variation in Pasture Target due to Aerosol quantities in New Zealand.

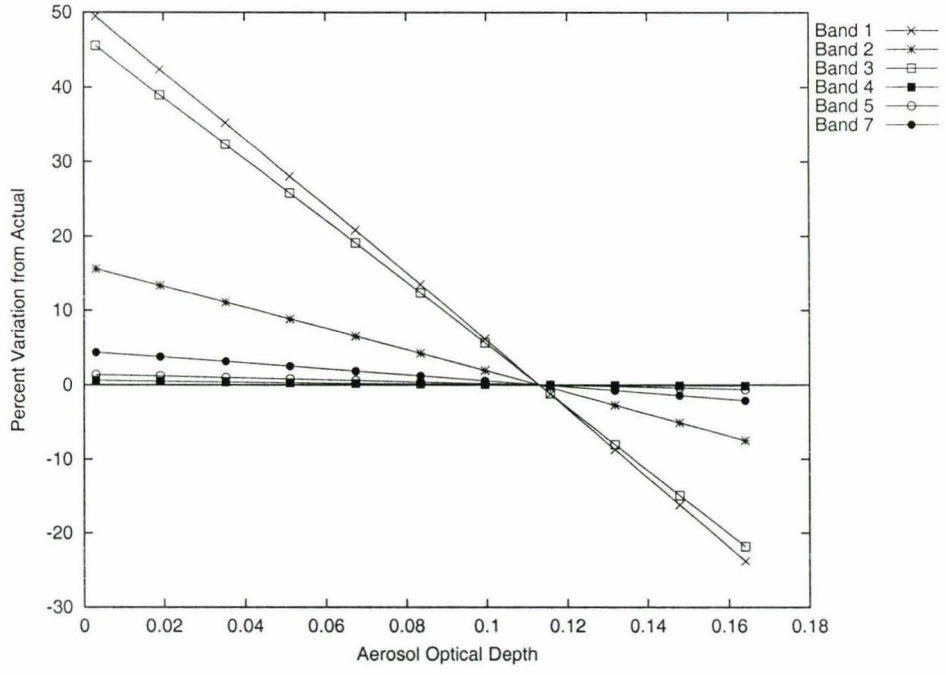

Figure 3.25: Variation in Soil Target due to Aerosol quantities in New Zealand.

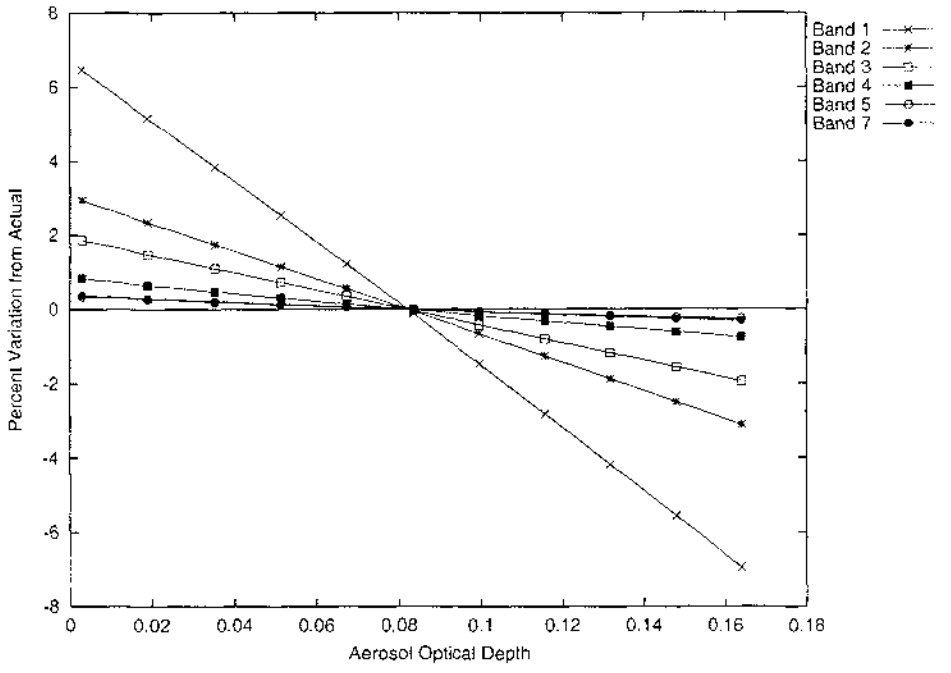

Water Vapour

Figures 3.26, 3.27 and 3.28 show the effect of changes in the amount of water vapour on the amount of reflectance. As expected, the infrared bands are affected the most (up to 3.7% for forest, 2.7% for pasture and 3.8% for soil). The shape of Figure 3.26 indicates that conditions on the day were much drier than the average for New Zealand and hence there is no variation to the left of where the lines converge. This is due to the altitude of the forest target.

Ozone

Ozone, like the aerosols, displays a degree of variation between the targets (Figures 3.29, 3.30 and 3.31). For the forest target, the maximum variation in reflectance is about 7%. For the pasture target, this is around 5.5% and for the soil target, it is around 3%. The reason that there is little variation to the left on the graphs is that the concentration of ozone is unusually low. This is due to the average concentration of ozone being much lower in summer, as noted in Section 3.1.

Figure 3.26: Variation in Forest Target due to Water Vapour quantities in New Zealand.

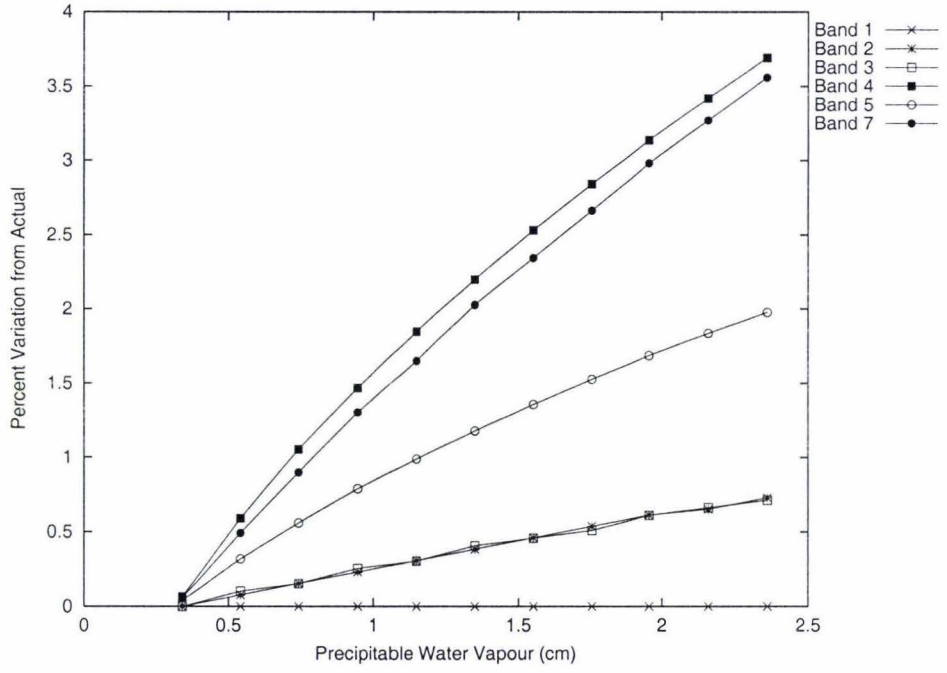

Figure 3.27: Variation in Pasture Target due to Water Vapour quantities in New Zealand.

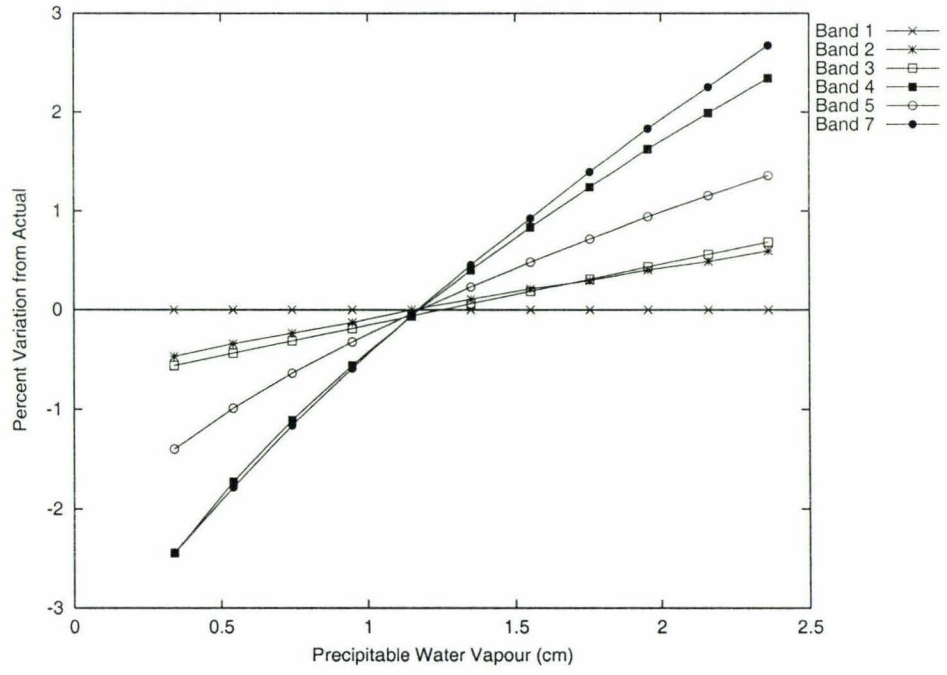

Figure 3.28: Variation in Soil Target due to Water Vapour quantities in New Zealand.

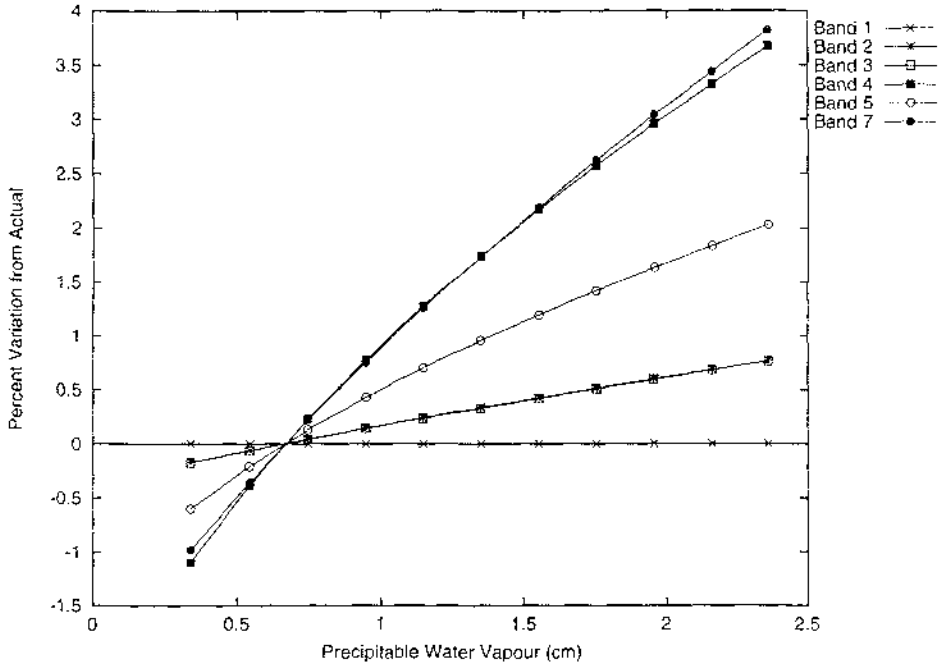

Figure 3.29: Variation in Forest Target due to Ozone quantities in New Zealand.

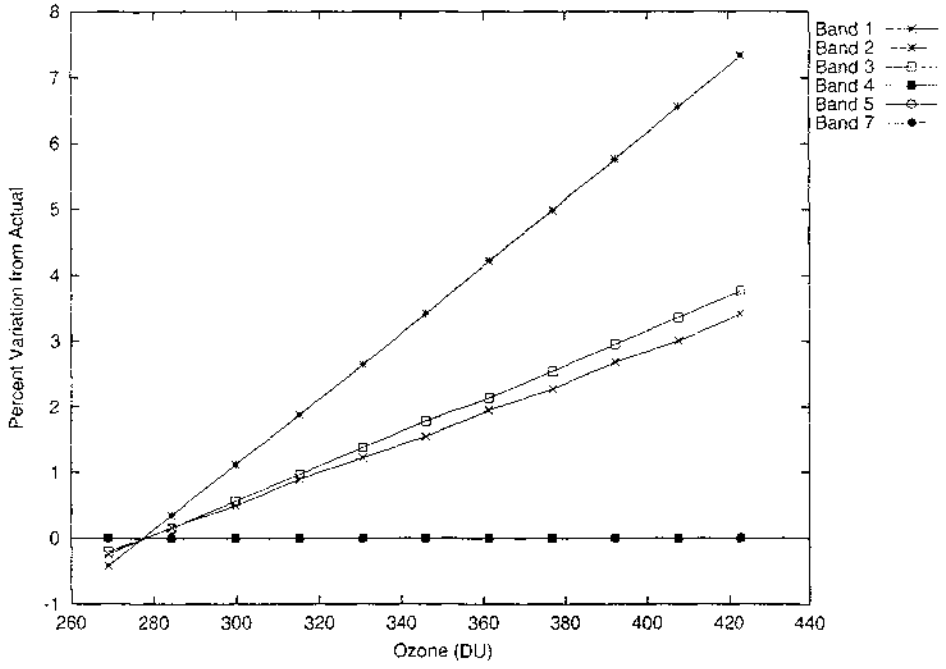

Figure 3.30: Variation in Pasture Target due to Ozone quantities in New Zealand.

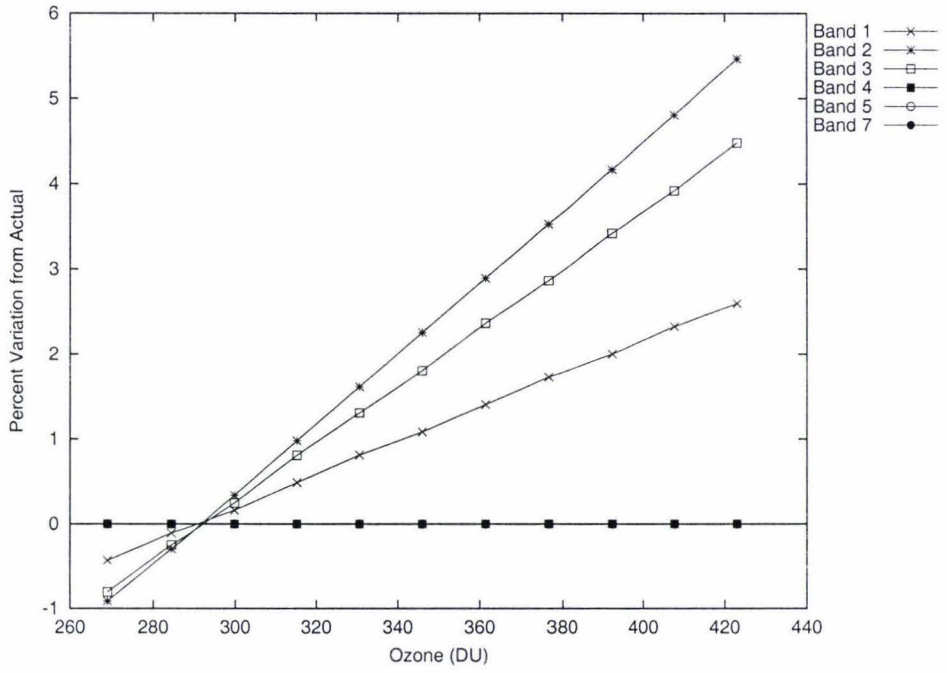

Figure 3.31: Variation in Soil Target due to Ozone quantities in New Zealand.

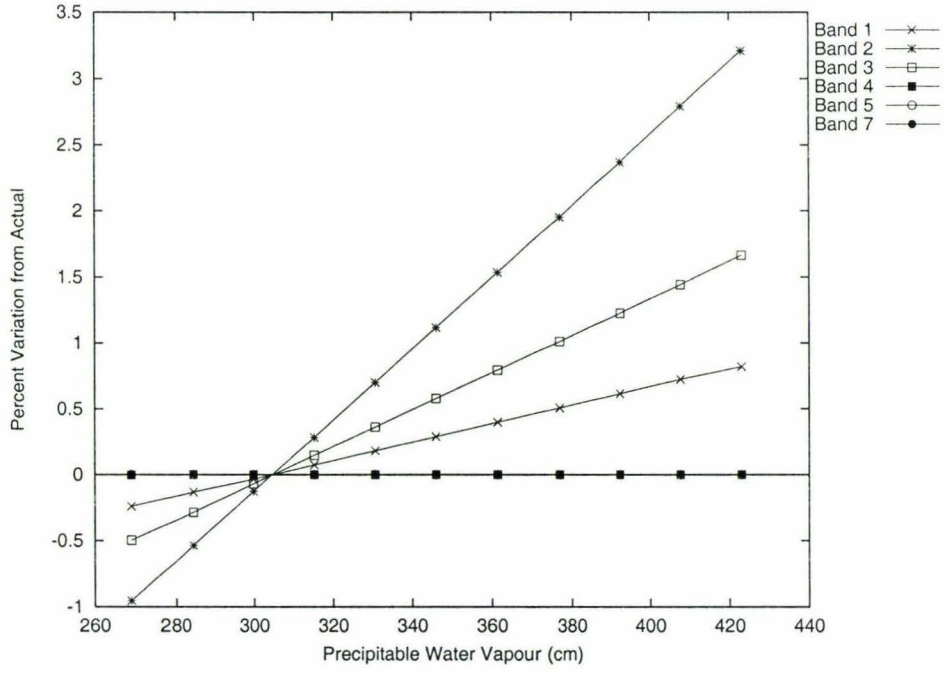

Summary

The findings for the New Zealand atmosphere are be summarised in Tables 3.5, 3.6 and 3.7.

Table 3.5: Sensitivity Results for Forest for New Zealand.

	Band 1	Band 2	Band 3	Band 4	Band 5	Band 7
Aerosol	69%	28%	34%	0.9%	2.8%	7.6%
Water Vapour	0%	0.7%	0.7%	3.7%	2%	3.6%
Ozone	3.4%	7.3%	3.8%	0%	0%	0%

Table 3.6: Sensitivity Results for Pasture for New Zealand.

	Band 1	Band 2	Band 3	Band 4	Band 5	Band 7
Aerosol	49.5%	15.6%	45.5%	0.6%	1.4%	4.4%
Water Vapour	0%	0.6%	0.7%	2.4%	1.4%	2.7%
Ozone	2.6%	5.5%	4.5%	0%	0%	0%

Table 3.7: Sensitivity Results for Soil for New Zealand.

	Band 1	Band 2	Band 3	Band 4	Band 5	Band 7
Aerosol	6.9%	3.1%	1.9%	0.8%	0.3%	0.4%
Water Vapour	0%	0.8%	0.8%	3.7%	2.0%	3.8%
Ozone	0.8%	3.2%	1.7%	0%	0%	0%

3.3 Ground Atmosphere Measurements

Here the results from the ground measurements are presented. The methods used are described in Section 2.3. Each recording and its associated Langley plot is presented separately and the results for aerosol optical depth are summarised in Table 3.9. The ozone and water vapour measurements were also recorded for each reading and are presented in Table 3.10.

3.3.1 Estimating Rayleigh Scattering

The optical depth given for Rayleigh scattering was taken from the tables and runs of 6S as summarised in Table 3.8. Note that the Rayleigh scattering was not affected by the setting of the zenith or azimuth angle or the amount of aerosols, ozone and water

Table 3.8: Optical Depth of Rayleigh Scattering.

	320nm	1020nm
6S US Standard 1962	0.916	0.00804
6S Mid Latitude Winter	0.910	0.00808
6S Mid Latitude Summer	0.908	0.00806
Penndorf's Tables [39].	0.926	0.00818
Average	0.913 $\pm$0.01	0.008090 $\pm$0.00009

Note: 1020nm figure interpolated from Penndorf's tables.

vapour. The model was asked to find the amount of Rayleigh scattering from sea level up to space and given the filter function of the MICROTOPS instrument defined for the 320nm and 1020nm wavelengths.

As this table shows, the values of Rayleigh scattering are reasonably close. The values from the tables are consistently higher. The average of these values were taken and errors given.

3.3.2 Langley Plots

A site was chosen on the roof of the Landcare building at Massey University (2732327E, 6087560N). This site was clear of obstruction and interference. The results of these readings are shown in Table 3.9.

The first reading was carried out on the morning of 16 May 2002. Because of the variable nature of the 1020nm readings it was decided to take five readings every 0.5 atmospheres. The times that the readings needed to be taken were estimated using the method described in Section 2.3.2. Readings that appeared to be inconsistent with other readings taken about the same time were removed from the data. It was decided that these readings were very likely to be erroneous. The Langley plot for 1020nm is shown in Figure 3.32, and the plot for 320nm is shown in Figure 3.33 for comparison. Note how the readings at 1020nm appear to show much more variability, primarily because they cover a much smaller range.

The 1020nm Langley plot has a number of readings on top of one another. It appears that successive readings taken at the around the same time have increasingly high values. This may be due to the sensors heating up as they are exposed to the sun for longer. As the values do not change the overall slope of the line, this is not a major problem. However, it would probably be better to shade the instrument for a few minutes between successive readings. All the readings seemed to be subject to this problem to a similar extent, with the readings later in the day being more susceptible,

Figure 3.32: Langley plot for readings taken on 16 May at 1020nm.

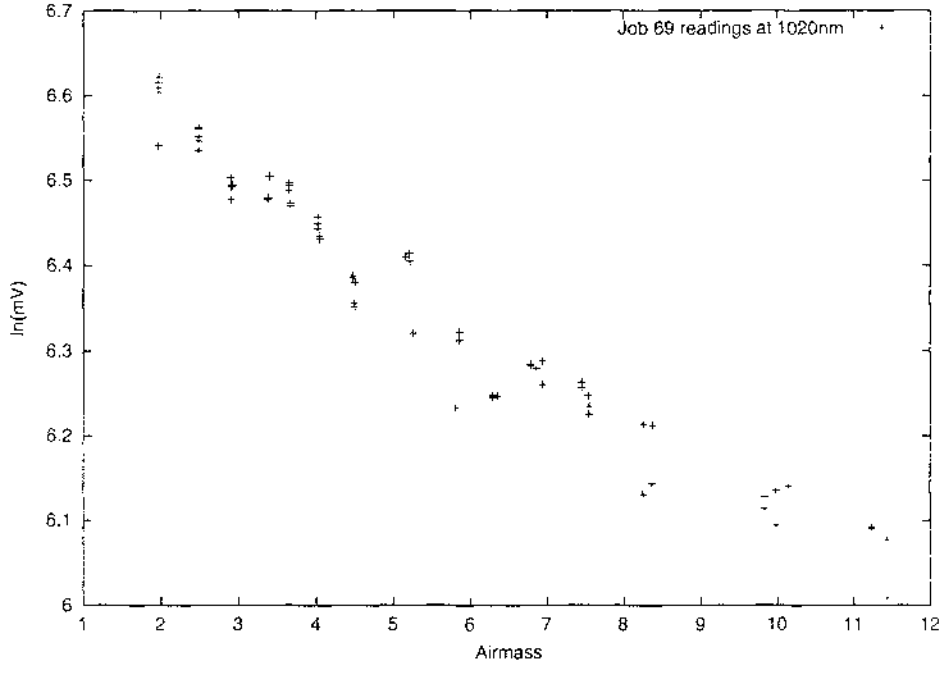

Figure 3.33: Langley plot for readings taken on 16 May at 320nm.

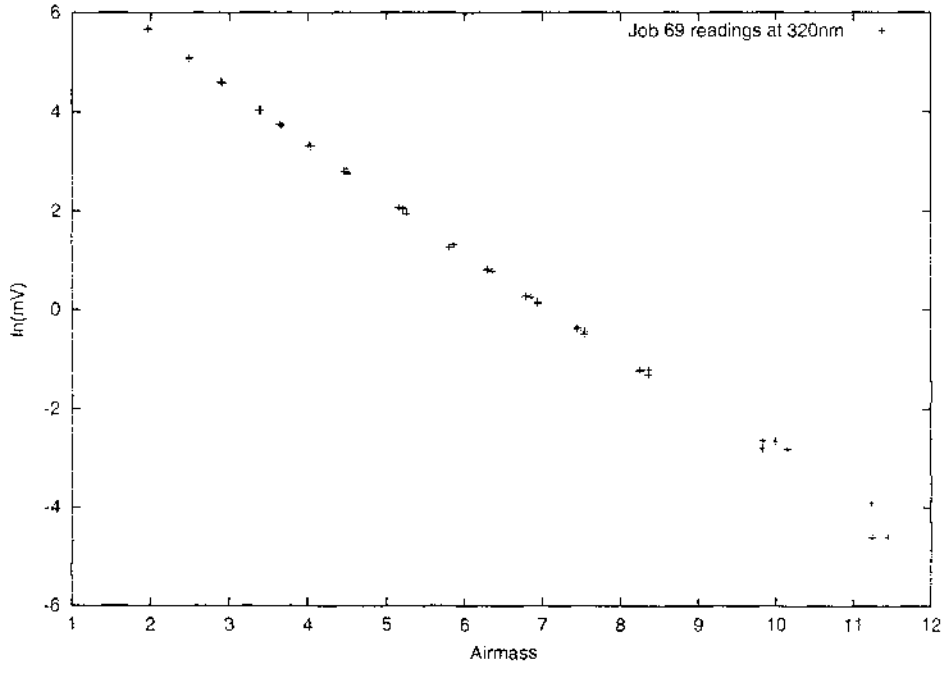

Figure 3.34: Langley plot readings taken on 10 August at 1020nm.

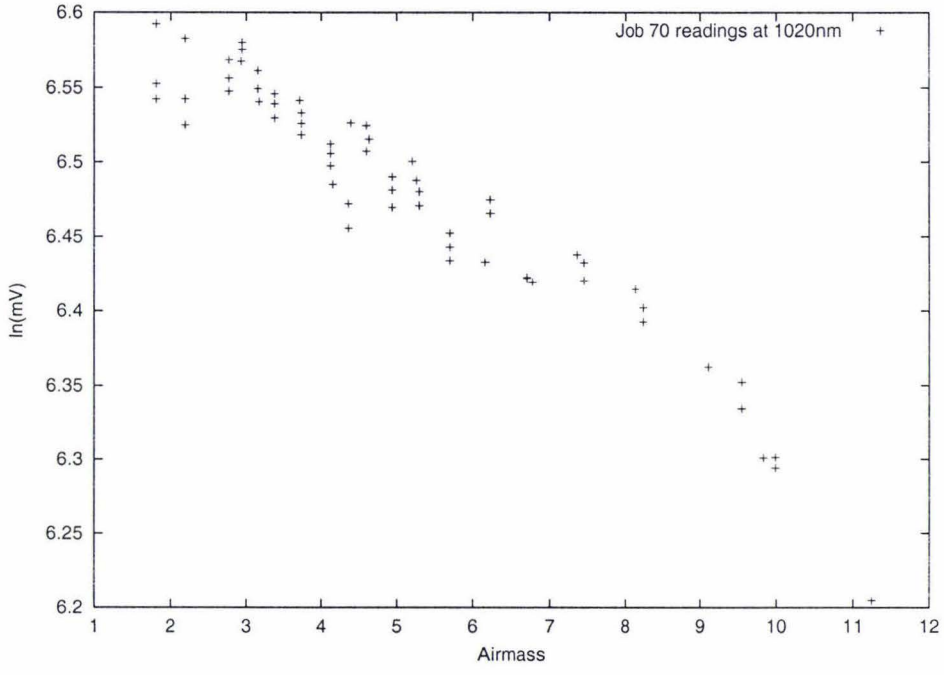

due to the sun being higher and brighter.

The next set of readings was performed on 10 August 2002. The gap between this set and the previous set was due to poor weather. The procedure followed was the same (i.e. readings taken about every 0.5 atmospheres), but due the different time of year, the readings were started at 7:50am. Figure 3.34 shows the Langley plot for the 1020nm measurements.

The next available day was 29 August 2002. There was some scattered cloud on this day, and a midday reading was not able to be taken because of the increasing cloud. In addition quite a number of measurements had to be discarded due to interference by cloud. However, despite the low number of readings, the resulting data were of reasonable quality so the results have been included here. Figure 3.35 shows the Langley plot of these data.

The next reading was taken on the 9 October 2002. This was a perfect cloudless day after a month of almost continuous rain. As a result, this day was particularly clear and features on distant hills were much more obvious than is normally the case. Most readings were valid and the Langley plot is shown in Figure 3.36.

Figure 3.35: Langley plot readings taken on 29 August at 1020nm.

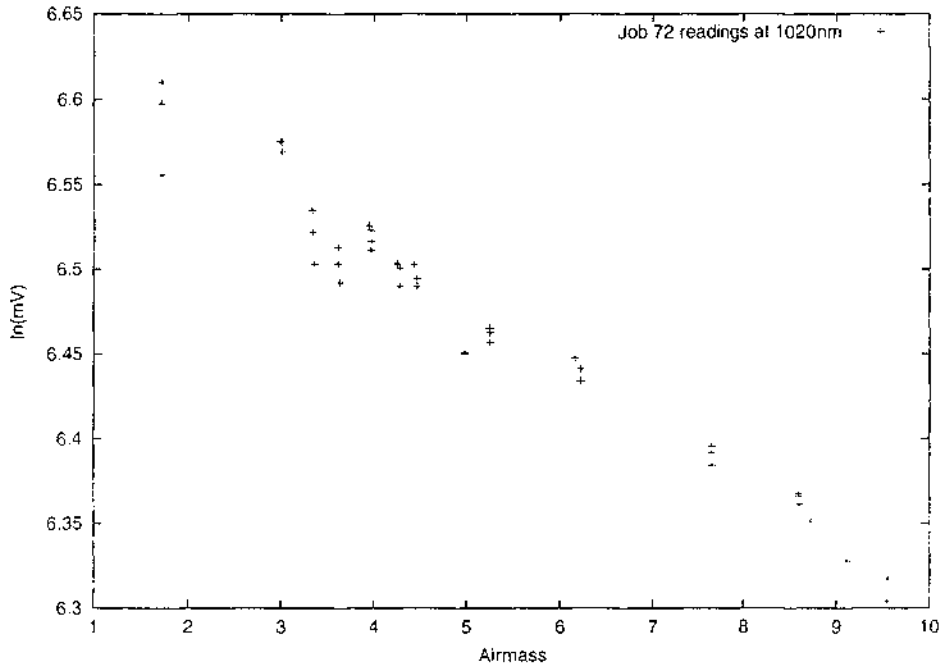

Figure 3.36: Langley plot readings taken on 9 October at 1020nm.

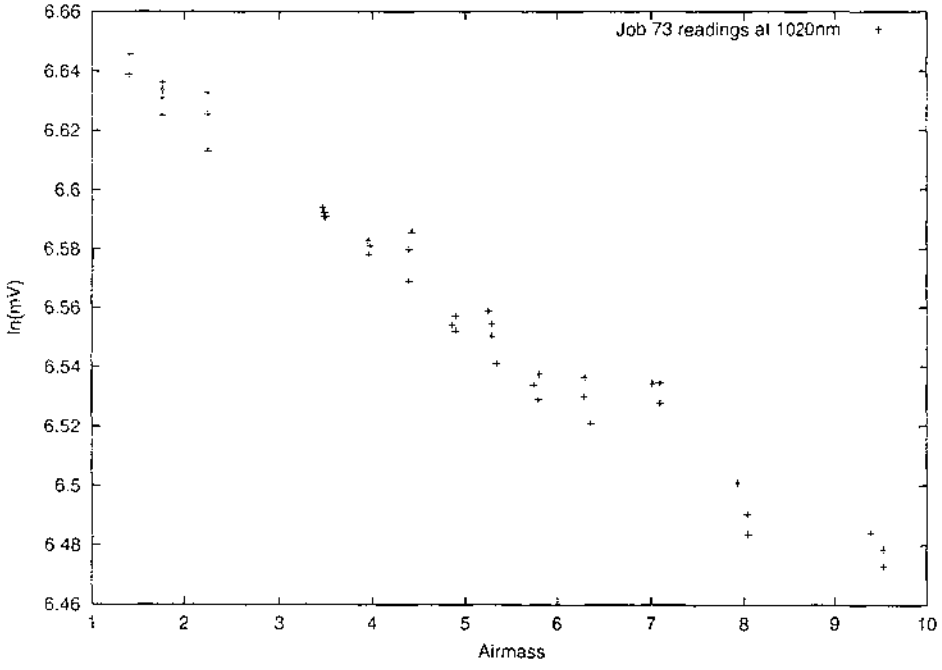

Table 3.9: Optical Depths from the Langley plots created from MICROTOPS readings.

Date	$\tau_{tot1020}$	$\tau_{Ray1020}$	$\tau_{aer1020}$	τ_{aer550}
16 May 2002	0.057±0.007	0.0081 ±0.0001	0.049 ±0.007	0.102
10 August 2002	0.033 ±0.004	0.0081 ±0.0001	0.025 ±0.004	0.051
29 August 2002	0.034 ±0.005	0.0081 ±0.0001	0.026 ±0.006	0.054
9 October 2002	0.021 ±0.003	0.0081 ±0.0001	0.013 ±0.003	0.027

Table 3.10: Results for Ozone and Water Vapour measurements taken with MICROTOPS.

Date	Water Vapour(cm)	Ozone(DU)
16 May 2002	0.76 ±0.22	291 ±21
10 August 2002	0.35 ±0.20	355 ±26
29 August 2002	0.53 ±0.20	387 ±12
9 October 2002	0.28 ±0.10	336 ±148

3.3.3 MICROTOPS Results

The results of the readings for aerosol optical depth at 1020nm taken on the roof of the Landcare building are shown in Table 3.9. Note that the Ozone Optical Depth is not listed because Ozone has no effect at this wavelength. Note also that the τ_{Ray} values are taken from Table 3.8.

The relationship between the aerosol optical depth at 1020nm and that at 550nm (used by MODIS) is established approximately by Equation 2.4. If τ_{aer550} for 16 May is compared with the average of the MODIS May monthly composite for 2001, it can be seen that the MICROTOPS reading is much higher than the MODIS, but the opposite is true for the other dates compared to the MODIS composites in 2001. See Section 3.3.4 for a comparison with MODIS data for the same day.

Table 3.10 presents the average readings taken by the MICROTOPS instrument at the same time as the readings for aerosol optical depth. Firstly, for water vapour, the reading for 16 May of around 0.76cm is lower than the May composite of 2000 average of about 1.08cm (see Figure 3.6). Even with the highest value in the error range, the reading is still lower than the MODIS data. The other values (10 and 29 August) are also much lower than the MODIS average for August 2001 (0.98cm). For October 2001, the values are again much lower than expected. However, the difference between these values and the composite average values are much greater. The one thing these values do have in common is the overall trend - down to a lowest value in July, then heading back up again. These readings seem to be inconsistent, so some climate data were downloaded for comparison as outlined in Section 2.3.6. See Section 3.3.5 for

the results of these calculations from climate data.

The MICROTOPS ozone values were consistently lower than the MODIS ozone values for 2001. The third MICROTOPS reading (29 August) of 395DU was closest to the average MODIS reading of 400DU for that month. The MODIS readings for 16 May and 10 August were outside the error bounds of the MICROTOPS readings. They are within the error bounds for 9 October, but the error given is high. The MICROTOPS measurements of 16 May and 9 October also had values for aerosol that do not match the measured MODIS aerosol values. A comparison of NIWA and MODIS data are presented in Section 3.3.6.

It is important to remember here that the MODIS data are for a different year to when the ground readings were taken. It is assumed that the same trends would be repeated for all years, but with minor variations. It is possible that the actual days when the readings were taken (generally unusually fines ones) are in fact not representative of the year at all. In addition, the MICROTOPS readings are taken at a specific time and location and compared to MODIS spatial averages over all of New Zealand and temporal averages over a whole month. The following Sections attempt to relate the data from MODIS to ground readings taken at the same time.

3.3.4 Results from MODIS Aerosol

The actual MODIS aerosol data were downloaded for the same days that the MICROTOPS readings were taken in 2002. The Aerosol Optical Depth figures for the area of Palmerston North are shown in Table 3.11. There are no data for 10 August because the orbit of the satellite was not favourable for data collection over New Zealand. There are two readings for 9 October because there were two images taken by MODIS on that day that included Palmerston North. The figures for 9 October are different. This does put into question the accuracy of these readings since they were taken only 40 minutes apart. Further, these readings do not correlate well with the data collected by the MICROTOPS (see Table 3.9). The obvious exception is the second MODIS reading on 9 October. It is exactly the same as the MICROTOPS reading for that day.

3.3.5 Results from Paraparaumu NIWA Water Vapour data

Data from NIWA's Climate database were downloaded and processed as described in Section 2.3.6. The NIWA data compared to the MODIS data for the Paraparaumu area is shown in Figure 3.37.

Table 3.11: Aerosol Optical Depth at 550nm from MODIS for days measured by MICROTOPS

Date	16 May	10 August	29 August	9 October
Reading 1	0.066	No Data	0.113	0.101
Reading 2		No Data		0.027
Average	0.066		0.113	0.064

Figure 3.37: NIWA and MODIS data for Paraparaumu.

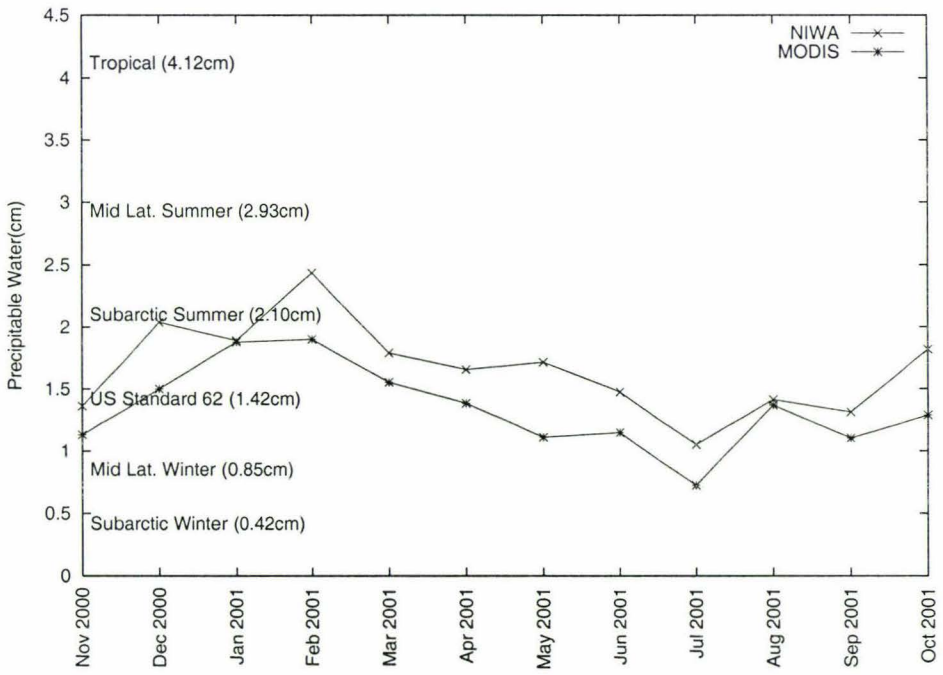

Also plotted are the amounts of water vapour that correspond to the six standard atmospheric models that come with 6S. There is a distinct difference between the NIWA data and the MODIS data. It is assumed that the NIWA data are more accurate, as it uses calibrated sensors aboard a balloon. Readings are taken by this sensor as it ascends through the atmosphere as described in Section 2.3.6. Although the MODIS data follow the same trend as the NIWA, it tends to consistently underestimate the amount of water vapour in the atmosphere. However, this difference is not as great as the differences between the NIWA data and some of the atmospheric models that could have been chosen. One way this could be explained is that the NIWA readings were the average of all the readings when there was no rain. The MODIS data however were all readings when there was less than 30% cloud. Therefore there will be cloudy days that were included in the NIWA average that were not in the MODIS. On these cloudy days the humidity may well have been higher because of the lack of sun to dry the atmosphere out. Therefore it is possible that the difference between the NIWA and MODIS data may be explained in this way. It is also possible that the error from the MODIS data may be showing up here as well. As mentioned in Section 1.3, the stated error in the MODIS water vapour figures is 10%. However the average difference between the NIWA and MODIS data are more like 20%. Therefore the difference is most likely a combination of this and the cloudy days problem mentioned above. These values are significantly higher than those recorded by the MICROTOPS (see Table 3.10). It would appear that the MICROTOPS is at fault as the NIWA data are known to be accurate.

3.3.6 Results from the Lauder NIWA Ozone data

This processing was performed as described in Section 2.3.6. Figure 3.38 shows the Lauder data compared to the MODIS data for Lauder. The data plotted for MODIS is for the pixel that contains Lauder taken from the monthly composites.

As this shows, the MODIS data appear to overestimate the amount of ozone in the atmosphere. However, both sets of data have the same overall trend throughout the year. Therefore MODIS cannot be relied upon to provide totally accurate results for ozone.

For August, the MICROTOPS results span the MODIS and NIWA data, but underestimate ozone for the other months.

Figure 3.38: Ozone recorded at Lauder compared to MODIS.

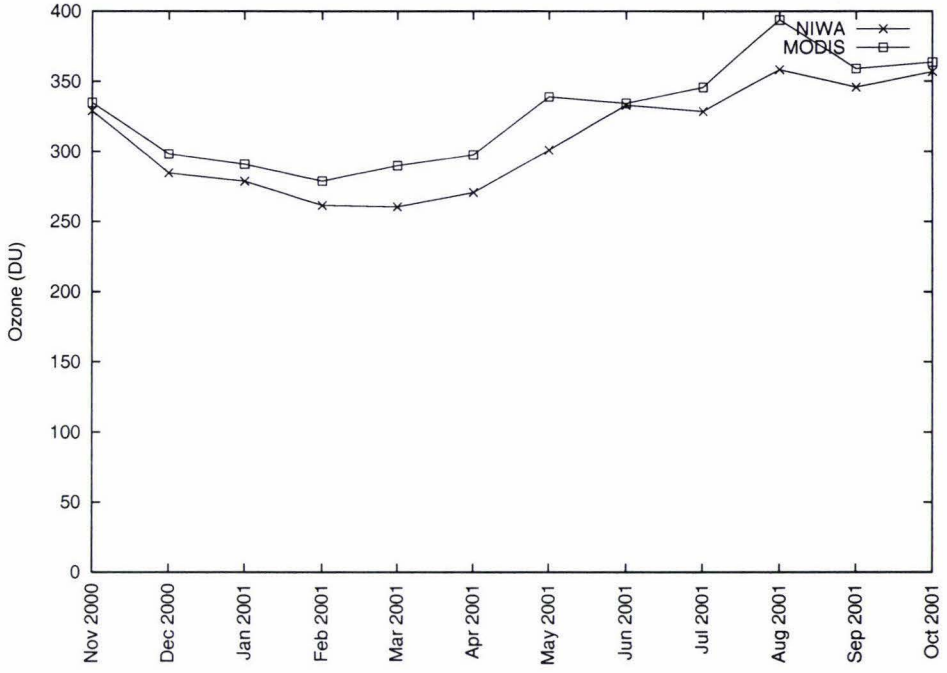

3.4 Comparison of Atmospheric Correction Methods

Here the performance of different correction methods is compared for defined areas in the Landsat scene. Additional targets where measurements were taken with the GER instrument are described in Section 3.5.

One difference that stood out was that large spatially corrected scenes can suffer from obvious "blocks". The sample image that was corrected did not suffer from this as the area was small, but it is more obvious in larger corrected scenes. These blocks result from the aerosol data being at a low resolution (10km). Differences in the amount of aerosols between adjacent MODIS pixels result in blocks of the Landsat scene being corrected differently and thus the output is uneven. This reflects the fact that the spatial resolution of the corrected reflectance image is no better than the lowest resolution of the data input; in this case the MODIS aerosol data. The visual effect could be reduced by applying distance weighted correction coefficients, but this would increase the time taken.

3.4.1 CPU times of Atmospheric Correction

Table 3.12 compares the different times taken for the correction techniques. All corrections were run on a Sun SuperSparc server with two 200MHz processors and 1.5GB

Table 3.12: Times taken for different atmospheric corrections.

Correction Type	Speed (minutes)
Monthly	7
Simple	8
Spatial	249
ATCOR 2	13
Lauder	13

Note: Time taken to import from HDF files ignored for Simple and Spatial.

Figure 3.39: Original Landsat subset (left) and spatially atmospherically corrected scene (right). Bands 1, 2 and 3.

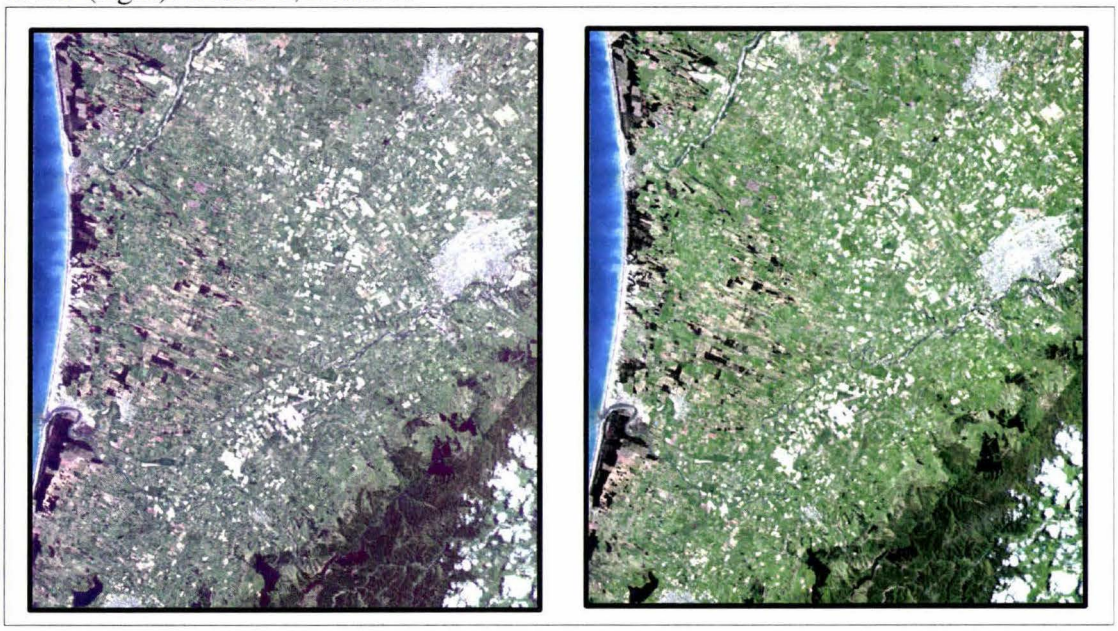

of RAM.

Figure 3.39 displays the output from the simple correction technique compared with the original image. Note how the uncorrected image is much bluer than the corrected image. This is because most of the affect of aerosols is in the blue end of the spectrum, and (this has been shown in Section 3.2) the corrections have reduced the amount of blue in the image.

3.4.2 Target Comparisons

The targets shown here are similar to the representative target measured by the GER (see Appendix A). This was not taken of the same area, or in the same conditions, but was meant as an indication of the reflectance to be expected. The locations of the

Figure 3.40: Landsat Extract including Palmerston North.

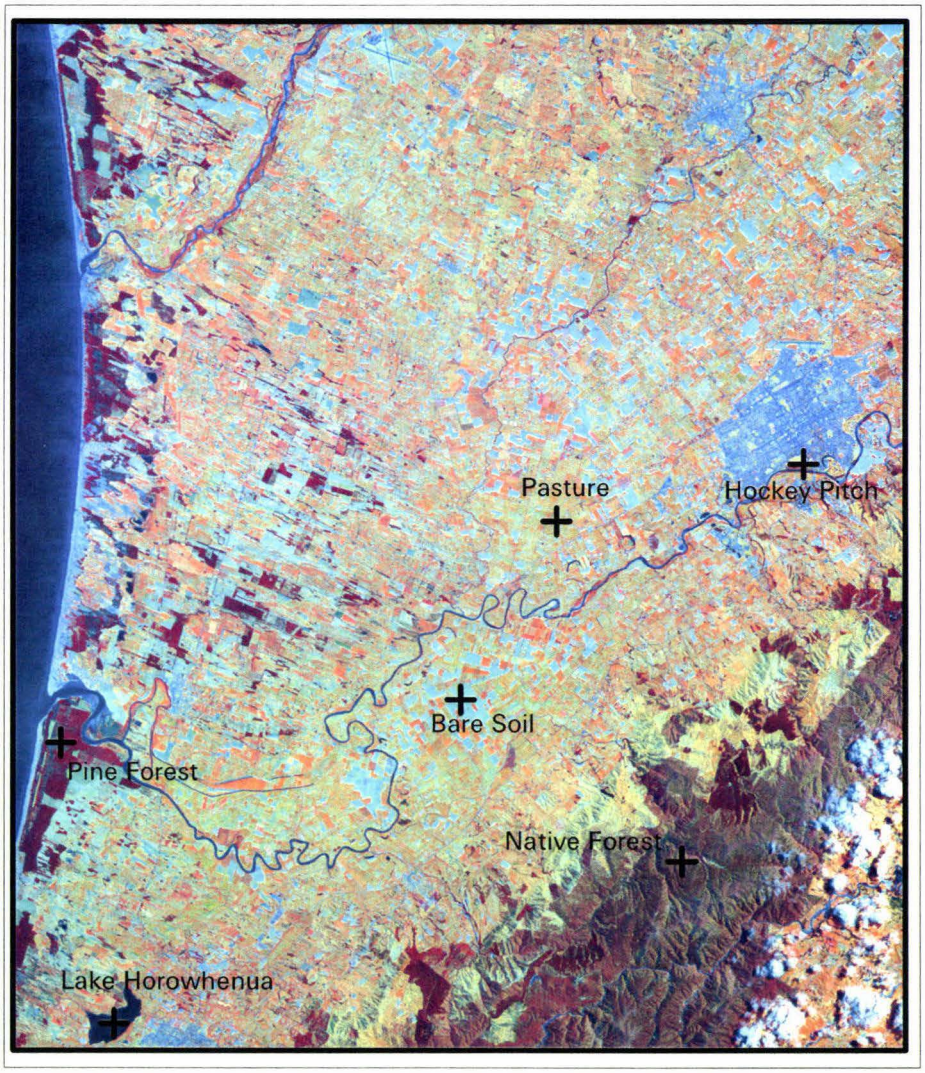

Figure 3.41: Selected Targets from the Landsat Extract.

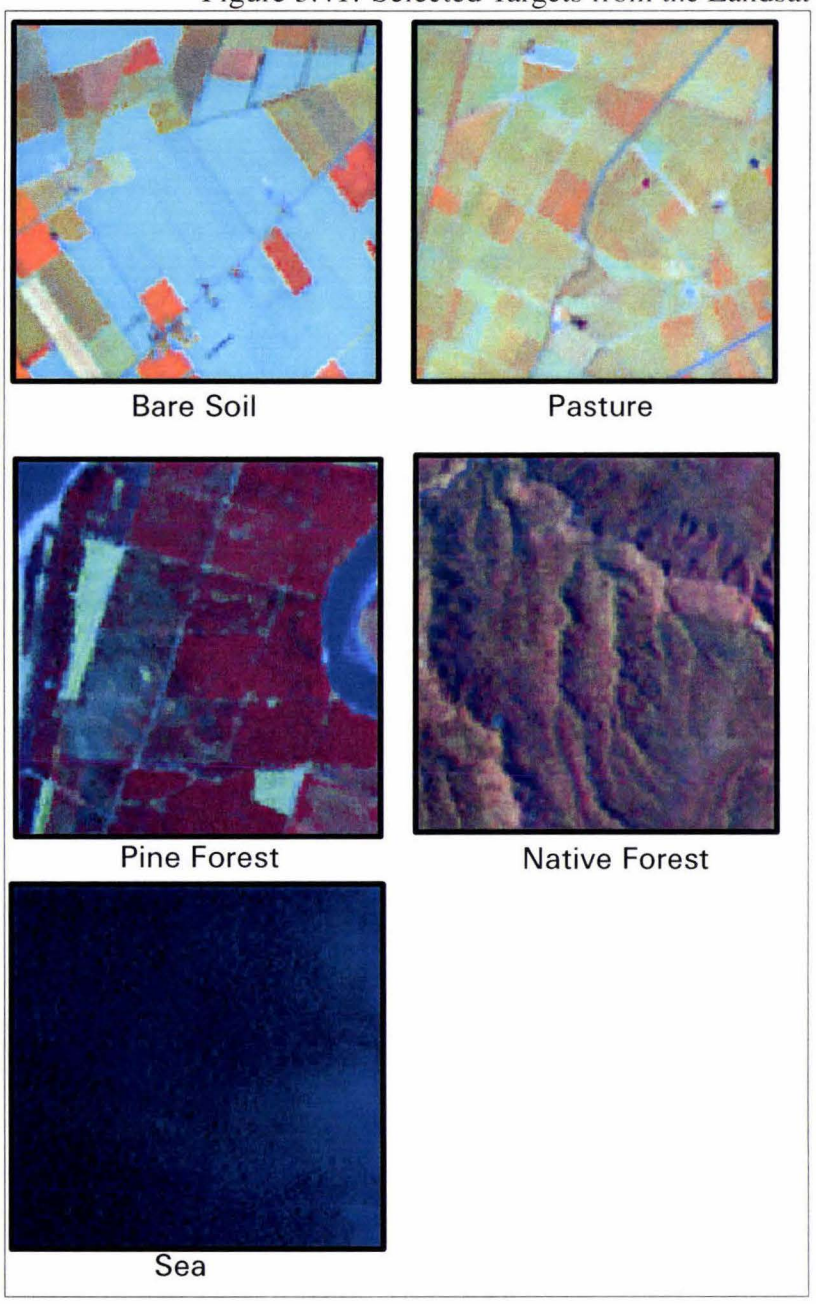

Table 3.13: Median reflectance of bare soil for different atmospheric corrections.

	Band 1	Band 2	Band 3	Band 4	Band 5	Band 7
Monthly Correction	0.083	0.110	0.142	0.238	0.314	0.273
Simple Correction	0.084	0.110	0.142	0.234	0.311	0.268
Spatial Correction	0.085	0.111	0.143	0.235	0.311	0.268
ATCOR 2	0.07	0.11	0.14	0.25	0.37	0.29
Reference Spectra	0.111	0.153	0.191	0.244	0.324	0.289

Table 3.14: Median reflectance of pasture for different atmospheric corrections.

	Band 1	Band 2	Band 3	Band 4	Band 5	Band 7
Monthly Correction	0.030	0.060	0.042	0.422	0.219	0.099
Simple Correction	0.030	0.061	0.043	0.415	0.217	0.097
Spatial Correction	0.030	0.061	0.042	0.416	0.217	0.0971
ATCOR 2	0.01	0.06	0.04	0.47	0.26	0.10
Reference Spectra	0.026	0.068	0.038	0.613	0.247	0.113

various targets referred to are shown in Figure 3.40 and Figure 3.41 has a more detailed view of the targets chosen.

Table 3.13 contains the median values for an area of bare soil on the Manawatu plains calculated using the different methods of atmospheric correction. The reflectance for Monthly, Simple and Spatial corrections are very similar. The reflectance for ATCOR 2 are reasonably close to these for all bands except bands 4 and 5. The reference spectra used compares consistently well to the correction methods in all bands except 3.

Table 3.14 contains the median reflectance for an area of pasture on the Manawatu plains calculated using the different methods of atmospheric correction. This was the largest area available without any areas of bare soil within it. Again, the three atmospheric corrections developed here have very similar reflectance and ATCOR 2 is not very different. All the bands are very similar to the reference spectra, except band 4 which is near infrared. Near infrared is the most responsive to vegetation, so it is expected that any differences between the reference spectra and the target chosen would show in this band.

Table 3.15 contains the median reflectance for the different atmospheric corrections for an area of Waitarere forest on the west coast, south of the mouth of the Manawatu River. All the corrections have very similar results. These in turn are similar to the results of the reference spectra, but again with the exception of Band 4. This is the same as the pasture target. The reference spectra for this target was taken from a

Table 3.15: Median reflectance of pine forest for different atmospheric corrections.

	Band 1	Band 2	Band 3	Band 4	Band 5	Band 7
Monthly Correction	0.011	0.016	0.012	0.231	0.065	0.026
Simple Correction	0.012	0.017	0.013	0.227	0.064	0.026
Spatial Correction	0.011	0.016	0.012	0.227	0.064	0.025
ATCOR 2	0.01	0.01	0.01	0.26	0.08	0.02
Reference Spectra	0.012	0.022	0.017	0.281	0.072	0.032

Table 3.16: Median reflectance of native forest for different atmospheric corrections.

	Band 1	Band 2	Band 3	Band 4	Band 5	Band 7
Monthly Correction	0.012	0.028	0.018	0.248	0.101	0.039
Simple Correction	0.013	0.029	0.019	0.244	0.101	0.039
Spatial Correction	0.015	0.030	0.020	0.246	0.101	0.039
ATCOR 2	0.01	0.02	0.01	0.028	0.12	0.04
Reference Spectra	0.012	0.022	0.017	0.281	0.072	0.032

helicopter.

Table 3.16 contains the median reflectance for the different atmospheric corrections for an area of native forest. This was chosen to be a reasonably homogeneous area in the northern Tararuas. This area consisted of two adjoining north west facing slopes. This was chosen because the values for the beech forest on a well lit area was of most interest. Steep valley walls and the like are not likely to return representative reflectance for beech forest as they are much darker than would typically be expected. Generally, the reflectance returned by the atmospheric correction techniques are similar, with the exception of the reflectance for the visible bands of the Spatial Correction. The reflectance returned are higher than the other correction techniques for Bands 1, 2 and 3. For Bands 2 and 3, however ATCOR 2 is much lower than the reflectance for the other corrections. Unfortunately, a reference spectra for native forest was not available. The best available was spectra for Manuka taken from a helicopter which turns out to be very close to the atmospheric corrections.

Table 3.17 contains the median reflectance for the different atmospheric corrections for an area of sea. This area is off the west coast north of Himatangi. Like the the other targets, the Monthly, Simple and Spatial corrections have similar reflectance. However, for some of the infrared bands there are negative reflectance. The Spatial correction has negative reflectance for all the infrared bands. The magnitude of these negative numbers is small, but indicates there is an error in either the input data, or in the correction methods themselves. ATCOR 2 has reasonably comparable values to the

Table 3.17: Median reflectance of sea for different atmospheric corrections.

	Band 1	Band 2	Band 3	Band 4	Band 5	Band 7
Monthly Correction	0.046	0.032	0.007	0.003	0.000	0.001
Simple Correction	0.046	0.032	0.007	0.003	0.000	0.001
Spatial Correction	0.042	0.028	0.003	-0.001	-0.003	-0.001
ATCOR 2	0.03	0.02	0.01	0.01	0.01	0.01
Reference Spectra	0.056	0.042	0.005	0.000	0.000	0.000

other corrections, apart from Bands 1 and 2 which are lower that the other methods. However, the numbers are all positive and not less than 0.01. This is a situation similar to that for Lake Horowhenua as described in Section 3.5. The reference spectra is higher than the atmospheric corrections for Bands 1 and 2, but comparable for the other bands.

3.5 Ground Cover Measurements

This section describes the results obtained from the GER 2600 instrument as described in Section 2.6.

3.5.1 Test reading

Although the instrument had recently been sent away for recalibration, it was important to check that the instrument was producing sensible results. On 22 August 2002 the instrument was assembled and taken outside. The weather was generally fine with scattered cloud. Between clouds, measurements were taken of concrete and grass. Figure 3.42 shows a graph of the reflectances at the different wavelengths recorded by the instrument for the targets. The radiance of the reference plate across the wavelengths is also shown at each time the reference plate was read. Even in the short time that the readings were taken the radiance from the sun varied as can be seen especially around 500nm. Note how the radiance varies over the spectrum in line with the atmospheric windows. Note also how the reflectance readings are prone to spikes and erroneous values when the reference radiance line is close to zero - especially noticeable at the longer end of the spectrum. This is because of the low signal to noise ratio at these points and the data are only reliable for those points where there is higher values for radiance coming from the sun.

The Landsat filter response for bands 1, 2, 3, 4, 5 and 7 are also shown in Figure

Figure 3.42: Test run of the GER 2600.

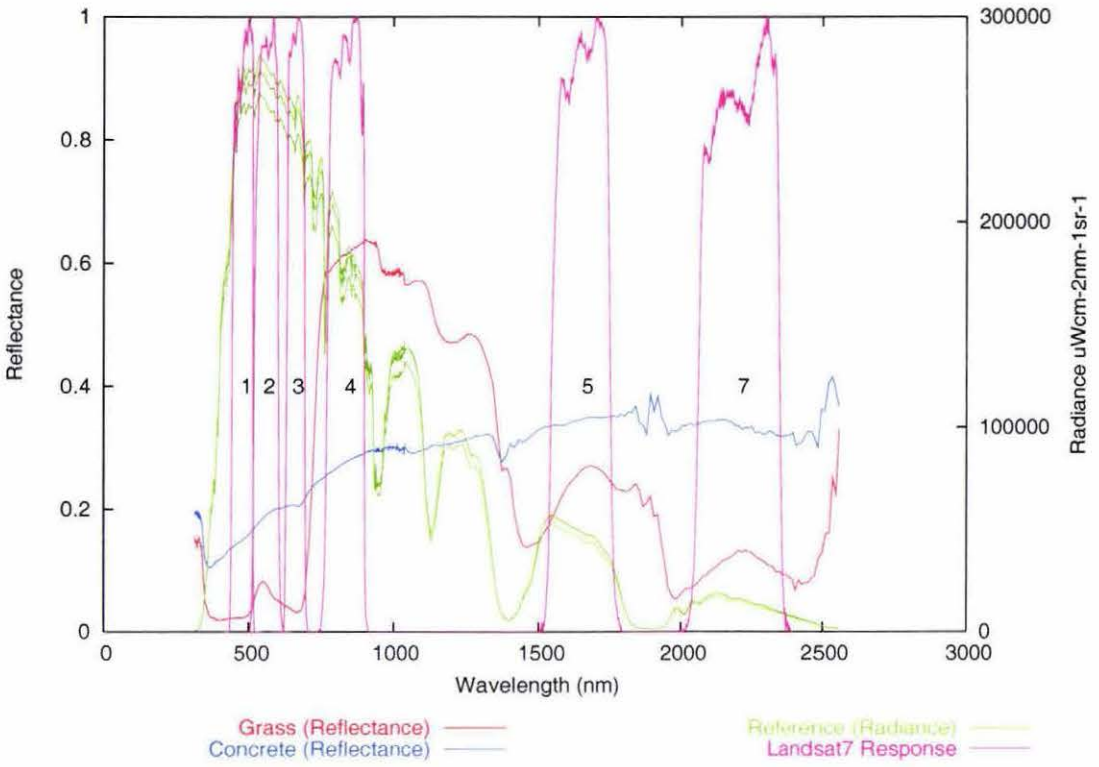

3.42. As this shows, the first three visible bands are bunched together at the point of maximum radiation from the sun. The other bands used are also placed on peaks in the radiation from the sun. Notice how the grass targets have a higher reflectance in the infrared bands, than the visible. This is also true for concrete, but the difference is not as much.

The Landsat filter function were then applied to the data and the results shown in Figure 3.18. Table 3.1 shows the reflectances of the three targets in the Landsat scene that were used for sensitivity analysis for comparison. As expected, for "Grass", the values in the green band are higher than the blue or red and the infrared bands are much higher than the visible. The readings for "Grass" are similar to the pasture target used for sensitivity analysis. "Concrete" has a similar response over all the Landsat bands.

3.5.2 The Hockey Pitch

The location of the corners of two hockey pitches (which lie side by side) were recorded using a Trimble Pro-XR GPS. The hockey ground with the GPS locations overlaid is

Table 3.18: Reflectance given by applying Landsat filter function to test data from the GER 2600.

	Band 1	Band 2	Band 3	Band 4	Band 5	Band 7
Grass	0.026	0.068	0.038	0.613	0.247	0.113
Concrete	0.151	0.189	0.207	0.276	0.345	0.334

Figure 3.43: Close up of Hockey ground with GPS positions overlaid.

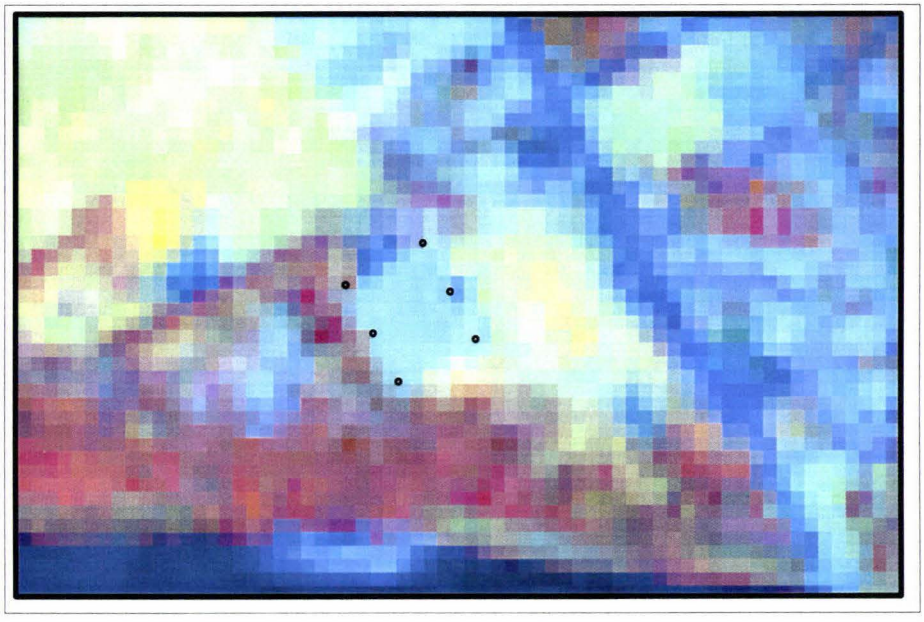

shown in Figure 3.43. This shows that the entire blue area in the scene is in fact the hockey ground. Initially, there was uncertainty where the hockey ground finished and the car park began, but it is obvious here that the car park is the darker area to the north of the hockey ground. Also visible in this figure is the cricket ground (east of the hockey ground), Ongley Park (north-west of the hockey ground) and the Manawatu River (at the bottom of the image). As mentioned in Section 2.6.2, one of the hockey pitches had been upgraded to a water based surface since the Landsat image had been taken. The one that had remained with the same covering is the top most (northern) one.

The positions of the northern hockey pitch were then input into the ERDAS Imagine software, and statistics for each area for the bands extracted for different atmospherically corrected images. This method worked well for the images that had been atmospherically corrected such as the ones generated by the monthly, simple and spatial correction methods. However, as mentioned in Section 2.5.2, the image that had

Table 3.19: Median values for Hockey Pitch with different atmospheric corrections.

	Band 1	Band 2	Band 3	Band 4	Band 5	Band 7
Uncorrected Radiance	88.4	88.3	66.2	77.0	17.0	4.9
Monthly Correction	0.114	0.161	0.150	0.278	0.288	0.252
Simple Correction	0.114	0.161	0.150	0.274	0.285	0.248
Spatial Correction	0.113	0.160	0.149	0.273	0.285	0.248
Lauder Based Correction	0.119	0.163	0.153	0.281	0.289	0.254
ATCOR 2	0.11	0.17	0.15	0.31	0.31	0.23
GER 2600	0.134	0.185	0.167	0.252	0.275	0.270

Table 3.20: Average absolute differences from GER readings for Hockey Pitch.

	Error
Monthly Correction	0.0196
Simple Correction	0.0190
Spatial Correction	0.0195
Lauder Based Correction	0.0181
ATCOR 2	0.0314

been atmospherically corrected by ATCOR has not been rectified. The area that the statistics were extracted for was selected by approximating the location of the hockey field by comparing it with the points overlaid on one of the corrected images. Note that this image has one quarter the number of pixels over the hockey field because it has not been pan sharpened, so still has 30 metre pixels.

The median values are shown in Table 3.19. For comparison the values taken with the GER 2600 are shown. Eight readings were taken on 9 October 2002 between 11:35am and 12:05pm. This corresponds to a sun elevation of between 50.22 degrees and 53.17 degrees. The sun elevation when the Landsat scene was recorded was 55.60 degrees. In ideal circumstances the readings should have been taken at around 1:00pm when the sun elevation would have been 55.71 degrees. However since cloud was starting to form it was decided that the readings should be taken as soon as possible. The eight readings were evenly spaced over the area of the northern hockey pitch. All these readings were very similar, so they were averaged. The plot of the average reflectance over the spectrum recorded by the GER is shown in Figure A.1.

All the readings shown here are in close agreement. The average absolute differences from the GER readings are shown in Table 3.20. For all bands except Band 2, the methods developed for this project are more accurate than ATCOR 2. This may be expected since the 6S based methods use information about the atmosphere at the time.

Table 3.21: Median values for Lake Horowhenua with different atmospheric corrections.

	Band 1	Band 2	Band 3	Band 4	Band 5	Band 7
Uncorrected Radiance	43.4	25.4	11.7	6.5	0.26	0.60
Monthly Correction	0.010	0.011	0.004	0.010	0.000	-0.001
Simple Correction	0.010	0.011	0.004	0.010	0.000	-0.001
Spatial Correction	0.005	0.006	-0.0004	0.006	-0.003	-0.003
Lauder Based Correction	0.017	0.017	0.009	0.015	0.003	0.001
ATCOR 2	0.00	0.00	0.00	0.00	0.00	0.00
GER (Hokowhitu Lagoon)	0.006	0.012	0.008	0.006	0.003	0.008

where ATCOR 2 uses predefined atmospheric models. This is discussed in more detail in Section 2.5. The Lauder method is actually more accurate than the other methods developed. This may be due to differences in the amounts of aerosols input into it as well as the different approach to atmospheric correction.

3.5.3 Lake Horowhenua

The behaviour of the atmospheric corrections over very dark targets is useful in confirming their accuracy. Lakes are generally very dark in satellite imagery and ideally the calculated reflectance for this lake should be close to zero. However errors in the correction can result in negative values. Table 3.21 shows the median retrieved reflectance for Lake Horowhenua. Note that the figures from the GER 2600 provided for comparison are taken from the Hokowhitu Lagoon, but should have very similar spectral properties. The Hokowhitu Lagoon appears in the Landsat scene, but is too small to have many pixels that do not include the edge of the Lagoon. The plot of the reflectance of the Lagoon target is shown in Figure A.7. These readings are the average of five readings taken from a pier on the lagoon. The GER was suspended out over the lagoon between the sun and the pier. One of the readings was discarded due to errors, and the other four readings were averaged.

The Monthly, Simple and Spatial methods have negative values for Band 7. The positive values for the spatial correction method are closest to zero, as may be expected since this should be the most accurate correction. However this method also has the most negative readings and the magnitude of the negative values in Bands 5 and 7 are greater. Thus, the corrections developed do not appear to be totally accurate as some small negative values appear in the infrared bands. However the magnitudes of these negative values are very small. These negative values could be the result of

erroneous input from MODIS, such as an overestimation of the amount of aerosol in the atmosphere.

The Lauder based correction is closer to the ATCOR 2 system, but uses data that are from a different source. It appears the amount of aerosol used is less because none of the bands have negative numbers. This would make some sense as the location where the aerosols were recorded is very clean.

Note that because ATCOR 2 produces an output file of unsigned 8 bit integers, it is impossible for it to record negative values for reflectance. The 6S based methods, however, can output negative values. Therefore it is unknown whether ATCOR 2 producing only zero indicates that it is more accurate in terms of finding reflectance for dark targets, or that it may internally - but because it only outputs positive numbers, its deficiencies may be masked.

If these numbers are compared to the readings taken by the GER 2600, it can be seen that the reflectance recorded is very close to zero. For all bands, ATCOR 2 underestimates the amount of reflection (to the limit of precision provided), and that the methods developed are about midway between the ATCOR 2 results and the GER readings.

Chapter 4

Discussion

4.1 MODIS data

The MODIS data showed significant variation in the concentrations of the main contributors to scattering and absorption in the atmosphere over New Zealand. These results are outlined in Section 3.1. In summary, the values for aerosol optical depth varied between 0.03 and 0.1. Precipitable water vapour varied between 0.6 and 1.7cm. Ozone varied between 280 and 400DU for the year of the study (November 2000 to October 2001). This confirms the suspicion that using one model for New Zealand throughout the year is not going to be accurate.

The quantities of aerosols, water vapour and ozone vary in an annual cycle (see Figures 3.2, 3.6 and 3.9). Both aerosols and water vapour reach a peak in late summer. For water vapour, this is related to the warmer air being able to hold more water vapour. In the case of aerosols this is related to less rain in summer to wash the particles out, and the higher humidity causing the particles to have a higher effective optical depth. This corresponds to what one would expect: fine days in winter are always much clearer than summer days. Table 1.1 lists the natural sources of aerosols. Each of these sources will be discussed in turn. Dust is probably a major contributor to this peak in summer, as there are areas of exposed dry soil from which wind can pick up dust. In winter the soil is kept moist and dust cannot be liberated into the atmosphere in the same way. Forest fires are not common in New Zealand so would probably have little, if any impact. However, farmers burning the remains of crops and burning of marginal high country land to encourage growth may have an impact. Further, bush fires in Australia are becoming a common occurrence and some of the smoke is likely to be carried across the Tasman Sea.

Salt spray almost certainly has an impact. Studying the aerosol composites in Figure 3.1 reveals areas around the coastal areas with higher values of aerosols. This is especially noticeable in the January 2000 image around the Manawatu and Horowhenua coastline, but is also seen around many parts of the North Island in the summer composites. Large scale volcanic activity is not common in New Zealand, and was not seen during the year of the study. There is no doubt that Sulfate, Ammonium and Nitrate based aerosols have some importance given the agricultural land use of most of New Zealand. However it is unlikely their contributions change significantly over the course of the year. Hydrocarbon from plants, however, probably also increases over summer as the warmer temperatures and longer sunshine hours are ideal for plant growth.

Man-made contributions to aerosols are probably higher in winter with wood being burnt for domestic heating, so it is the natural sources of aerosols that are responsible for the increase in summer. During autumn the amounts of aerosols generally decrease, with a spike in April (possibly autumn burning by farmers). The values in winter stay reasonably constant through May, June and July, before picking up again in spring. This could be due to the increase in wind and unsettled weather generally seen about this time. As the sensitivity analysis will show, estimating the amount of aerosols is most important for an accurate atmospheric correction.

Other reasons for the variation in aerosol optical depth over the year are related to water. These allow for a constant amount of aerosols being added to the atmosphere throughout the year, but explain the effects seen differently. The first reason is in winter there is more rain, and this could be responsible for washing more of the aerosols out of the atmosphere during the winter months. The second reason is related to the interaction of water vapour and aerosols. There is a hygroscopic effect caused by water vapour condensing around an aerosol particle. This increases the optical depth of the atmosphere while the amounts of aerosols stay constant. This is a plausible conclusion as the amount of water vapour is also high in summer. O'Neill *et al.* [37] calculate the growth of aerosols due to increasing humidity as shown in Table 4.1. Note that this is for sulfates and nitrates; dust and soot are assumed to be insoluble. Sulfates are mainly from the sea so it is likely that these are a significant contributors to the aerosols seen over New Zealand. As the table shows, this type of aerosol can double its dry size at 95% humidity. It is likely that this would also increase in the resulting aerosol optical depth.

As for water vapour, the increase in summer is related to warmer air being able to carry more water vapour. Ozone has the reverse trend to aerosols and water vapour.

Table 4.1: Mean radius (in μm) of aerosols due to changes in relative humidity (from O'Neill *et al.* [37]).

	Dry	70%	80%	90%	95%
Sulfates	0.1	0.1	0.1472	0.1741	0.2090
Nitrates	0.3	0.3988	0.4474	0.5525	0.7030

That is, in late summer the values are low, and in late winter and early spring the values are highest. This is bad news for sun seekers since ozone is an important absorber of carcinogenic ultra violet light, and therefore has the lowest values when people generally are at the beach and need the protection. However, in winter when people are generally wrapped up, there is the most protection from ultraviolet rays!

4.2 Sensitivity Analysis with 6S

The sensitivity analysis for the values seen in the New Zealand atmosphere indicates a large variation in the retrieved reflectance. These values are summarised in Tables 3.5, 3.6 and 3.7.

The greatest variation happens for the forest target. This is because the target is relatively dark and so input from the atmosphere is a very high percentage of the low actual reflectance values (69% due to aerosols in the blue band). The other targets are progressively lighter, so the effect of atmosphere is a smaller percentage of the reflectance values (49.5% for pasture due to aerosol in the blue band, and 6.9% for soil). This means that if an area of forest or pasture was being monitored, it would be important to get the atmospheric correction right because there is the potential for significant variation in the retrieved reflectance due to the variation in the atmosphere over New Zealand. In the extreme case, two readings for the same forest target at different dates could result in two readings that are 69% different even though there is no change on the ground. The same could happen for the pasture target, but with a smaller difference of 49.5%. However if a lighter coloured target, such as bare soil, was being monitored, the maximum difference between readings would be around 7%. Thus depending on the accuracy of the monitoring required, atmospheric correction may not be so important for soil. But it would almost certainly be required for forest and pasture targets.

As for the effects on the different bands, aerosols and ozone have the greatest effect in the visible, water vapour in the infrared. Aerosols have the greatest effect on the retrieved reflectance. Therefore when doing an atmospheric correction, it would be

most important to get the values for aerosols. As described above, the percentage amount of variation due to aerosol is dependent on the brightness of the target. The effect of aerosols on the infrared is minimal. Water vapour and ozone have less of an effect on the retrieved reflectance. The amount of variation due to water vapour is around 1.4 - 3.6% in the infrared, and only very small effects in the visible. The effect of the water vapour is most obvious for the forest and soil targets, and least for the pasture targets. This is probably due to the actual values for the pasture target being dryer than the others. Ozone has an effect only in the visible, but the percentage variation is dependent on the brightness of the target. For the forest target the maximum variation is around 7.3% in the green band, but for soil the maximum variation is 3.2%, also in the green band. Thus generally, aerosols cause the greatest percentage variation, for the visible, then ozone which is quite a bit smaller, and also in the visible, and lastly water vapour which is mainly in the infrared.

In summary, not only is there a large variation in the amounts of aerosols, water vapour and ozone in the New Zealand atmosphere; it also causes a significant variation in the retrieved reflectance. This is an important finding, as it proves that atmospheric conditions have a large impact, and need to be modelled for monitoring change using Landsat imagery.

4.3 Ground Atmosphere Measurements

It needs to be found how much confidence can be placed in the MODIS data. To test the MODIS data, a ground based instrument was used as described in Section 2.3. The results of the readings are described in Section 3.3.3.

The results for aerosol optical depth do not seem to be in line with the MODIS data (see Tables 3.9 and 3.11). The May reading is higher than the MODIS data and the others lower. It should be remember that there is a significant error in the MODIS aerosol readings over land (see Section 1.3). These readings are somewhat inconclusive in proving the accuracy of the MODIS data. However there is some circumstantial evidence that MODIS overestimates the amount of aerosols in the atmosphere as discussed in Section 4.5. It could be that the May reading with the MICROTOPS was in fact erroneous and the other readings where the sampled aerosol was much lower than MODIS could indeed be the true case. More readings are required for this to be proved.

Because the readings have not been taken at a number of different locations and

compared to the MODIS data, there can not be certainty that the variations in the MODIS data in each scene are correct. It would be interesting to do a series of readings across the lower north island for instance, to confirm that the high values of aerosols seen around the coast do in fact exist, and that other spatial variations in the MODIS data are in fact accurate. In addition some readings in mid summer would prove that the variations seen over the whole year do in fact exist.

As discussed in Section 3.3.3, the readings taken for water vapour were inconclusive. However the data obtained from NIWA seems in agreement with the broad trend of the MODIS data as shown in Section 3.3.5. With reasonable certainty it can be concluded that the difference in the magnitude of the values is due to the fact that the Met Service data were all readings when it was not raining, while the MODIS were readings only when there was no cloud. Thus it is likely that the higher amount of water vapour in the NIWA readings is due to days when conditions were overcast and it may well have been raining. The NIWA data include such times, while the MODIS data do not. In addition, part of the error can be explained by the error in the MODIS data, which is stated at 10%.

The ozone data from the ground based instrument seem reasonably similar to the MODIS data. Further, the instrument is known to be very accurate at recording ozone. Therefore there can be confidence in the ozone figures supplied by MODIS. For a better comparison, data recorded at Lauder over the same year as the MODIS data at Lauder was used. This confirmed the accuracy of the MODIS data, but showed that there was a small overestimation in the amount of ozone by MODIS.

To determine how these errors in MODIS data effect the accuracy of atmospheric correction, the absolute difference between the MODIS readings and the ground measurements were averaged. These differences were taken between the averaged monthly readings for water vapour and ozone, and for each of the three readings for aerosols. This results in an error of ± 0.044 for aerosol optical depth, ± 0.322cm for water vapour and ± 18.1DU for ozone. The error for aerosol optical depth is consistent with the errors stated for the MODIS data (see Section 1.3) and the ozone measurement is relatively accurate (5% error). However the error for water vapour is around twice as much as stated (approximately 20% instead of 10%).

Using the sensitivity results obtained in Section 3.2 the uncertainty in percentage reflectance was obtained. This was related to the retrieved reflectance of the target and the range of reflectance obtained. These results are summarised in Tables 4.2, 4.3 and 4.4. The greatest differences are attributable to uncertainty in the amount of aerosols.

Table 4.2: Uncertainty in retrieved reflectance due to errors in MODIS data for Forest Target.

	Aerosol	Water Vapour	Ozone	Total
Band 1	30.48%	0%	0.41%	30.89%
Band 2	12.12%	0.11%	0.92%	13.15%
Band 3	14.92%	0.13%	0.46%	15.51
Band 4	0.47%	0.81%	0%	1.28%
Band 5	1.22%	0.44%	0%	1.66%
Band 7	3.36%	0.69%	0%	4.05%

Table 4.3: Uncertainty in retrieved reflectance due to errors in MODIS data for Pasture Target.

	Aerosol	Water Vapour	Ozone	Total
Band 1	20.50%	0%	0.37%	20.87%
Band 2	6.43%	0.18%	0.75%	7.36%
Band 3	18.84%	0.25%	0.65%	19.74%
Band 4	0.19%	0.82%	0%	1.01%
Band 5	0.56%	0.47%	0%	1.03%
Band 7	1.81%	0.86%	0%	2.67%

As expected, the errors are greatest for the forest target because of its darkness.

In summary, a number of ground measurements were performed and compared them to MODIS data for the same year. The aerosol values are not equal to the MODIS values - sometimes with a significant error. This can result in a significant error in the retrieved reflectance, especially for darker targets, such as forest. Therefore caution should be exercised when using aerosol values from MODIS in an atmospheric correction. However, the results for water vapour and ozone were reasonably close, giving confidence for using MODIS ozone and water vapour in atmospheric correction.

Table 4.4: Uncertainty in retrieved reflectance due to errors in MODIS data for Soil Target.

	Aerosol	Water Vapour	Ozone	Total
Band 1	3.69%	0%	0.13%	3.82%
Band 2	1.66%	0.17%	0.49%	2.32%
Band 3	1.04%	0.17%	0.26%	1.47%
Band 4	0.44%	1.09%	0%	1.53%
Band 5	0.18%	0.59%	0%	0.77%
Band 7	0.20%	0.97%	0%	1.17%

4.4 Methods of Atmospheric Correction

As described in Section 2.4, three methods for performing atmospheric correction have been developed. These methods are a compromise between processing time and accuracy. The first system, the monthly correction, is ideal if it is not possible to obtain the MODIS data for the scene. For example, it may be an old image taken before MODIS started recording data. This method assumes that the yearly trends seen in the year's data that has been downloaded are the same for other years. It uses the information in the monthly composites created in this study and applies the corrections for the amounts of aerosols, water vapour and ozone in them to the scene.

The next method relies on having the MODIS data taken shortly after the Landsat scene. It uses the average values of the MODIS data and applies the correction to the entire Landsat scene. This means that it is reasonably fast to do the processing, and uses the actual MODIS data for the scene. Any regional variations over the MODIS scene, however, will be ignored. For example, if one particular area has a particularly high amount of aerosol from, for example sea spray, the correction will not reflect this.

Alternatively, the most ambitious method developed matches the actual MODIS data spatially with the Landsat scene. Therefore the correction applied to a Landsat pixel will be generated from the corresponding MODIS pixels. This is intended to allow compensation for any spatial variation in atmospheric conditions. This would allow, for instance, an area of high aerosol concentration and an area of low aerosol concentration to be corrected for accurately, for example, the higher concentration of aerosols often seen at the coast. However, this process is very time consuming - 6S must be run at the highest resolution of the MODIS data (1km). The means for a Landsat scene which is 180 by 180 km, calculating the correction would take approximately 66 hours on the server used. There are other concerns with this approach - mainly with the reliance it places on the accuracy of the MODIS data. As seen in Section 3.1, the ozone data in particular are susceptible to noise and dropouts. Further, the geometric correction of the MODIS data have been found to be less than perfect - up to 3km out in some cases. It would be possible to implement a system that used a larger spatial scale, maybe 10 by 10km. Thus 6S would be run fewer times, cutting down the processing time, but retaining some use of the spatial variation in the MODIS data.

The ATCOR 2 package is described in Section 2.5. As already mentioned, there are problems with its approach of using atmospheric models, its inability to input MODIS based real atmosphere readings into a correction system is a real disadvantage. How-

ever, it cannot be denied that the range of sensors it supports and the fact it plugs into ERDAS Imagine is very useful.

In Section 3.4 the differences in output of the different correction methods is shown. It can be seen that most of the differences between the Monthly, Simple and Spatial methods are very small. It is also shown that the reflectance returned by ATCOR 2 are in general agreement with the other correction techniques, although the numbers returned for Band 4 are generally slightly higher than the other correction techniques. This may be due to the different inputs that are used in ATCOR 2's atmospheric database.

As for the comparison of the reference spectra against the corrections, there are some discrepancies. This may be due to the different circumstances in which the reference spectra were collected. On the whole, however, the reference spectra were reasonably close to the values from the atmospheric corrections. To obtain accurate reference spectra, ground measurements of known targets with a Spectroradiometer are required and these are discussed in Section 4.5.

4.5 Comparison with Ground Readings

As can be seen by the comparisons between the methods of atmospheric correction and of the ground based readings, the corrections used are reasonably accurate (see Section 3.5). Generally, the difference between the ground readings and the atmospherically corrected figures are small enough to be explained by errors in the MODIS data (see Section 4.3).

The corrections also compare favourably with the output of the commercial ATCOR 2. However, they do result in negative values for dark targets, such as Lake Horowhenua. The fact that that corrected reflectance is higher in the near infrared than they are in the red (see Table 3.21) tends to indicate that too much aerosol has been input into the correction process. This is because aerosol has more effect in the red band than the infrared. As can be seen, the red band is negative, while the infrared is positive, lending some weight to this hypothesis.

The values for the Lauder based correction seem better for the dark targets. Positive numbers were returned for Lake Horowhenua. Excluding the different mechanisms for performing the correction, it seems likely that the amount of aerosol from Lauder is closer to the actual for New Zealand than the MODIS data. It is hard to know what is happening with ATCOR 2 for dark targets. The same aerosol measures are being given

as the other methods, but expressed as a visibility. The values returned are zero where the other methods have some small positive values and a few negative values. ATCOR 2 could well be implemented internally such that it does not output negative numbers. The lack of resolution in the values returned (values between 0 and 0.01 cannot be expressed) also makes it difficult to know the exact accuracy of the system.

As for the hockey pitch, the values retrieved by the GER instrument are much closer to the values for atmospheric correction. Again, the differences in reflectance may be attributed to errors in the MODIS data. All the bands have slightly higher values for reflectance with the GER with the exception of Band 4. This is similar to what is happening for the Lake Horowhenua target lending weight to the "too much aerosol" hypothesis. But the fact that the GER values are generally in line with the corrections tends to indicate the corrections are on track. They also tend to confirm the results of the ATCOR 2 system are not too far from the actual despite the shortcomings and generalisations of the system.

Chapter 5

Conclusion and Future Work

5.1 Conclusion

In this thesis the use of MODIS data for characterising the behaviour of the New Zealand atmosphere over the course of one year has been demonstrated. One year's worth of data (1 November 2000 - 31 October 2001) was downloaded and demonstrated the behaviour of the concentrations of aerosol, water vapour and ozone over that year. Aerosol optical depth varies between about 0.03 in winter and 1.0 in late summer. Precipitable water varies between 0.6cm in winter and 1.6cm in late summer. Ozone varies between 280 Dobson Units in summer and 400 Dobson Units in winter. More detailed information for each month in the form of composites made from all the MODIS observations for the month was prepared for display.

It has been shown that the MODIS data have a significant error in estimating the amount of aerosol. This has been shown by the use of a MICROTOPS instrument, and also by the results of atmospheric correction which have been over corrected in Band 3 - a sign of too much aerosol being input. As for the water vapour part of the MODIS measurements - a comparison of these with the data recorded with weather balloons released from Paraparaumu was performed. Although close, the MODIS data tend to underestimate the amount of water vapour in the atmosphere. The ozone readings were compared to that recorded by the MICROTOPS instrument and to readings taken by NIWA. These indicated that MODIS is reasonably accurate at measuring ozone, but overestimates the amount slightly. These errors in MODIS readings mean that for dark targets such as forest, there can be a significant variation in the retrieved reflectance (up to 30%).

Sensitivity analysis was undertaken to determine how much these variations in

the various components of the atmosphere affected the retrieved reflectance. It was concluded that variations in aerosol optical depth have the biggest effect on the retrieved reflectance. The effect is focused on the visible part of the spectrum. Varying the aerosols through the range seen in the New Zealand atmosphere, the retrieved reflectance varied from that calculated on the conditions for the day by up to 69% for a dark target such as beech forest. This was less for the lighter targets of pasture (49%) and soil (6.9%). Variations in the concentration of ozone were of secondary importance, and were also focused on the visible part of the spectrum. Ozone contributed to between 0.8% and 5.5% variation in the retrieved reflectance. Water vapour had the least effect, and mainly in the infrared. Water vapour contributed to a variation of between 2.7% and 3.7% depending on the brightness of the target.

Some methods for performing atmospheric correction that vary in input and processing time consumed were developed. These generally return very similar results for the targets that were compared. It was concluded that the Simple correction, where the values for aerosols, water vapour and ozone are averaged from the MODIS scene coincident to the Landsat scene to be corrected are used as inputs to the model, is best if the MODIS data are available for that scene. Otherwise, it is recommended that the Monthly correction which uses the composite image created for the month of the Landsat scene to be corrected be used. This enables scenes to be corrected that were taken before MODIS was launched. This assumes that the behaviour of the New Zealand atmosphere that was witnessed in the year of the study is the same for every year. Spatial correction, where the variations in the MODIS data over the scene are taken into account, was found to be too time consuming and did not increase accuracy significantly.

A comparison was done between the outputs of the atmospheric corrections that were developed and those of a commercial product (ATCOR 2). It was found that for most targets the results were very similar. However, over very dark targets such as lakes ATCOR 2 was not susceptible to negative numbers as these other methods were. The results of these corrections were also compared with readings of specific targets taken with a GER 2600 Spectroradiometer. A close correlation was found between these and the results of the atmospheric corrections. In addition the output of the original correction based on point data were compared. These results were comparable to the other corrections.

Thus a number of MODIS based atmospheric corrections have been developed and have demonstrated their accuracy with other correction techniques and ground based

readings.

5.2 Future Work

The understanding of the behaviour of the New Zealand atmosphere would be greatly enhanced if more MODIS data were downloaded. This would give an indication of whether the trends observed in this study continue for all years and whether the values are representative. This would give researchers more confidence when using the Monthly correction technique.

To gain a better understanding of the accuracy of the MODIS aerosol data, it would be good to acquire more MICROTOPS readings, and preferably compare those against MODIS data for the same day. This may give an indication of trends in the errors of MODIS aerosol data. Comparison with other sensors that produce similar data, such as MERIS and MISR would also be extremely useful.

Further, more representative targets could be collected using the Spectroradiometer and this would give researchers more confidence when doing an atmospheric correction if the output from such a correction matches these targets. This process has been started in this study but large targets such as lakes and river beds would be helpful.

Appendix A

Reference Spectra

This appendix contains a collection of reference spectra of different targets. These were either collected by using a GER 2600 Spectroradiometer, or from the ATCOR 2 package as indicated in brackets.

Figure A.1: Reference Spectra for Artificial Hockey Pitch (GER).

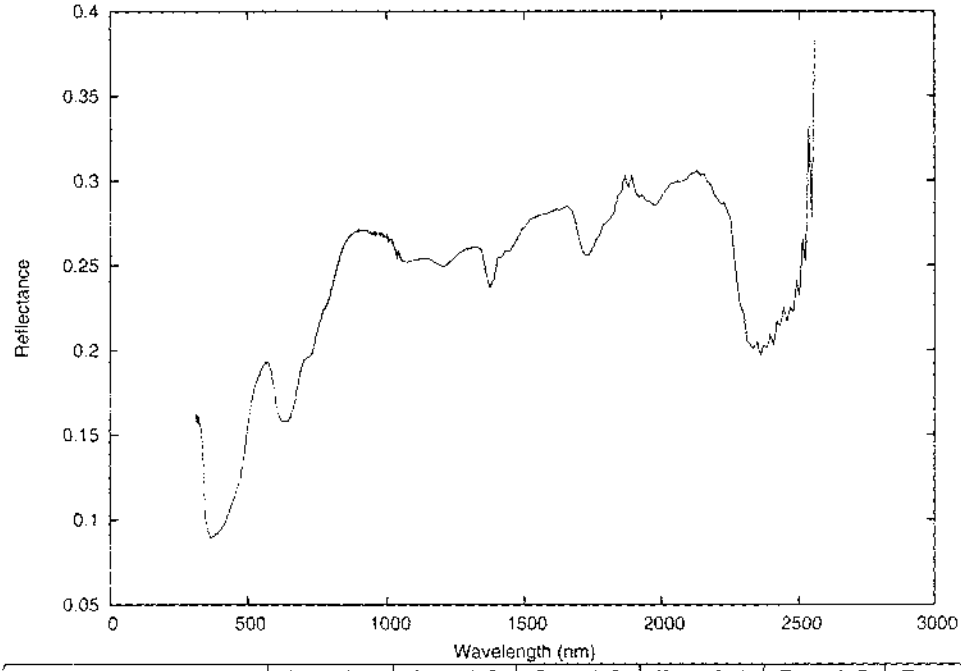

	Band 1	Band 2	Band 3	Band 4	Band 5	Band 7
Landsat Response	0.1335	0.1853	0.1671	0.2522	0.2754	0.2700

Figure A.2: Reference Spectra for Manuka (GER).

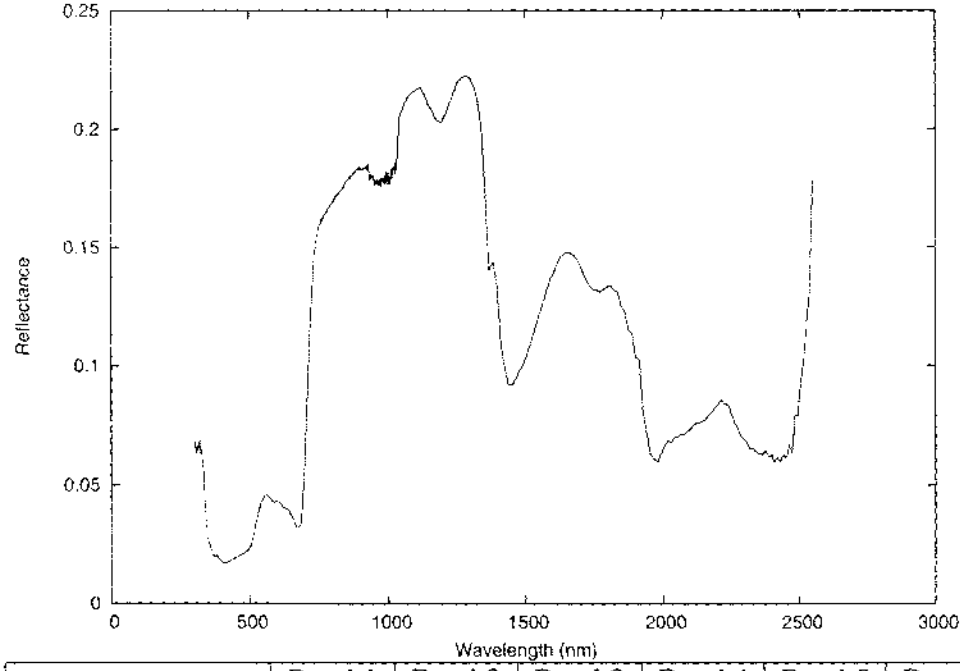

	Band 1	Band 2	Band 3	Band 4	Band 5	Band 7
Landsat Response	0.0120	0.0223	0.0166	0.2809	0.0724	0.0317

Figure A.3: Reference Spectra for Regrowing Bush (GER).

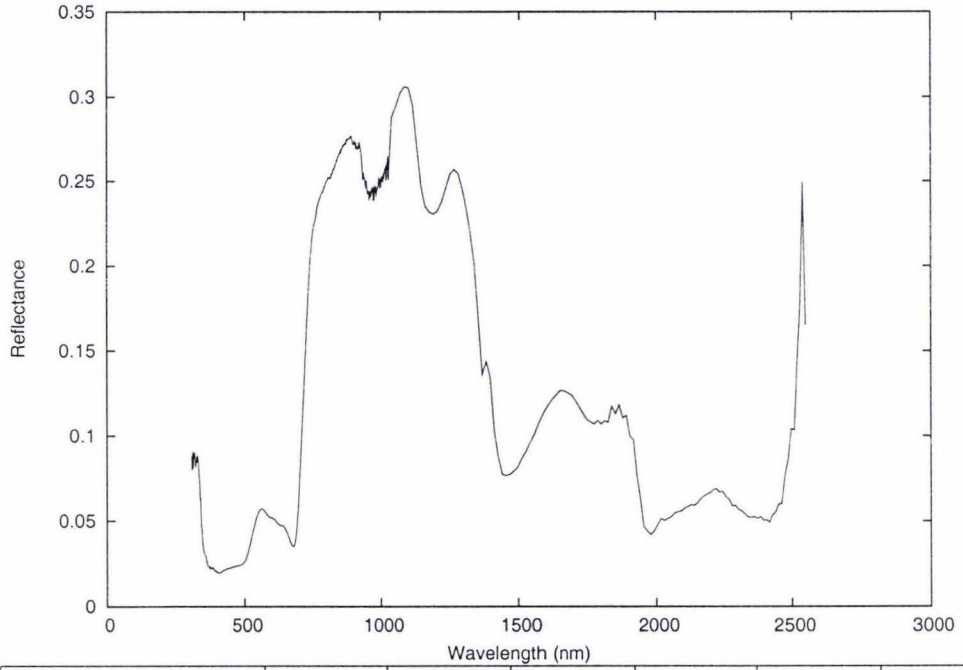

	Band 1	Band 2	Band 3	Band 4	Band 5	Band 7
Landsat Response	0.0251	0.0517	0.0421	0.2595	0.1176	0.0605

Figure A.4: Reference Spectra for Pine (GER).

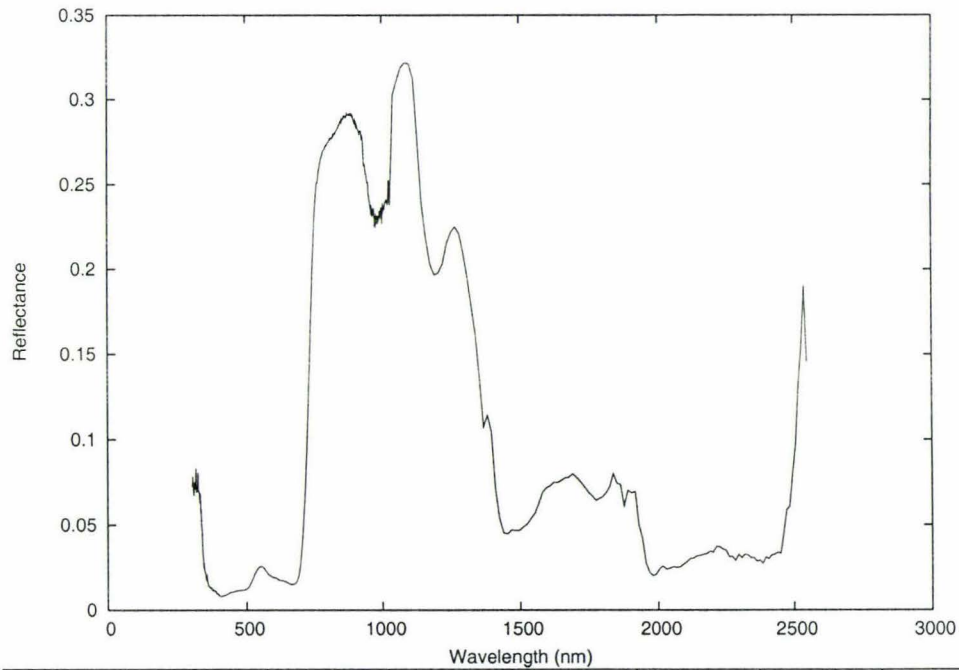

	Band 1	Band 2	Band 3	Band 4	Band 5	Band 7
Landsat Response	0.0120	0.0223	0.0166	0.2809	0.0724	0.0317

Figure A.5: Reference Spectra for Soil (GER).

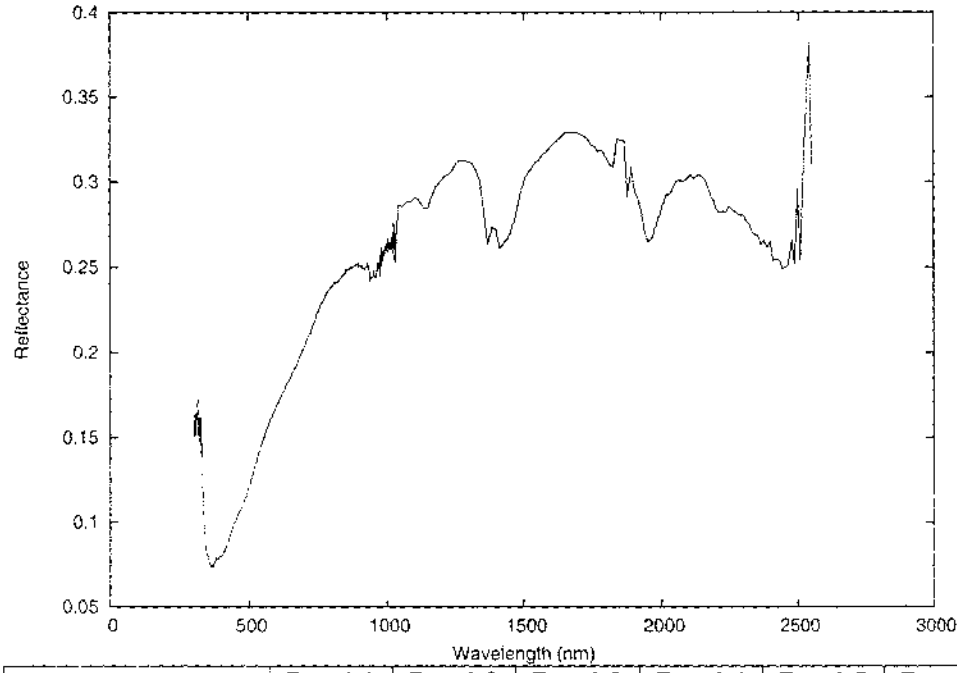

	Band 1	Band 2	Band 3	Band 4	Band 5	Band 7
Landsat Response	0.1114	0.1529	0.1905	0.2441	0.3240	0.2885

Figure A.6: Reference Spectra for Asphalt (GER).

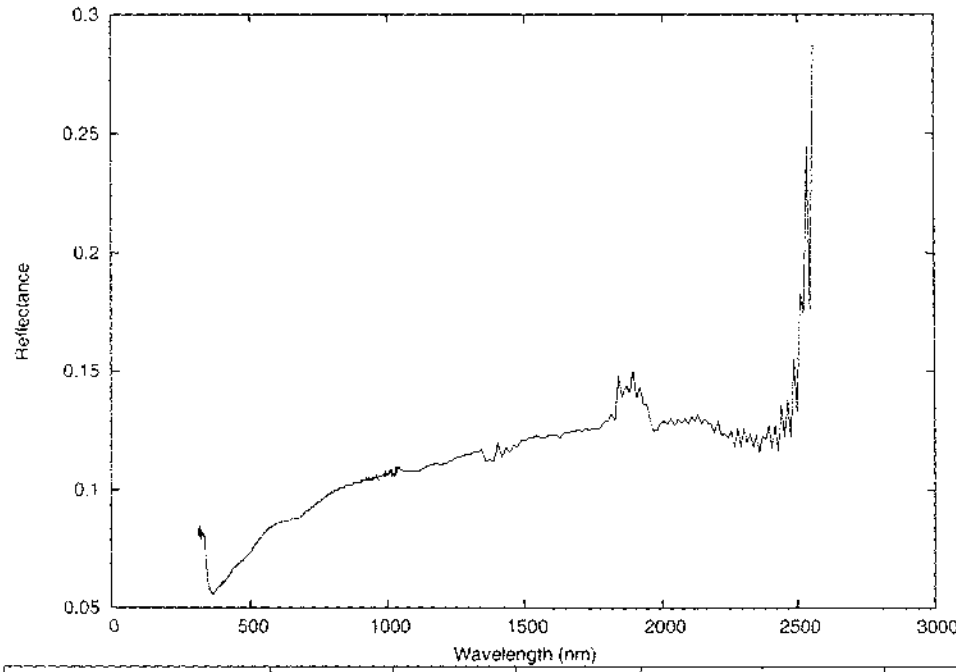

	Band 1	Band 2	Band 3	Band 4	Band 5	Band 7
Landsat Response	0.0714	0.0827	0.0879	0.1007	0.1240	0.1254

Figure A.7: Reference Spectra for a Hokowhitu Lagoon (GER).

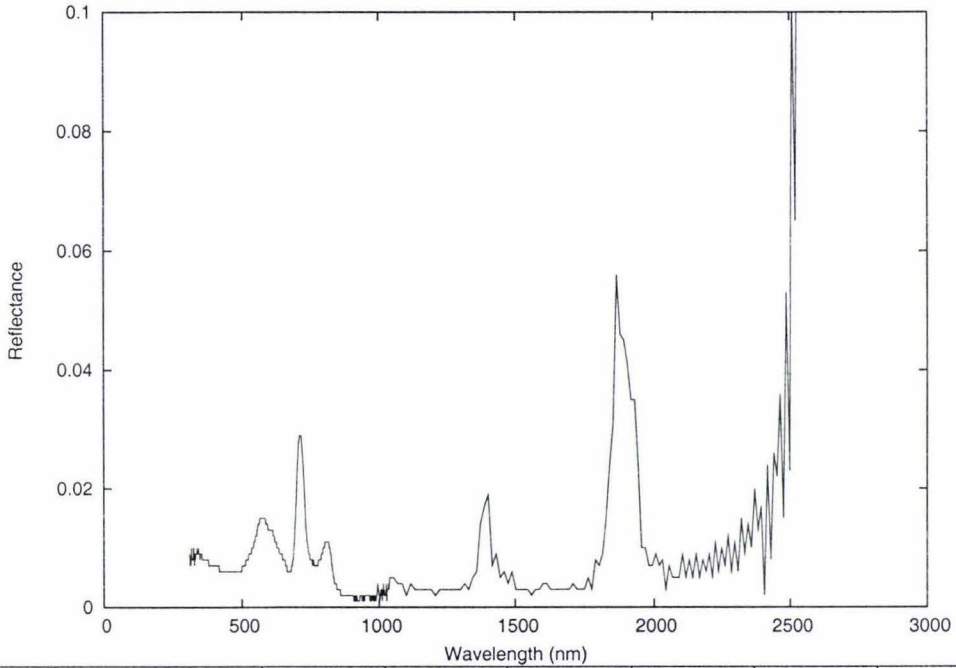

	Band 1	Band 2	Band 3	Band 4	Band 5	Band 7
Landsat Response	0.0062	0.0124	0.0079	0.0057	0.0032	0.0079

Figure A.8: Reference Spectra for Sea (ATCOR).

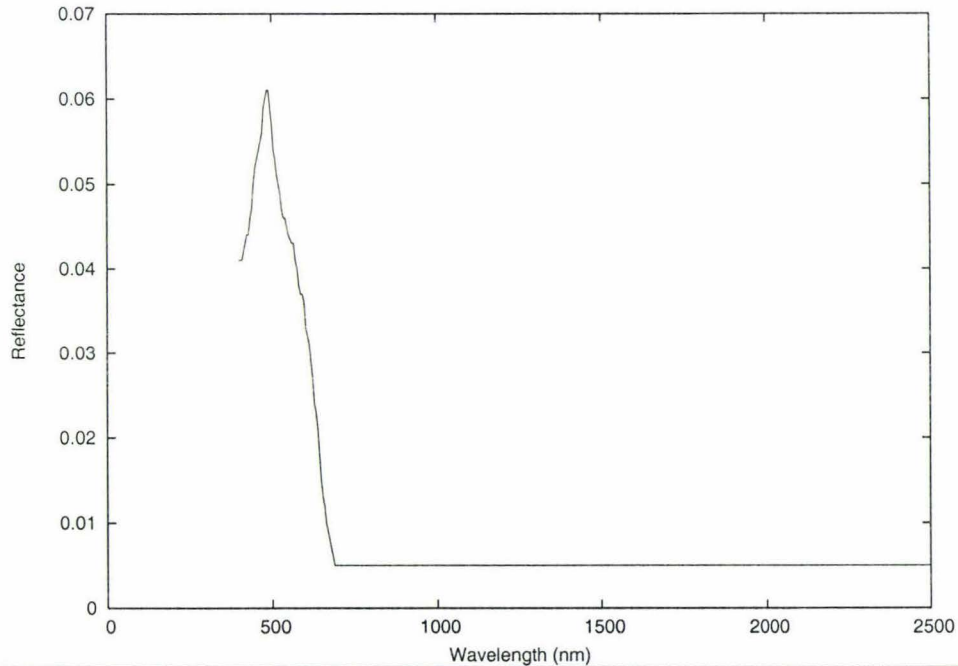

	Band 1	Band 2	Band 3	Band 4	Band 5	Band 7
Landsat Response	0.0558	0.0421	0.0054	0.000	0.000	0.000

Figure A.9: Reference Spectra for Concrete (GER).

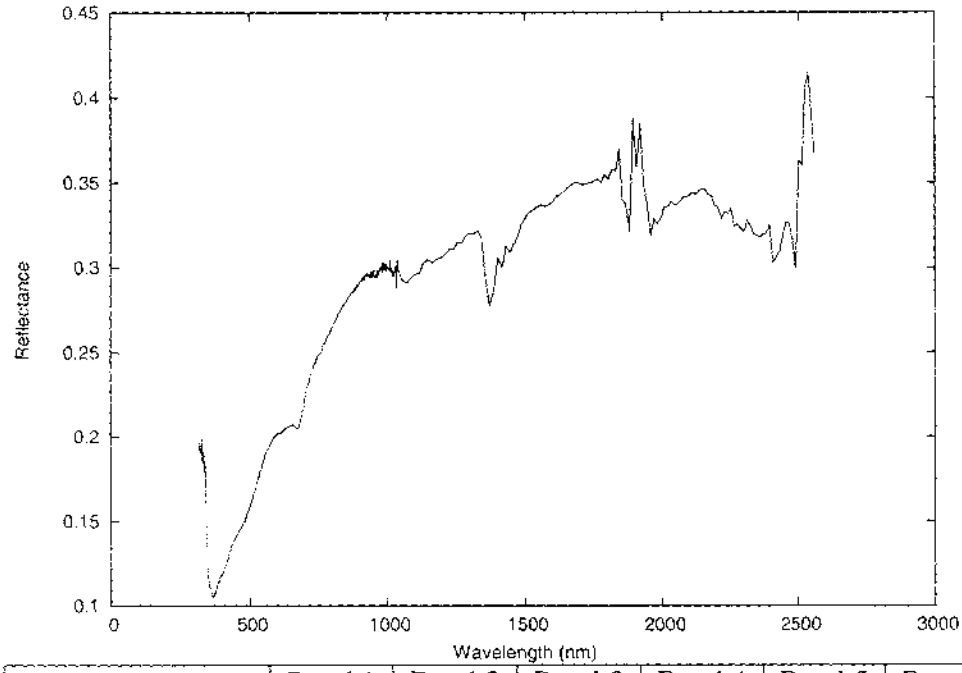

	Band 1	Band 2	Band 3	Band 4	Band 5	Band 7
Landsat Response	0.1509	0.1894	0.2074	0.2755	0.3446	0.3341

Figure A.10: Reference Spectra for Grass (GER).

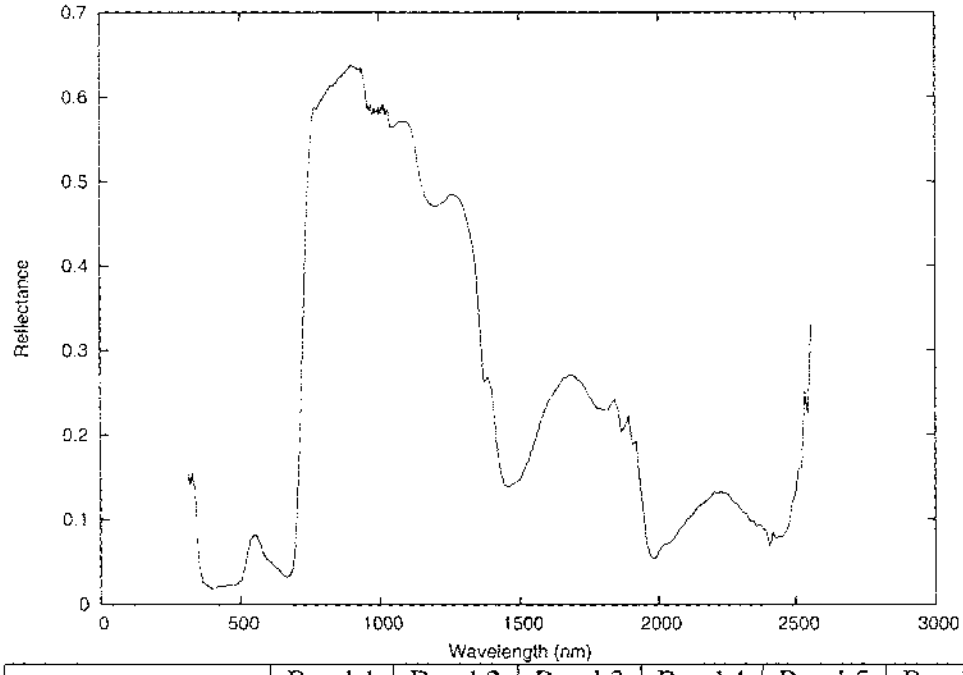

	Band 1	Band 2	Band 3	Band 4	Band 5	Band 7
Landsat Response	0.0258	0.0676	0.0378	0.6133	0.2474	0.1134

Bibliography

[1] MODIS Atmosphere Home. http://modis-atmos.gsfc.nasa.gov/index.html

[2] Terra: The EOS Flagship. http://eos-am.gsfc.nasa.gov/index.html

[3] EOS Tracking. http://liftoff.msfc.nasa.gov/realtime/JTrack/eos.html

[4] Landsat7 Science Data Users Handbook. http://ltpwww.gsfc.nasa.gov/IAS/handbook/handbook_toc.html

[5] TERRA: What are Aerosols? http://terra.nasa.gov/FactSheets/Aerosols/.

[6] MODIS Atmosphere Data products. http://eosdatainfo.gsfc.nasa.gov/eosdata/terra/modis/modatm_dataprod.html

[7] MODIS Atmosphere: MOD04_L2: Format and Content. http://modis-atmos.gsfc.nasa.gov/MOD04_L2/format.html

[8] MODIS Atmosphere: MOD05_L2: Format and Content. http://modis-atmos.gsfc.nasa.gov/MOD05_L2/format.html

[9] MODIS Atmosphere: MOD05_L2 (Water Vapour Product).http://modis-atmos.gsfc.nasa.gov/MOD05_L2/index.html

[10] MODIS Atmosphere: MOD07_L2: Format and Content.http://modis-atmos.gsfc.nasa.gov/MOD07_L2/format.html

[11] MODIS Atmosphere: MOD07_L2 (Atmosphere Profile Product).http://modis-atmos.gsfc.nasa.gov/MOD07_L2/index.html

[12] MODIS Water Vapour Known Problems. http://modis-atmos.gsfc.nasa.gov/MOD05_L2/qa.html

[13] National Centre for Supercomputing Applications, 1999: *HDF User's Guide.* ftp://ftp.ncsa.uiuc.edu/HDF/HDF/Documentation/HDF4.1r5/Users_Guide/

[14] Ozone and the atmosphere protective ozone. http://daac.gsfc.nasa.gov/CAMPAIGN_DOCS/ATM_CHEM/protective_ozone.html

[15] Allen, A.G., Dick, A.L., Davison, B.M. 1997: Sources of atmospheric methanesulphonate, non-sea-salt sulfate, nitrate and related species over the temperate South Pacific. *Atmospheric Environment.* 31 (2): pp191-205. January 1997

[16] Batchelor, R.L., 2001: *An Experimental Investigation into the Scattering of UV Radiation by Air Pollution.* Undergraduate Project Report, University of Canterbury. Department of Physics & Astronomy.

[17] Blum, J.R., Rosenblatt, J.I. 1972: *Probability and Statistics.* Page 442. W.B. Saunders Company.

[18] Chahine, M.T., McCleese, D.J., Rosenkrantz, P.W., Staelin, D.H., 1983: Interaction Mechanisms Within the Atmosphere. *Manual of Remote Sensing.* American Society of Photogrammetry.

[19] Chavez, P.S., 1988: An Improved Dark-Object Subtraction Technique for Atmospheric Scattering Correction of Multispectral Data. *Remote Sensing of Environment.* Vol 24. No 3, pp 459-479. April 1988.

[20] Chu, Strabala, Platnick, Moody, King, Mattoo, Hucek, & Ridgway, 2000: *MODIS Atmosphere QA Plan.* Version 2.2. http://modis-atmos.gsfc.nasa.gov/_docs/QA_Plan_2000_07.pdf

[21] Forgan, B.W., Liley, J.B. 1997:Aerosols and UV in New Zealand. In *UV Radiation and its effects: an update.* The Royal Society of New Zealand. December, 1997.

[22] Gao, B., Kaufman, Y.J., 1998: *The MODIS Near-IR Water Vapour Algorithm.* http://modis-atmos.gsfc.nasa.gov/_docs/atbd_mod03.pdf

[23] Geophysical & Environmental Research Corp. 1996: *GER 2600 User Manual.* Geophysical & Environmental Research Corporation, Millbrook, NY USA.

[24] Hu, C., Muller-Karger, F.E., Andrefouet, S., Carder, K.L. 2001: Atmospheric correction and cross-calibration of LANDSAT-7/ETM+ imagery over aquatic environments: A multi platform approach using SeaWiFS/MODIS. *Remote Sensing of Environment.* Vol 78. Issues 1-2. October 2001. pp 99-107.

[25] Kasten, F. and Young, T., 1989: Revised optical air mass tables and approximation formula. *Applied Optics* Vol. 28, No. 22.

[26] Kaufman, Y.J., Tanré, D., 1998: *Algorithm for Remote Sensing of Tropospheric Aerosol from MODIS.* `http://modis-atmos.gsfc.nasa.gov/_docs/atbd_mod02.pdf`

[27] Lee, D.S., Dollard, G.J., Derwent R.G., Pepler S. 1999: Observations on gaseous and aerosols components of the atmosphere and their relationships. *Water, Air and Soil Pollution.* 113. pp 175-202.

[28] Liang, S., Fang, H., Chen, M. 2001: Atmospheric Correction of Landsat ETM+ Land Surface Imagery-Part I: Methods. *IEEE Transactions on Geoscience and Remote Sensing.* Vol 39. No 11. November 2001. pp 2490-2498.

[29] Lu, D., Mausel, P., Brondizio, E., Moran, E. 2002: Assessment of atmospheric correction methods for Landsat TM data applicable to Amazon basin LBA research. *International Journal of Remote Sensing.* Vol 23. No 13. pp 2651-2671.

[30] Meeus, J., 1991: *Astronomical Algorithms.* Published by: Willmann-Bell, Inc. P.O. Box 35025 Richmond, Virginia 23235.

[31] Menzel, W.P., Gumley, L.E., 1998: *MODIS Atmospheric Profile Retrieval - Algorithm Theoretical Basis Document.* `http://ltpwww.gsfc.nasa.gov/MODIS-Atmosphere/_docs/atbd_mod07.pdf`

[32] Michalsky, 1988, The Astronomical Almanacs algorithm for approximate solar position (1950-2050). *Solar Energy* Vol. 40, No. 3, pp 227-235.

[33] Molina L.T., Molina M.J. 1986: Absolute Absorption Cross Sections of Ozone in the 185 to 350nm Wavelength Range. *Journal of Geophysical Research,* 91(D13):14501-14508.

[34] Morys, M., Mims, F.M., Anderson, S.E., 1996: Design, calibration and performance of MICROTOPS II hand-held ozonometer. In *User's Guide*, Solar Light Co. Inc.

[35] New Zealand Meteorological Service, 1978: Modification of the Ozone Layer due to human activities and some possible geophysical consequences. *New Zealand Meteorological Service Technical Information Circular* no. 167.

[36] Nilsson, Annika, 1996: *Ultraviolet reflections: Life under a thinning ozone layer.* John Wiley & Sons.

[37] O'Neill, N.T., Royer, A., Hubert, L., 1990: Remote Sensing of Aerosols from Space: Information Content of Monochromatic Atmospheric Reflectance's. *Remote Sensing of Environment.* 34 (3): 193-206 December 1990.

[38] Ouaidrari, H., Vermote, E.F., 1999: Operational Atmospheric Correction of Landsat TM Data. *Remote Sensing of Environment.* Vol 70. No 1. October 1999. pp 4-15.

[39] Penndorf, R., 1957: Tables of the Refractive Index for Standard Air and the Rayleigh Scattering Coefficient for the Spectral Region between 0.2 and 20.0μ and Their Application to Atmospheric Optics. *Journal of the Optical Society of America*, Vol 47, No 2.

[40] Richards, J.M., 1971: A simple expression for the saturation vapour pressure of water in the range -50 to 140 deg. *C. J. Phys. D.: Appl. Phys.*, 4:L15-L18, 1971.

[41] Richter, R., 2002: *ATCOR for ERDAS IMAGINE, User Manual.* Geosystems GmbH, Riesstr. 10, D-82110 Germering, Germany.

[42] Shepherd, J.D., 1997: *Land Surface Temperature Retrieval from AVHRR.* Thesis submitted for the degree of Doctor of Philosophy in Physics. University of Waikato.

[43] Shepherd, J.D., Dymond, J.R., 2000: BRDF Correction of Vegetation in AVHRR Imagery. *Remote Sensing of Environment.* Vol 74. No 3. December 2000. pp 397-408.

[44] Song, C., Woodcock, C.E., Seto, K.C., Lenney, M.P., Macomber, S.A. 2001: Classification and change detection using Landsat TM data: When and how to

correct atmospheric effects? *Remote Sensing of Environment.* Vol 75. No 2. February 2001. pp 230-244.

[45] Tanré, D., DeRoo, C., Duhaut, P., Herman, M., Morcrette, J.J., 1990: Description of a computer code to simulate the satellite signal in the solar spectrum: the 5S code. *International Journal of Remote Sensing.* Vol 11. No 4. April 1990. pp 659-668.

[46] Vermote, E., Tanré, D., Deuzé, J.L, Herman, M. and Morcrette, J.J., 1997: *Second Simulation of the Satellite Signal in the Solar Spectrum (6S).* `ftp://kratmos.gsfc.nasa.gov/pub/6S/`

[47] Zhang, M., Carder, K., Muller-Karger, F.E., Lee, Z., Goldgof, D.B., 1999: Noise Reduction and Atmospheric Correction for Coastal Applications of Landsat Thematic Mapper Imagery. *Remote Sensing of Environment.* Vol 70. No 2. November 1999. pp 167-180.

[48] Zhao, W.J., Tamura, M., Takahashi, H., 2001: Atmospheric and spectral corrections for estimating surface albedo from satellite data using 6S code. *Remote Sensing of Environment.* Vol 76. No 2. May 2001. pp 202-212.